

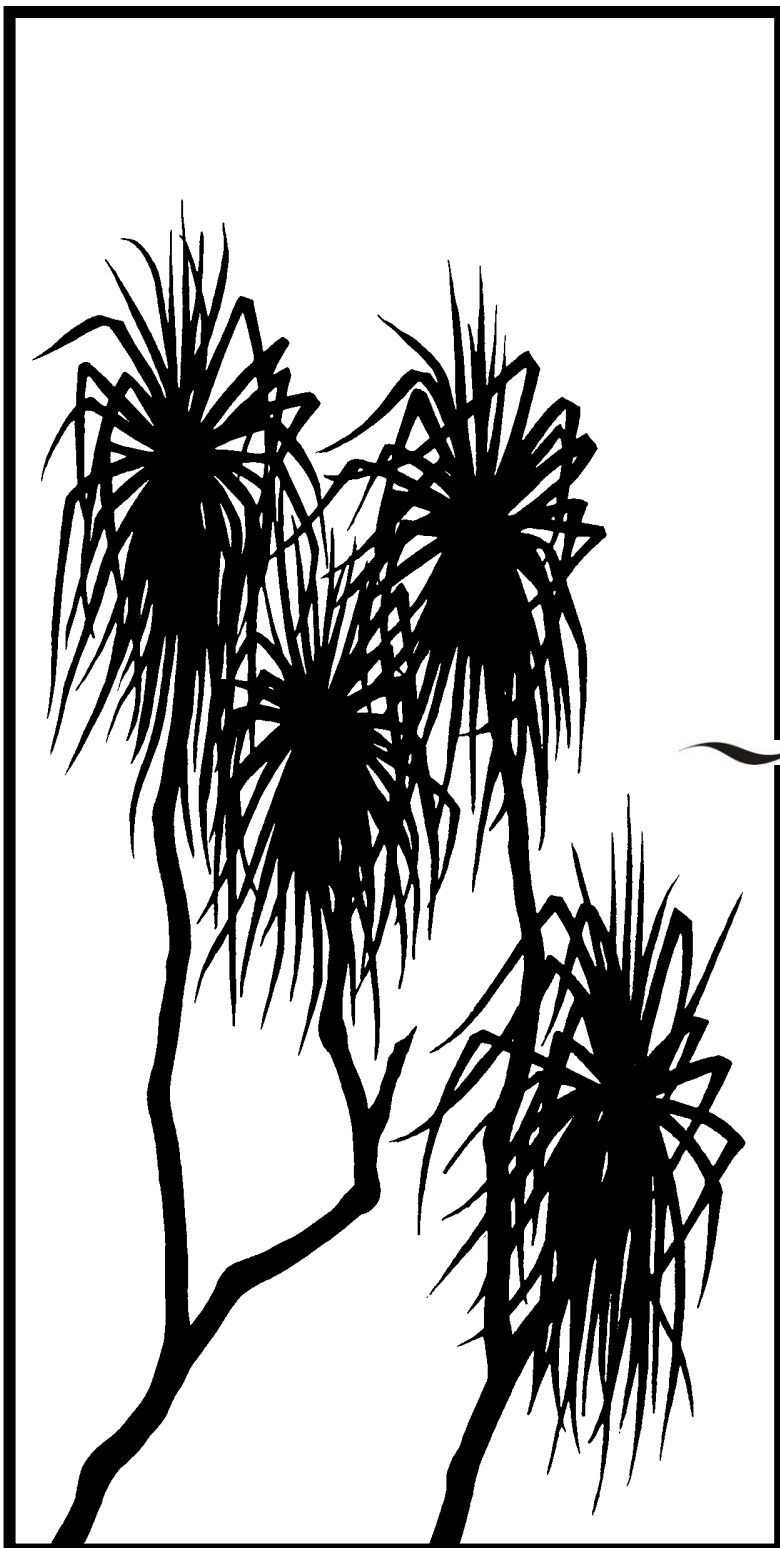


Australian Government

Department of Sustainability, Environment,
Water, Population and Communities
Supervising Scientist

*internal
report*

616



Pre-mining radiological
conditions in the Ranger
Project Area

A Bollhöfer, A Beraldo,
K Pfitzner, A Esparon & G Carr

February 2013

Release status – unrestricted
Project number – RES-2005-001

This page has been left blank intentionally.

Pre-mining radiological conditions in the Ranger Project Area

A Bollhöfer, A Beraldo, K Pfitzner, A Espanon & G Carr

Supervising Scientist Division
GPO Box 461, Darwin NT 0801

February 2013

Project number RES-2005-001

Registry File SG2005/0127

(Release status – unrestricted)



Australian Government

**Department of Sustainability, Environment,
Water, Population and Communities**
Supervising Scientist

How to cite this report:

A Bollhöfer, A Beraldo, K Pfitzner, A Espanon & G Carr 2013. Pre-mining radiological conditions in the Ranger Project Area. Internal Report 616, February, Supervising Scientist, Darwin.

Project number – RES-2005-001

Location of final PDF file in SSDX Sharepoint:

[http://publications.nt.environment.gov.au/PublicationWork/Publications and Productions/Internal Reports \(IRs\)/Nos 600 to 699/IR616_Pre-mining radiological conditions](http://publications.nt.environment.gov.au/PublicationWork/Publications and Productions/Internal Reports (IRs)/Nos 600 to 699/IR616_Pre-mining radiological conditions)

Location of all key data files for this report in SSDX:

<http://ssd.nt.environment.gov.au/SSDX/Chemical and Radiological Site Assessment/SPIRE Radiological/SPIRE Anomaly 2>

Authors of this report:

Andreas Bollhöfer – Environmental Research Institute of the Supervising Scientist, GPO Box 461, Darwin NT 0801, Australia

Annamarie Beraldo – Environmental Research Institute of the Supervising Scientist, GPO Box 461, Darwin NT 0801, Australia. Address at time of publication: Sinclair Knight Merz, GPO Box 2145 Parap NT 0804, Australia

Kirrilly Pfitzner – Environmental Research Institute of the Supervising Scientist, GPO Box 461, Darwin NT 0801, Australia

Andrew Espanon – Environmental Research Institute of the Supervising Scientist, GPO Box 461, Darwin NT 0801, Australia

G Carr – Environmental Research Institute of the Supervising Scientist, GPO Box 461, Darwin NT 0801, Australia. Address at time of publication: Northern Land Council, GPO Box 1222, Darwin, NT 0801, Australia

The Supervising Scientist is part of the Australian Government Department of Sustainability, Environment, Water, Population and Communities.

© Commonwealth of Australia 2013

Supervising Scientist

Department of Sustainability, Environment, Water, Population and Communities
GPO Box 461, Darwin NT 0801 Australia

This work is copyright. Apart from any use as permitted under the Copyright Act 1968, no part may be reproduced by any process without prior written permission from the Supervising Scientist. Requests and enquiries concerning reproduction and rights should be addressed to Publications Enquiries, Supervising Scientist, GPO Box 461, Darwin NT 0801.

e-mail: publications_ssd@environment.gov.au

Internet: www.environment.gov.au/ssd (www.environment.gov.au/ssd/publications)

The views and opinions expressed in this report do not necessarily reflect those of the Commonwealth of Australia. While reasonable efforts have been made to ensure that the contents of this report are factually correct, some essential data rely on references cited and/or the data and/or information of other parties, and the Supervising Scientist and the Commonwealth of Australia do not accept responsibility for the accuracy, currency or completeness of the contents of this report, and shall not be liable for any loss or damage that may be occasioned directly or indirectly through the use of, or reliance on, the report. Readers should exercise their own skill and judgment with respect to their use of the material contained in this report.

Printed and bound in Darwin NT by Supervising Scientist Division

Contents

Executive summary	ix
1 Introduction	1
1.1 Background	1
1.1.1 Ranger Environmental Requirements	1
1.1.2 Use of airborne gamma surveys in exploration and site characterisation	2
1.1.3 Existing pre-mining ground data at Ranger	3
1.2 Objective	4
2 Selection of an undisturbed radiologically anomalous site	5
2.1 The MODAT database	5
2.2 Existing airborne gamma surveys	6
2.2.1 The Alligator River Geophysical Survey	7
2.2.2 1996 Rio Tinto Airborne Gamma survey	8
3 Methods	10
3.1 1976 airborne gamma survey specifications	10
3.2 1997 airborne gamma survey specifications	10
3.3 Ground truthing	11
3.3.1 Gamma dose rate measurements	11
3.3.2 Radon flux density measurements	13
3.3.3 Radon in air measurements	15
3.3.4 Soil activity concentration measurements	16
4 Results	18
4.1 1976 airborne gamma survey data	18
4.2 1997 airborne gamma survey	19
4.3 Gamma dose rates measured in the field	20
4.4 Radon	21
4.4.1 Radon flux densities	21
4.4.2 Radon activity concentration in air	21
4.5 Soil activity concentrations	22
4.5.1 Laboratory HPGe measurements	22
4.5.2 In situ NaI measurements	25
5 Conversion factors	26
5.1 Terrestrial gamma dose rate to ^{226}Ra soil activity concentration	26
5.2 ^{226}Ra soil activity concentration to ^{222}Rn flux density	27
5.3 Terrestrial gamma dose rate to ^{222}Rn flux density	28

5.4 Converting the 1976 AGS U data to terrestrial dose rate in the field	29
5.4.1 Modelling the 1997 AGS line data to the field gamma dose rate data	30
5.4.2 Modelling the 1976 raster to the 1997 raster airborne gamma data	35
5.4.3 Converting 1976 eU data to terrestrial gamma dose rates and radon flux densities	36
6 Discussion	37
6.1 Pre-mining external γ dose rates, radon flux densities and ^{226}Ra activity concentrations in the greater Ranger region	37
6.2 Orebody 1, Orebody 3 and Anomaly 2	40
6.2.1 Gamma dose rates and ^{226}Ra activity concentrations	40
6.2.2 Radon flux density	40
6.2.3 Airborne radon activity concentration	41
6.2 Djalkmara and Corridor Creek Land Application Areas	42
6.3 Environmental background	42
7 Conclusions	44
References	45
Appendix A Results of external gamma dose rate and in-situ soil activity concentration measurements	49
Appendix B Radon flux density	88
Appendix C Airborne radon activity concentrations	90
Appendix D Soil activity concentrations	92

Figures

Figure 1 Contours of total counts measured during the 1969 AGS over the Ranger area (Ryan 1972)	3
Figure 2 Known uranium (and uranium/gold) anomalies in the ARR (from Pfitzner & Martin 2003)	5
Figure 3 Spatial coverage of the existing AGS data available over the ARR, as available from NTGS (from Pfitzner & Martin 2003)	6
Figure 4 (a) Ikonos satellite data (2001, displayed as false colour composite) subset shown in Figure 3 and (b) corresponding 1976 equivalent uranium (eU) AGS raster data, with MODAT uranium anomalies overlaid.	8
Figure 5 Eupene et al (1975) map of aerial radiometric contours of total count (TC) overlaid on airborne data from the 1976 AGS.	9
Figure 6 Extent and flight lines of the 1997 Rio Tinto airborne gamma survey, overlaid on an aerial photograph from March 2007.	9
Figure 7 Location of the 2007–08 ground gamma survey points	12
Figure 8 Location of the 2007–08 ground gamma survey points overlaid on the total counts signal above Anomaly 2 from the 1997 AGS	13
Figure 9 Location of the radon exhalation sampling points overlaid on the total counts signal above Anomaly 2 from the 1997 AGS	15
Figure 10 Set up of the GS-512 field gamma spectrometer	16
Figure 11 Counts (> 25 counts per sec) in the uranium channel of the 1976 AGS over the whole scene	18
Figure 12 Counts (>250 counts per second) in the uranium channel of the 1976 AGS over the Ranger mine region	19
Figure 13 Counts (>250 counts per second) in the uranium channel of the 1976 AGS over Anomaly 2	19
Figure 14 Counts (>4500 counts per second) in the TC channel of the 1997 AGS over Anomaly 2	20
Figure 15 Field gamma dose rates measured over Anomaly 2 between 2007–09	20
Figure 16 Radon flux densities measured over the Anomaly 2 area between 2007–09	21
Figure 17 Radon activity concentrations measured in air at 30 cm, 50 cm and 150 cm above ground over the Anomaly 2 area for the dry season 2009	22
Figure 18 (a) Measured ^{234}Th activity concentration plotted against derived ^{238}U for sample activity concentrations between (a) 40 – 40 000 $\text{Bq}\cdot\text{kg}^{-1}$, and (b) 40 – 10 000 $\text{Bq}\cdot\text{kg}^{-1}$	23
Figure 19 (a) ^{226}Ra activity concentration and (b) $^{226}\text{Ra}/^{238}\text{U}$ activity concentration ratio plotted against ^{238}U activity concentrations in samples from Anomaly 2	23

Figure 20 Calculated terrestrial gamma dose rates [$\mu\text{Gy}\cdot\text{hr}^{-1}$] from laboratory HPGe radionuclide activity concentration measurements plotted versus the measured terrestrial gamma dose rates at sites 1A-25A.	25
Figure 21 Calculated terrestrial gamma dose rates (using equation 2) in $\mu\text{Gy}\cdot\text{hr}^{-1}$ plotted versus measured terrestrial gamma dose rates performed in August 2007 using the NaI detector.	25
Figure 22 In situ and laboratory measured soil ^{226}Ra activity concentration plotted against the measured terrestrial gamma dose rates, all data shown.	26
Figure 23 In situ (NaI) (o) and laboratory (HPGe) (•) measured soil ^{226}Ra activity concentration plotted against measured terrestrial gamma dose rates ($< 2 \mu\text{Gy}\cdot\text{hr}^{-1}$)	27
Figure 24 ^{222}Rn flux densities plotted against the measured (HPGe) ^{226}Ra soil activity concentrations. Only the loamy sand and fine gravel sample types are included in the line of best fit.	28
Figure 25 ^{222}Rn flux densities plotted against the measured (in situ) terrestrial gamma dose rates.	29
Figure 26 Shapefile created in ArcGIS for the 2007–2009 ground survey (grey), flight lines and flight line numbers (black arrows) and individual ground survey points (orange)	31
Figure 27 Variable buffers overlaid on shapefile created in ArcGIS for the 2007–2009 ground survey.	32
Figure 28 Coefficient of determination R^2 obtained between average ground gamma dose rates for varying buffer radii measured in the field and TC measured in 1997 on board the plane	32
Figure 29 Correlation between averaged terrestrial gamma dose rates and the TC (s^{-1}) channel of the 1997 AGS. Buffer radius of 90 m, n=54.	33
Figure 30 Correlation between averaged terrestrial gamma dose rates and eU ($\text{Bq}\cdot\text{kg}^{-1}$) channel of the 1997 AGS. Buffer radius r=90 m, n=54.	33
Figure 31 Buffers (n=29) with even distribution of ground survey points chosen to establish the correlation between the ground survey and the 1997 AGS data. Buffer radius r=90 m	34
Figure 32 Correlation between averaged terrestrial gamma dose rates and the TC (s^{-1}) channel of the 1997 AGS for buffers with evenly distributed ground survey points only. r = 90 m, n = 29	34
Figure 33 Correlation between averaged terrestrial gamma dose rates and eU ($\text{Bq}\cdot\text{kg}^{-1}$) channel of the 1997 AGS for buffers with evenly distributed ground survey points only. r=90 m, n=29.	35
Figure 34 Full extent of the 1997 raster imagery. The total counts of the 1997 AGS are shown, with light colours indicating high values.	35
Figure 35 Averaged eU data ($\text{Bq}\cdot\text{kg}^{-1}$) from the 1997 AGS plotted versus the 1976 eU data (s^{-1}) of the respective grid cell.	36

Figure 36 Shapefiles overlaid on aerial photo of the greater Ranger region (left) and on the counts in the eU channel of the 1976 AGS of the same extent (right). 38

Figure 37 Shapefiles overlaid on aerial photo of Ranger only (left) and on the counts in the eU channel of the 1976 AGS of the same extent (right) 39

Figure 38 Radon activity concentrations measured in air at 30 cm, 50 cm and 150 cm above ground over the Anomaly 2 area for the dry season 2009. 41

Tables

Table 1 Uranium concentrations, terrestrial gamma dose rates ^{226}Ra activity concentrations and radon flux densities determined for orebodies 1 and 3 and background sites from Kvasnicka and Auty (1994)	4
Table 2 Survey parameters of the 1976 Rio Tinto Alligator River geophysical survey	10
Table 3 Survey parameters of the 1997 Rio Tinto Ranger uranium mine AGS flown by World Geoscience Corporation Ltd	11
Table 4 Details of the instruments used for the gamma dose rate surveys at Anomaly 2	11
Table 5 Conversion factors used to calculate ^{238}U , ^{232}Th and ^{40}K activity concentrations and expected terrestrial gamma dose rates from given soil uranium, thorium and potassium concentrations	24
Table 6 Comparison of typical footprints for ground-based and airborne gamma surveys	30
Table 7 Pre-mining mean (95% confidence intervals) external gamma dose rates E [$\mu\text{Gy} \cdot \text{hr}^{-1}$] (including cosmic component), ^{222}Rn flux densities and soil ^{226}Ra activity concentrations in the Ranger area	37
Appendix A1 γ dose rates and in-situ γ -spectrometry results from Anomaly 2 survey (4 pixels at 70 m x 70 m each) conducted 21–24 August 2007.	49
Appendix A2 γ dose rate results from Anomaly 2A survey conducted 21–24 July 2008. Measured values were read off the analogue dial in the field, calculated values used the calibration equation.	53
Appendix A3 γ dose rate results from Anomaly 2B survey (northeast of Anomaly 2A) conducted 1–5 September 2008	67
Appendix A4 γ dose rate results from survey between Anomalies 2A and 2B, and on top of Anomaly 2C (southwest of Anomaly 2A), conducted 8–10 October 2008	77
Appendix B Radon flux density results for individual charcoal canisters deployed during Anomaly 2 survey conducted 14–17 July 2009	88
Appendix C Results of airborne radon activity concentrations [$\text{Bq} \cdot \text{m}^{-3}$] for sites 1A–25A	90
Appendix D Results of soil activity concentrations [$\text{Bq} \cdot \text{kg}^{-1}$] and gamma dose rate measurements [$\mu\text{Gy} \cdot \text{hr}^{-1}$] for sites 1A–25A at Anomaly 2.	92

Executive summary

Ground gamma surveys, radon exhalation and soil ^{226}Ra activity concentration measurements were conducted between 2007 and 2009 over an undisturbed analogue site, Anomaly 2, to the south of Ranger mine. This anomaly exhibits radiation levels that are higher than typical background levels in the region, similar to the outcropping orebodies 1 and 3, that have been mined out between 1981 and 2012. The purpose of the measurements was to groundtruth a historic airborne gamma survey (AGS) that was flown over the area in 1976, before mining started, to be able to determine the pre-mining radiation source term and extrapolate to the whole extent of the AGS including the unmined RPA.

Algorithms were developed to upscale the ground gamma data in ArcGIS to make the spatial resolution comparable to the resolution of the 1976 AGS (300 m line spacing). This was done via an intermediate step, correlating the ground data with data from a higher resolution AGS flown in 1997 by Rio Tinto (100 m line spacing) that also covered the area of Anomaly 2.

The minimum footprint area that can be assessed is set by the optimum buffer radius determined when up-scaling the external gamma dose rates measured on ground to the AGS data. For the current case this is approximately 4 ha. Thus, the correlation models developed allow estimates to be made of the pre-mining baseline gamma dose rates, ^{226}Ra soil activity concentrations and ^{222}Rn fluxes for any selected area larger than 4 ha covered by the 1976 AGS over the greater Ranger area.

Comparison with published data on external gamma dose rates, ^{226}Ra soil activity concentrations and ^{222}Rn exhalation flux densities in the Ranger region before mining started shows that our model estimates are in good agreement with radiation and radionuclide activity levels estimated previously via direct measurement on top of orebody 3 and orebody 1, and from previous environmental radiation surveys.

The GIS model will also allow an estimate of pre-mining uptake of uranium series radionuclides into biota over the footprint of the Ranger mine, assuming secular equilibrium of the radionuclides in soils and using uptake factors determined for bush Tucker in the region (eg Martin et al 1998, Ryan et al 2005, Doering et al in prep). This will facilitate the calculation of pre-mining ingestion doses to humans from the consumption of traditional foods harvested on site, in addition to an estimate of the internal and external radiation doses to wildlife.

Our approach for determining pre-mining radiological conditions can be used at any mine and industrial site where historical AGS data are available and an undisturbed analogue exists to groundtruth the AGS data. Areal extent and thus resources for the ground survey will ultimately depend on the resolution of the historic AGS.

1 Introduction

1.1 Background

1.1.1 Ranger Environmental Requirements

The Environmental Requirements (ERs) for the Ranger uranium mine set out the Commonwealth's environmental protection conditions with which the company (Rio Tinto) must comply. These are conditions of the Authority to mine prescribed substances on the Ranger Project Area, issued under section 41 of the *Atomic Energy Act 1953*. The Primary Environmental Objectives of the ERs are to ensure that World Heritage attributes and biodiversity are maintained and the health of ecosystems and members of the public are protected during operation of the mine, and to rehabilitate the Ranger Project Area to:

an environment similar to the adjacent areas of Kakadu National Park such that, in the opinion of the Minister with the advice of the Supervising Scientist, the rehabilitated area could be incorporated into the Kakadu National Park (Commonwealth of Australia 1999).

With regards to the radiological conditions after rehabilitation of the Ranger Project Area the major objectives are:

stable radiological conditions on areas impacted by mining so that, the health risk to members of the public, including traditional owners, is as low as reasonably achievable; members of the public do not receive a radiation dose which exceeds applicable limits recommended by the most recently published and relevant Australian standards, codes of practice, and guidelines; and there is a minimum of restrictions on the use of the area.

The 'Code of Practice and Safety Guide for Radiation Protection' and 'Radioactive Waste Management in Mining and Mineral Processing' (ARPANSA 2005) are the most recently published and relevant documents for benchmarking the radiation protection objectives of the ERs. The Code

applies to the control of occupational and public radiation exposures, and the management of radioactive waste generated, at all stages of mining and mineral processing from exploration to final site rehabilitation

and provides a regulatory framework

to manage the protection of workers, members of the public and the environment from harmful effects of radiation exposures arising from mining or mineral processing and from the waste resulting from these activities both now and in the future.

The Code specifies a public dose limit of 1 mSv in a year, which is derived from ARPANSA's Recommendations for Limiting Exposure to Ionizing Radiation (2002). In addition, both the Code and Safety Guide make clear that the principle of optimisation of protection is to be applied to radiation practices, including site rehabilitation, to help ensure that the magnitude of individual doses, the number of people exposed, and the likelihood of incurring exposures are kept as low as reasonably achievable, economic and social factors being taken into account.

Natural background sources are generally excluded from regulatory control, and the doses received from natural background sources are not amenable to dose limits. The ERs state that

Radiation doses received from natural background sources or as the result of undergoing medical procedures are not subject to the system and are not to be included in the calculation of radiation doses.

Consequently, radiological conditions in the area before mining commenced need to be established in order to determine the above natural background magnitude of exposure to radiation after rehabilitation of Ranger mine. Such a baseline assessment needs to summarise all potential exposure pathways, which include the terrestrial gamma, the inhalation and the ingestion pathways.

In a high natural background radiation area such as the area around Ranger mine, where uranium orebodies 1 and 3 and several other anomalies are known to exist (Eupene et al 1975, Hegge et al 1980), determining the difference between post-rehabilitation and pre-mining annual radiation doses presents a challenge. Although there are some early studies that assessed the uranium mineralisation that occurred at and around the Ranger ore bodies, these studies were usually focussed on determining the radiation levels and the extent of the outcropping anomaly or orebody (eg Eupene et al 1975), rather than determining an area wide average gamma dose rate or soil uranium activity concentration. In addition, although many pre-mining environmental studies have been conducted (see for example Conway et al 1974) they provide relatively little quantitative radiological data that are spatially referenced appropriately to accurately assess the baseline radiological conditions in the greater Ranger region. Only Kvasnicka (1993) and Kvasnicka and Auty (1994) have reported outcomes from a pre-mining dose assessment for the Ranger uranium mine.

1.1.2 Use of airborne gamma surveys in exploration and site characterisation

Airborne gamma surveys (AGS) coupled with ground truthing surveys have previously been used for area wide assessments of current radiological conditions at rehabilitated and historic mine sites. Martin et al (2006) for example determined the radiological conditions at the rehabilitated Nabarlek mine through extensive groundtruthing of an AGS flown in July 1997 at a nominal line spacing of 100 m and a flying height of approximately 50 m. In 2000, an AGS was flown across the South Alligator River valley at a line spacing and flying height of 50 m (Pfitzner & Martin, 2000). This survey was flown to identify location and magnitude of radiological contamination in the South Alligator River valley from uranium mining and milling activities in the 1950s and 60s and to aid in rehabilitation planning for the area (Pfitzner et al 2001, Bollhöfer et al 2002). At the historic Sleinbeck mine an AGS was flown in August 2002, and geophysical data were collected along 25 m spaced flight lines at an average flying height of only 40 m (Pfitzner et al 2003, Bollhöfer et al 2007a, 2008). A similar tight line spacing of the AGS was used for an assessment of the radiological conditions at the old Rum Jungle mine site in October 2006 (Bollhöfer et al 2007a). This is an unusually tight line spacing but it is required for mine site assessment, where features can be very small in size, often less than 0.1 ha.

In contrast, surveys for mineral exploration are usually flown at a much coarser resolution with a line spacing in the order of 500 m and flying height > 100 m. AGSs were first extensively used for uranium exploration in 1949 in the Northwest Territories of Canada (Darnley 1972). In the Pine Creek Geosyncline, airborne gamma spectrometry has also been the principle tool for uranium exploration (Tucker et al 1980). The Ranger orebodies for example were discovered during an AGS flown in 1969 by Noranda (Australia) (Ryan 1972). Large anomalies were also detected over Nabarlek (Tipper & Lawrence 1972) and Koongarra in 1970 (Foy & Pedersen 1975). The Rum Jungle South uranium orebody was discovered in late 1959 by ground follow-up of weak radiometric anomalies detected by AGSs flown in 1952, 1956 and 1957 (AAEC 1963, Berkemann 1968).

Despite the coarser resolution of AGSs flown for mineral exploration compared to site remediation assessment, the method is still sufficient to detect and qualitatively map landscape scale changes in radiological conditions. An AGS flown in the late 1970s by the Bureau of Mineral Resources for example (1500 m line spacing, 150 m flying height) detected large radiometric anomalies at the former Rum Jungle mines, due to contamination of large areas with uranium bearing material (Tucker et al 1980). Despite this it was not until the late 1990s that AGS were routinely used to assess the radiological status of historical mine sites or other areas contaminated by naturally occurring radioactive material (NORM) residues (eg Winkelmann et al 2001, Coetze et al 2006, Martin et al 2006, Bollhöfer et al 2008).

1.1.3 Existing pre-mining ground data at Ranger

Ryan (1972) and Eupene et al (1975) published qualitative results of an AGS flown by Noranda in 1969 in the greater Ranger region. Contour lines are shown of the total counts measured during that AGS (Figure 1).

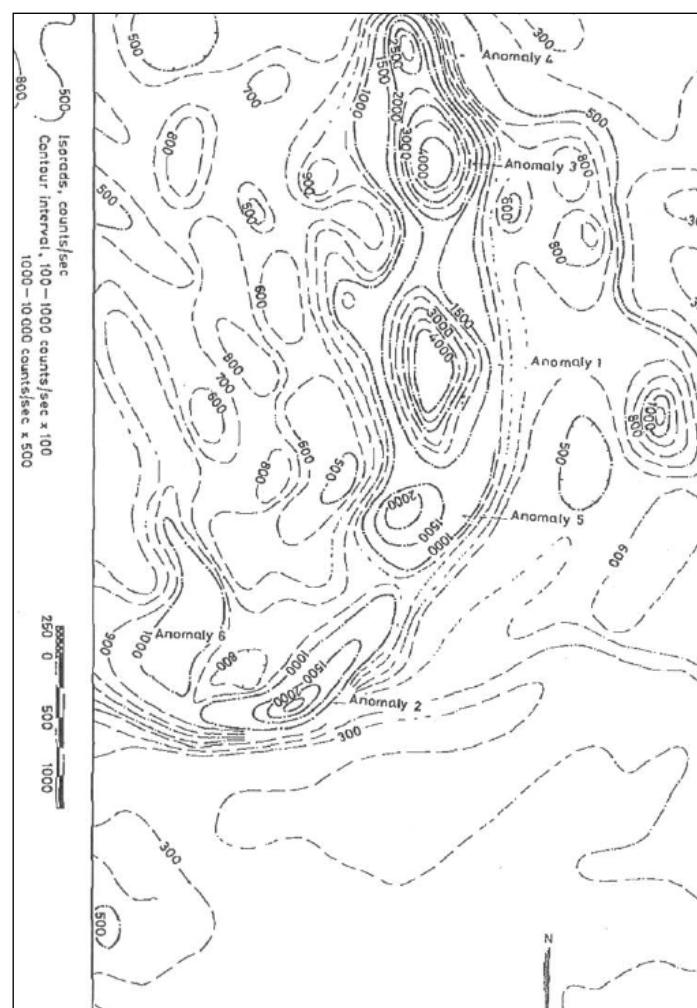


Figure 1 Contours of total counts measured during the 1969 AGS over the Ranger area (Ryan 1972).

Apart from Anomalies 1 and 3 (now pits 1 and 3), the data confirm the location of additional radiological anomalies that exist in the greater Ranger region. Anomaly 4 to the north of orebody 3 is now located within the Djalkmarra land application area and Anomaly 5 is located within the Corridor Creek land application area (see also Bollhöfer et al 2010). The

pre-mining data in particular highlight an existing anomaly to the south of the Ranger lease, which was called Anomaly 2.

Subsequent work on the ground at Ranger focussed on mapping the area and delineating the extent and magnitude of the radiological anomalies, and indicated the possible presence of substantial mineralisation (Eupene et al 1975). The first proposal for mining of uranium in the Alligator Rivers Region came jointly from the then Australian Atomic Energy Commission and Ranger Uranium Mines Pty Ltd for the development of the Ranger deposits (Johnston & Needham in Supervising Scientist 1999). An Inquiry into this proposal, the Ranger Uranium Environmental Inquiry (RUEI), or Fox Inquiry, was set up by the Commonwealth Government in 1975. Although the Inquiry investigated site specific environmental aspects of the proposed Ranger project, little data on the radiation background in the region is given in the two reports. For the lowland surrounding the Ranger prospect, a typical background external gamma dose rate of $0.1 \mu\text{Gy}\cdot\text{hr}^{-1}$ is given.

Data from an assessment of the pre-mining radiation background for the Ranger uranium mine are published in Kvasnicka (1993) and Kvasnicka and Auty (1994). A summary of uranium concentrations, terrestrial gamma dose rates ^{226}Ra activity concentrations and radon flux densities given in these publications is shown in Table 1.

Table 1 Uranium concentrations, terrestrial gamma dose rates ^{226}Ra activity concentrations and radon flux densities determined for orebodies 1 and 3 and background sites from Kvasnicka and Auty (1994).

	U_3O_8 [%]	γ -dose rate [$\mu\text{Gy}/\text{hr}$]	^{226}Ra [Bq/g]	Rn [Bq/ m^2/s]
Orebody 3	$0.037 \pm 0.030^{\text{a}}$	0.58	$1.35 \pm 1.09^{\text{c}}$	$2.5 \pm 2.0^{\text{e}}$
Orebody 1	$0.061 \pm 0.063^{\text{a}}$	0.96 ^b	$2.23 \pm 2.30^{\text{d}}$	$4.1 \pm 3.4^{\text{e}}$
Background		0.06 – 0.08	0.07 – 0.12	0.13 – 0.22 ^e

a: determined from results of U_3O_8 in the top 1 m of core samples from exploratory drilling on the orebodies

b: determined from the ratio of U_3O_8 of orebodies 1 and 3, multiplied by the dose rate measured on top of orebody 3.

c: determined from the measured γ -dose rate on orebody 3.

d: determined from the ratio of U_3O_8 of orebodies 1 and 3 and measured γ -dose rate on orebody 3

e: determined using a radon flux density per radium activity concentration ratio of $1.85 (\text{Bq}/\text{m}^2/\text{s})/(\text{Bq/g})$ measured on orebody 3

1.2 Objective

The objective of this study was to use and groundtruth historic AGS data to retrospectively determine the pre-mining radiological conditions in the greater Ranger region. This required identifying a suitable undisturbed radiological anomaly from the historic AGS data, groundtruthing the AGS data for the anomaly through field measurements and then extrapolating the groundtruthed data for the anomaly to the greater Ranger region.

2 Selection of an undisturbed radiologically anomalous site

2.1 The MODAT database

The Mineral Occurrence Database (MODAT) was developed within the Northern Territory Geological Survey to give spatially accurate point data of known mineral occurrences within the Northern Territory (NTGS 2007). More than 2800 metallic and non-metallic mineral occurrences are currently listed in this database.

The database also provides an overview of radiation anomalies in the Northern Territory and Pfitzner and Martin (2003) have investigated this database with a particular focus on uranium (and thorium) commodities in the Alligator Rivers Region. They have identified 198 known commodities in the Alligator Rivers Region, 164 of which are uranium anomalies of various sizes from 1 tonne to 10000 tonnes of uranium contained in the deposit. These uranium deposits were also classified according to their status.

Operating Mine: significant mineral deposit that is currently being mined.

Abandoned Mine: significant mineral deposit with recorded past production.

Prospect: mineral deposit with an exploration history but no production recorded.

Mineral Occurrence: minor mineral deposit, no production or significant exploration history.

Figure 2 shows the uranium anomalies in the Alligator Rivers Region with some of the anomalies annotated. For more detailed information, refer to Pfitzner and Martin (2003).

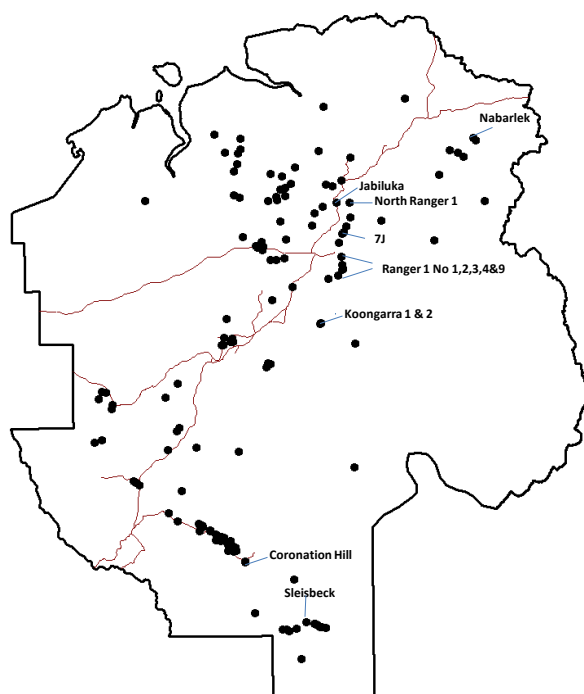


Figure 2 Known uranium (and uranium/gold) anomalies in the ARR (from Pfitzner & Martin 2003).

Ranger 1 No 1 and 3 are examples of an operating uranium mine, the historic Sleinbeck mine and Nabarlek are examples of abandoned (and now rehabilitated) mine sites. The Koongarra, Ranger 1 No 2, 4 and 9 and the North Ranger 1 uranium deposits are examples of known

uranium prospects in the Alligator Rivers Region that have a an exploration history but have no production recorded. As the purpose of this study was to determine pre-mining radiological conditions, it was these types of deposits, deposits that were not disturbed significantly over the past three decades, that were of interest to our project.

2.2 Existing airborne gamma surveys

Existing airborne gamma-ray survey (AGS) data covering the ARR were reviewed in order to evaluate potential undisturbed anomalies that could be groundtruthed as a pre-mining analogue to the Ranger ore bodies.

Some AGS data is available free of charge from the Northern Territory Geological Survey, and Figure 3 shows the extent of the available data in addition to the extent of high resolution AGS data acquired over the rehabilitated Nabarlek mine (Martin et al 2006), the historic Sleinbeck area (Pfitzner et al 2003, Bollhöfer et al 2008), and the upper South Alligator River valley (Pfitzner & Martin 2001, Pfitzner et al 2001a,b). Not the entire Alligator Rivers Region has been surveyed, and only the Koolpin and Alligator River Geological surveys were flown before mining started, in 1974 and 1976, respectively. The Ranger 1 deposits were covered by the Alligator River Geological Survey only.

To avoid correcting for inter-survey differences in resolution, flying height, detector volume and other parameters, ideally the pre-mining AGS data from the Ranger deposits and data from a potential analogue should have been acquired during the same survey, using the same survey specifications and instrumentation. Consequently, it was decided to study the Alligator River Geological Survey in more detail (labelled Alligator in Figure 3) and investigate whether this survey delineated radiation anomalies that may be suitable as a pre-mining analogue for the Ranger 1 and 3 orebodies.

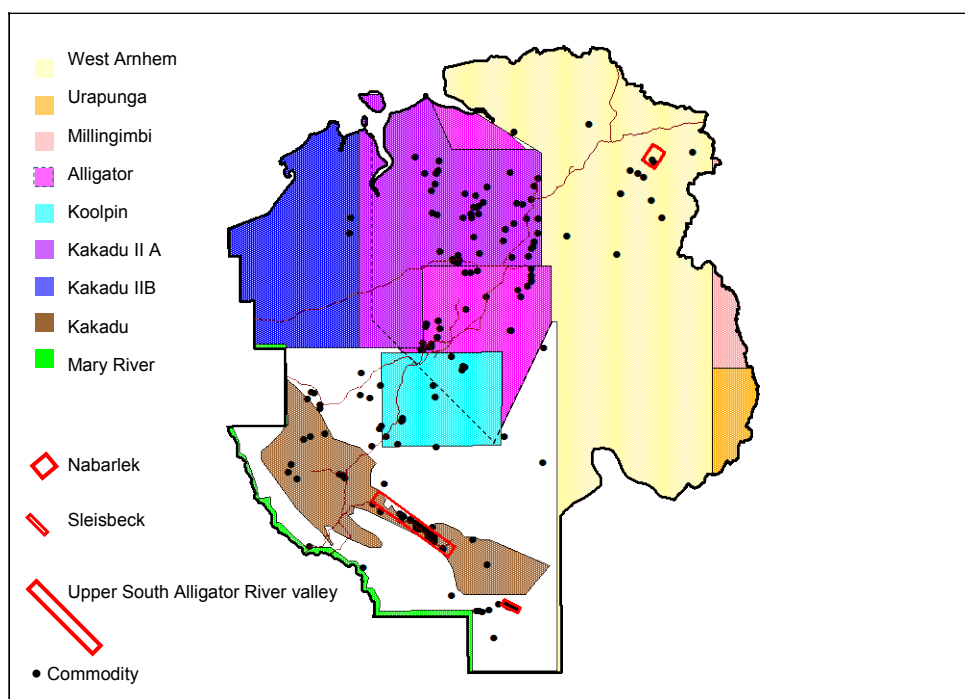


Figure 3 Spatial coverage of the existing AGS data available over the ARR, as available from NTGS (from Pfitzner & Martin 2003).

2.2.1 The Alligator River Geophysical Survey

The *Alligator River Geophysical Survey* was flown in 1976. The 1976 AGS data were acquired from Rio Tinto by the NT Government, and are available on the public domain. Data were re-processed in 2000 by the Northern Territory Geological Survey (NTGS) and then resampled by NTGS at a pixel size of 70 m x 70 m in 2003. These data were acquired by *eriss* from the Northern Territory Geological Survey (NTGS) in 2003, and were re-processed in 2005 and then re-supplied by the Northern Territory Department of Mines and Energy in 2006. Figure 3 shows the coverage of the *Alligator River Geophysical Survey*.

During the conceptual stage of this project, the Koongarra uranium deposit was considered a possible location as a pre-mining analogue for Ranger mine. The deposit was discovered in 1969 during several AGS flown by Noranda Ltd in the Alligator Rivers Region, which also identified other high intensity anomalies in the Ranger ore body 1 region (Ryan 1972, Eupene et al 1975).

Subsequent groundtruthing of the identified anomaly at Koongarra showed a surface radiation anomaly that increased 4-fold in intensity in 3.4 m depth below the surface (Giblin 2004). The uranium mineralisation at Koongarra occurs in two ore bodies separated by about 100 m, with the primary ore mineral being pitchblende (UO_2). Koongarra orebody 1 is covered by a 30 m deep layer of weathered schists (Dickson & Snelling, 1980) with secondary mineralisation present from just below the surface to the base of the weathered zone approximately 25–30 m down. Orebody 2 is about 50 m below the surface with only minor development of secondary mineralisation (Snelling 1980).

A comparison of signal intensity in the 1976 AGS with the location of known uranium occurrences in the MODAT database (Figure 4a) suggested that the signal in the AGS from the Koongarra orebodies was weak (Figure 4b), due to the fact that much of the mineralisation of the Koongarra deposit is covered by superficial sands, sometimes several metres thick. Consequently, the gamma signal from the uranium ore body is attenuated and weak at the surface and the signal measured on board the plane is small. It is important to note that generally, the gamma signal measured in air originates from radionuclides located in the top 0.5 m of the soil, while deeper lying radionuclides only contribute a few percent or less (depending on photon energy) to the signal (ICRU 1994, Saito & Jacobs 1994).

In contrast, Ranger 1 Anomaly 2 to the south of the Ranger lease is outcropping in places and characterised on ground by three strong separate radiometric anomalies (Hegge et al 1980). It also exhibits a strong airborne gamma signal in the 1976 data, as can be seen in Figure 4b. Anomaly 2 has been excluded from the Ranger Project Area, following the recommendations of the Ranger Uranium Environmental Inquiry in 1975. Although some drilling occurred on the anomaly (Ryan 1972), it is largely undeveloped.

In Figure 5 (left) radiation contours published in Eupene et al (1975), which show the total counts acquired during the 1969 Noranda airborne survey of Ranger, are overlaid on the airborne gamma data from the 1976 Alligator Rivers Geophysical Survey. In Figure 5 (right) the pre-mining 1976 airborne signal in the Ranger vicinity by extent and intensity (top 70% of values found in Ranger subset are shown coloured) is overlaid on the land surface image acquired by the IKONOS satellite in 2001 (from Esparon et al 2009). Based on the assessment of the historical AGS data it was decided to obtain groundtruthed data in the greater region of Anomaly 2 and to achieve this objective, an extensive fieldwork program to the south of the Ranger lease was commissioned in 2007.

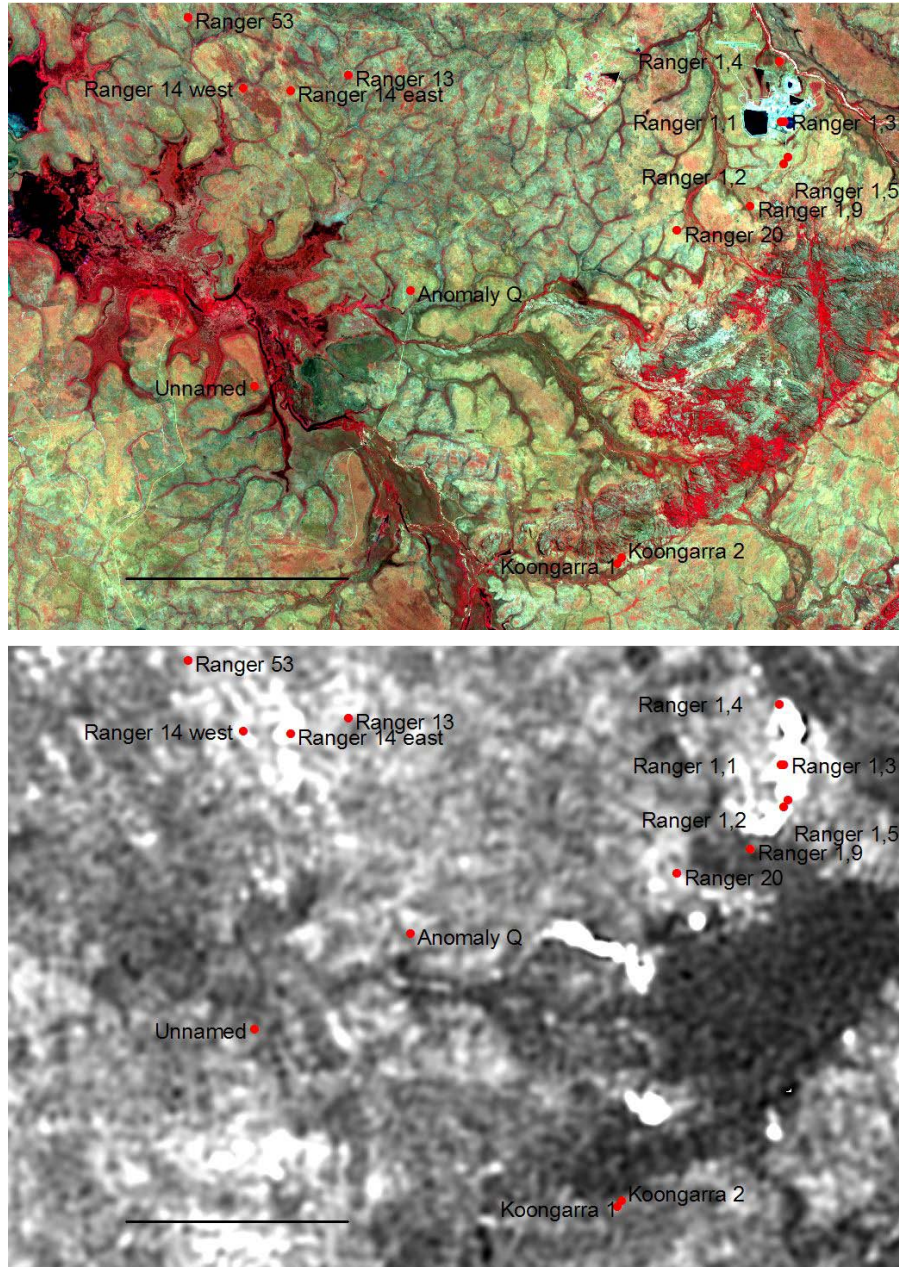


Figure 4 (a) Ikonos satellite data (2001, displayed as false colour composite) subset shown in Figure 3 and (b) corresponding 1976 equivalent uranium (eU) AGS raster data, with MODAT uranium anomalies overlaid. Light colours in (b) indicate a high intensity signal in the eU channel. Note the dark colour in the Koongarra region.

2.2.2 1996 Rio Tinto Airborne Gamma survey

In 2008 AGS data was made available to SSD by ERA. This AGS was commissioned by ERA and flown by World Geoscience Corporation Ltd in 1997, 20 years after the Alligator Rivers Geophysical Survey, at a lower flying height and a higher spatial resolution than the 1976 survey. The survey covered the Anomaly 2 area and it was considered appropriate to investigate whether data from that survey could be used for groundtruthing of the 1976 AGS as well. Initially, the data was used to delineate the exact location of the Anomalies.

Figure 6 shows the extent of the 1997 AGS. Although the survey included all of the active mining area, including the land application areas and Jabiru East, only the total counts (TC) data measured on board the plane to the south of the lease are shown, with the red colour

indicating count rates above 13 500 counts per second. The locations of Anomalies 2A and 2B are clearly visible in this image.

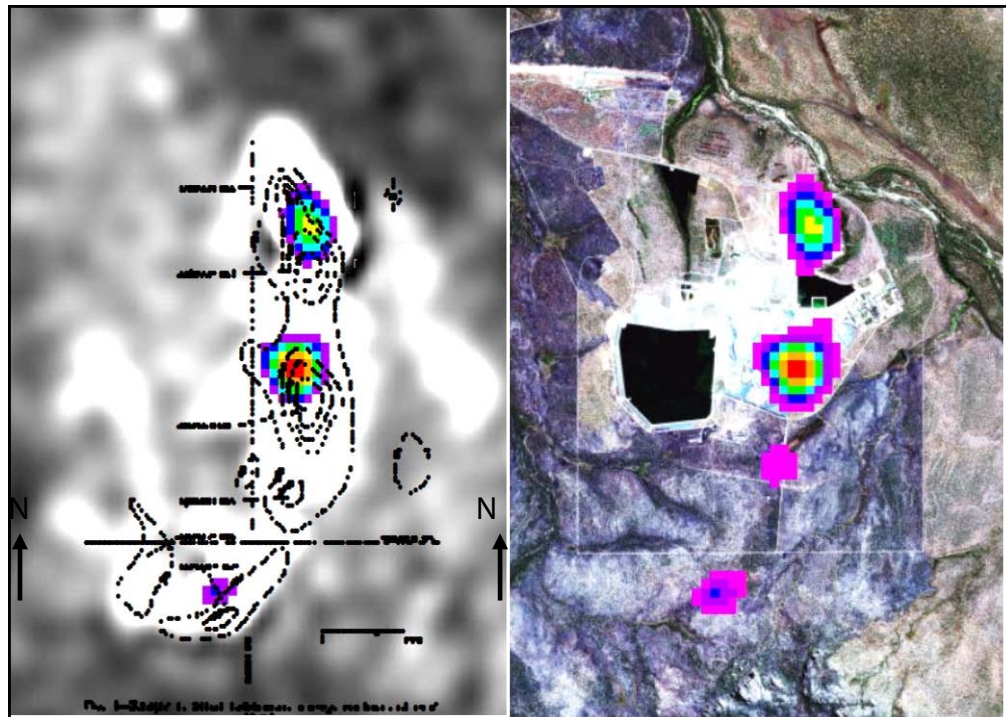


Figure 5 Eupene et al (1975) map of aerial radiometric contours of total count (TC) overlaid on airborne data (left) from the 1976 AGS. In addition, 1976 TC data with the top 70% of the values coloured are overlaid on an IKONOS (2001, displayed as true colour) optical satellite image on the right.

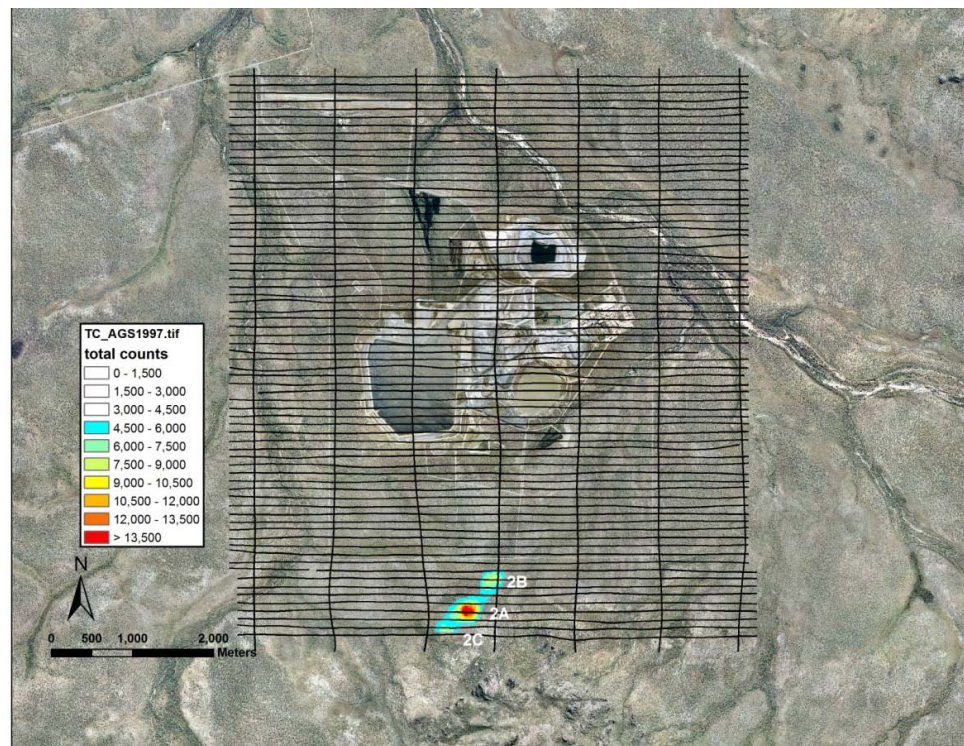


Figure 6 Extent and flight lines of the 1997 Rio Tinto airborne gamma survey, overlaid on an aerial photograph from March 2007. Only the total counts measured during the AGS south of the Ranger lease are shown. Anomalies 2A and 2B are clearly visible. A third Anomaly, 2C, lies to the southwest of Anomaly 2A.

3 Methods

3.1 1976 airborne gamma survey specifications

Figure 3 shows the coverage of the *Alligator River Geophysical Survey* overlaid on Ikonos satellite data from the Alligator Rivers Region. The survey was flown in 1976 by *Geometrics*, and, both magnetic and radiometric data were acquired. The data was then obtained by the Northern Territory Geological Survey from Rio Tinto in September 2000. Data were processed by the NTGS and supplied to *eriss* in 2003. Data were then re-processed in 2005 for the Northern Territory Geological Survey by Intrepid Geophysics, separated into magnetic and radiometric files and the flight direction added, and re-supplied to *eriss* in 2006.

Although the NTGS data has had a height correction applied (the digital numbers have changed from integer to floating point) no height information is available. There is no documentation on how the data was re-processed apart from the fact that the radon has been stripped (in the ‘reprocessed’ column), whereas the ‘original’ column has only been stripped of the noise. Radon was not stripped point by point but rather an average has been stripped as a result of radon in air on the overall image. The ‘reprocessed’ column also probably had some levelling applied (for the high frequency noise) (R Clifton, NTGS, pers comm). The algorithms applied to correct the data in the reprocessed columns are, however, not known.

Table 2 shows a summary of the known survey parameters. There is no information available on the specifications of the NaI detector on board the plane. Readings for radiometrics were taken every second and raw counts per second in the equivalent uranium (*eU*), equivalent thorium (*eTh*), potassium (K) and total count (TC) were measured. Line data were then processed and raster data were produced with a pixel size of 70 m x 70 m.

Table 2 Survey parameters of the 1976 Rio Tinto Alligator River geophysical survey.

Survey parameter	
Survey date	1976
Flight line direction	030 – 210
Line spacing	300 m
Flying height	unknown
Total km flown	21700 (approx)
Counts reported	TC, <i>eU</i> , <i>eTh</i> , K
Spectrometer	Unknown
Volume	Unknown

3.2 1997 airborne gamma survey specifications

ERA has made available data from an AGS flown in 1997 by World Geoscience Corporation Ltd over the Ranger area, including Anomaly 2. Table 3 shows a summary of the survey parameters of the 1997 Rio Tinto AGS.

3.3 Ground truthing

3.3.1 Gamma dose rate measurements

Gamma dose rates were measured using three environmental dose rate meters. The details of the three instruments (GM1, GM2 & GM3) are provided in Table 3. GM1 has been calibrated by Australian Radiation Services Pty. Ltd in June 2006, April 2008 and December 2010. Results of the calibration showed that the environmental dose rate meter operated within its specifications.

Table 3 Survey parameters of the 1997 Rio Tinto Ranger uranium mine AGS flown by World Geoscience Corporation Ltd.

Survey parameter	
Survey date	July – August 1997
Flight line direction	090 – 270
Line spacing	200 m
Flying height	50 m
Total km flown	Unknown
Counts reported	eU, eTh, K, TC
Spectrometer	256 channel PGAM-1000
Volume	33.56 litres

The Mini-Instruments Environmental Meter Type 6-80 have both an analogue display giving the measured dose rate in $\mu\text{Gy}\cdot\text{hr}^{-1}$ and a digital display of counts in a pre-selected time, usually 100 s. Gamma dose rates can be calculated from the measured count rate. GM2 and GM3 were cross calibrated against GM1 at three areas that exhibited gamma dose rates between 0.1 and 1 $\mu\text{Gy}\cdot\text{hr}^{-1}$ and the values for the corrections factors applied to the measured count rates are shown in Table 4.

Table 4 Details of the instruments used for the gamma dose rate surveys at Anomaly 2.

	GM1	GM2	GM3
Description	Environmental dose rate meter		
Manufacturer	Mini-instruments		
Model	6-80	6-80	6-80
Serial number	01065	01064	01049
Correction factor (Aug 07 – Sep 08)	0.92 ± 0.04	0.92 ± 0.02	
Correction factor (Oct 2008)	1.01 ± 0.02	0.97 ± 0.02	

3.3.1.1 August 2007

Initially, four 70 m x 70 m pixels of the 1976 AGS were surveyed using GM1. It was planned to take measurements within a pixel characterised by low counts in the AGS (background), on Anomaly 2A and 2B and between the two anomalies. Following recommendations made in ICRU Report 75 (2006), gamma dose rates were measured at 40 random points within each of those 70 m x 70 m pixels, and the average dose rates for each 70 m x 70 m area was determined.

160 gamma dose rates and in-situ soil activity concentrations were measured. GPS readings were taken at each measurement site for all gamma dose rate and soil activity concentration surveys. Figure 7 shows the locations of gamma dose rate measurements. Figure 8 shows a

close up of Anomaly 2 and the location of the gamma dose rate measurements taken in 2007 and 2008, overlaid on the total counts measured during the 1997 AGS of the area.

3.3.1.2 July 2008

A gamma dose rate survey was conducted over the main Anomaly (Anomaly 2A) in July 2008. The purpose of this survey was to delineate the exact position and the extent of Anomaly 2A. The line spacing of the survey was approximately 15 m, and the distance between measurement points approximately 10 m. An area of approximately 9 ha was surveyed and 663 gamma dose rates measured.



Figure 7 Location of the 2007–08 ground gamma survey points.

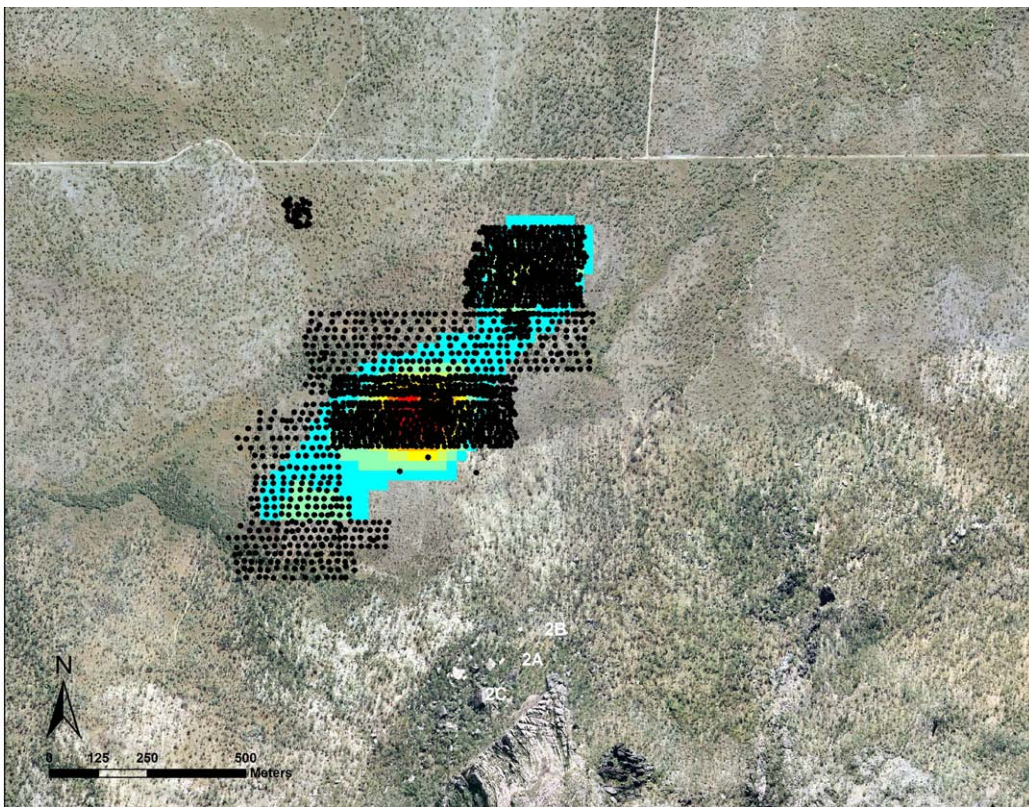


Figure 8 Location of the 2007–08 ground gamma survey points overlaid on the total counts signal above Anomaly 2 from the 1997 AGS.

3.3.1.3 September 2008

A gamma dose rate survey was performed in September 2008. This survey aimed to delineate the exact position and the extent of Anomaly 2B which is located to the north of Anomaly 2A. The line spacing was approximately 10 m with measurements taken at 10 m intervals. An area of approximately 6.6 ha was surveyed and 491 dose rate measurements taken.

3.3.1.4 October 2008

A fourth gamma dose rate survey was performed in October 2008, to fill in the area between Anomalies 2A and 2B, and to extend the area surveyed to the south west of Anomaly 2, to delineate the intensity and position of a third Anomaly, which will be called Anomaly 2C. The survey extended to a small tributary to Gulungul Creek, which can be seen on Figure 8 just south of Anomaly 2A. In this survey 533 measurements were taken.

3.3.2 Radon flux density measurements

Radon gas is produced in rock or soil grains from the decay of ^{226}Ra to ^{222}Rn through alpha decay. Radon then exhales from the ground into the atmosphere. Radon exhalation is a two-step process. First, a small quantity of the total radon produced in the ground emanates from the rock or soil grain surface into the soil gas. In the second step, a fraction of the radon gas diffuses to the ground surface and exhales from the soil into the air above (see for example Porstendorfer 1994, Lawrence 2005, Akber et al 2011).

Emanation from the solid grain into the soil gas depends on various factors, such as: the ^{222}Rn production rate (which depends on the ^{226}Ra activity concentration), the distribution of ^{226}Ra within the grain (production near the surface leads to higher probability of escape into soil

gas), and the grain size (the smaller the grain the higher is the surface area to volume ratio and emanation coefficients increase).

Exhalation of radon from the soil gas to the surface also depends on a number of variables including soil porosity and permeability, soil thickness, soil moisture, precipitation, wind velocity, barometric pressure and temperature (Porstendorfer 1994). Porosity facilitates radon exhalation and disturbing the soil allows any trapped radon to escape. Deeper layers of the soil make a decreasing contribution to surface exhalation but typically radon can reach the surface from depths of several meters. An estimate of diffusion length for 100 µm dry grain size material is 2 – 2.5 metres and a typical value for soil is 1.5 m (Porstendorfer 1994). Radon exhalation also has a complex dependence on soil moisture – values increase as the moisture content increases from dryness, and then decrease to nearly zero as soil moisture approaches saturation (Lawrence 2005, Lawrence et al 2009).

3.3.2.1 Deployment of radon cups

Radon flux density can be measured by trapping the radon that exhales from the ground surface in canisters filled with activated charcoal. The charcoal canisters used in this study were brass cylindrical design ('radon cups') with an internal diameter of 0.061 m. If the 'open face' of a brass charcoal canister is sealed against a surface, then all the radon emanating from the surface will diffuse into the canister and be adsorbed onto the charcoal. Deployment of a number of radon cups provides simultaneous measurements of numerous locations and was the method of choice for the Anomaly 2 survey. The radon flux density over the period of exposure can then be estimated using:

$$J = \frac{R \cdot t_c \cdot \lambda^2 \cdot \exp(\lambda t_d)}{\varepsilon \cdot a \cdot [1 - \exp(-\lambda t_e)] \cdot [1 - \exp(-\lambda t_c)]} \quad (1)$$

where J (Bq·m⁻²·s⁻¹) is the average radon flux density, R is the net count rate (s⁻¹) – after background subtraction – obtained during the counting period t_c (s), λ (s⁻¹) is the decay constant for radon, t_d (s) is the delay period from the end of exposure to the beginning of the counting interval, ε (s⁻¹·Bq⁻¹) is the counting efficiency of the system, a (m²) is the area of the canister, t_e (s) is the period of exposure of the charcoal in the canister (Spehr et al 1983).

The derivation of equation 1 is based on a number of assumptions (Bollhöfer et al 2005) including that the radon exhalation from the ground is constant over the exposure period. Existing data indicate that diurnal variations in ²²²Rn flux densities in the Alligator Rivers Region are small (Todd et al 1998, Lawrence et al 2009), and so the assumption of constant radon flux densities is reasonable. In addition, our data are not corrected for the effects of water vapour uptake by the charcoal. Provided that adsorption of gases (primarily water vapour) does not lead to saturation of the charcoal, as is the case during the dry season, all of the radon exhaled is adsorbed on the charcoal, and no correction for humidity is required.

The charcoal canisters contain 25 grams of charcoal retained behind a wire mesh. Prior to deployment the cups are heated overnight at ~110° C to drive out any residual radon and water adsorbed on the charcoal.

Radon flux density was measured over the extent of Anomaly 2 in July 2009 at 25 locations. The locations of the sampling points are shown in Figure 9. Three radon cups were deployed at each location on 14 July 2009 and collected after a period of three days. The locations are shown in Figure 9. To prevent leakage of radon around the edge of the canisters they were embedded in the earth to a depth of about 1 cm or, if the surface was too hard or irregular, the rim was sealed with mud or a 'putty'. There was no rainfall during the deployment period.

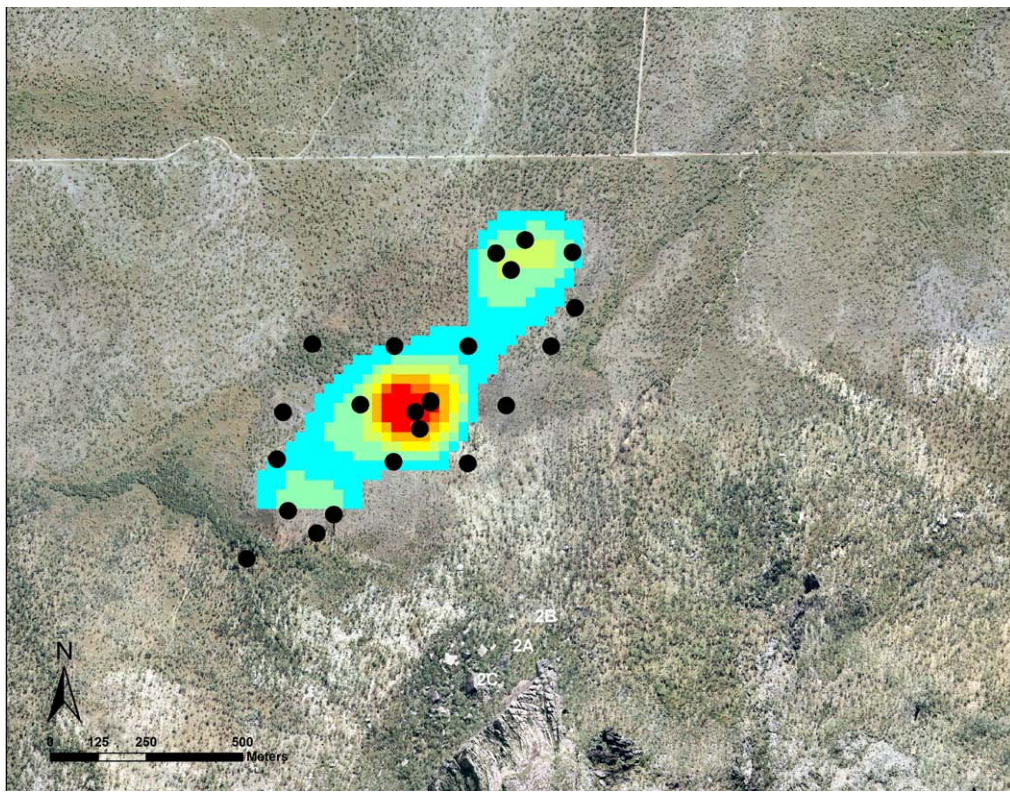


Figure 9 Location of the radon exhalation sampling points overlaid on the total counts signal above Anomaly 2 from the 1997 AGS.

3.3.2.2 Setup of counting system

A NaI gamma spectrometer, housed in a lead castle to reduce background, at the *eriss* laboratories in Darwin was used to determine the activity of radon decay products adsorbed on the charcoal. Each radon cup was counted for 600 s. Four regions of interest (ROI) representing the photopeaks for ^{214}Pb at 242, 295 and 353 keV and for ^{214}Bi at 609 keV were used to determine the activity of radon progeny adsorbed onto the charcoal. The net count rate R was obtained by subtracting the background count rate from the gross count rate in those regions of interest.

The system was calibrated against a charcoal canister of known ^{226}Ra activity. This calibration canister was prepared using twenty-five grams of charcoal and a solution containing 327 Bq activity of ^{226}Ra that was carefully added to the canister (Bollhöfer et al 2005). The canister was sealed after the solution had dried and, after delay of 25 days to allow ^{222}Rn to reach secular equilibrium with ^{226}Ra , was counted several times to obtain a statistically robust measurement of counting efficiency. The average counting efficiency was $10.6\% \pm 0.2\%$.

The procedure for counting radon cups includes a delay of at least 3 hours between the collection of the canisters and the start of the count period to allow the progeny, ^{214}Pb (half-life 27 mins) and ^{214}Bi (half-life 20 mins), to in-grow towards a secular equilibrium with their progenitor, ^{222}Rn (half-life 3.82 days).

3.3.3 Radon in air measurements

The activity concentration of radon in air [$\text{Bq}\cdot\text{m}^{-3}$] was measured using track etch detectors supplied by Radiation Detection Systems (*RDS*), Adelaide. Two track etch detectors were

deployed at about 1.5 m height above ground for 3 months (14 July to 22 October 2009) at each radon exhalation measurement location (1A to 25A). A small shade made of polystyrene was attached to the track etch detectors to avoid the track etch detector housing from exposure to direct sunlight. At 6 locations (sites 3A, 13A, 14A, 15A, 17A, 21A) two additional track etch detectors were deployed each at 30 cm and 50 cm height, respectively, to determine radon concentrations for a person lying down or sitting on the ground. Durrani and Ilic (1997) describe in detail the methodology of radon measurements using track etch detectors.

3.3.4 Soil activity concentration measurements

3.3.4.1 In-situ soil activity concentration measurements

Soil activity concentrations were measured with a 512 channel portable NaI gamma detector (*Geofyzika*, now *SatisGeo*, model GS-512) during the August 2007 gamma survey at each gamma dose rate measurement point. Measurements were taken for 600 seconds, 1 metre above ground using a tripod as shown in Figure 10.

The GS-512 displays and stores the concentrations of K, U, Th in %, or mg kg^{-1} respectively. It is assumed that ^{226}Ra is in secular equilibrium with ^{238}U , and the uranium measurements are generally reported as equivalent uranium ($e\text{U}$). However, it is the ^{226}Ra activity concentration that is determined, using the ^{214}Bi gamma rays detected at 1.73-1.76 MeV as a proxy for ^{226}Ra , rather than measuring uranium directly. Data for ^{40}K (1.46 MeV) and the thorium-series radionuclide ^{208}Tl (2.31 MeV) as a proxy for ^{232}Th were also obtained and are reported in Appendix A1.

Spectra are stored in the 512 channels of the GS-512 spectrometer. K, U and Th concentrations are determined by so called stripping (IAEA, 1989), through a matrix multiplication of the count rates with pre determined calibration constants. The instrument was calibrated in October 2003, and its stability was tested regularly by measuring the activity concentration on a test spot at the Darwin laboratories.

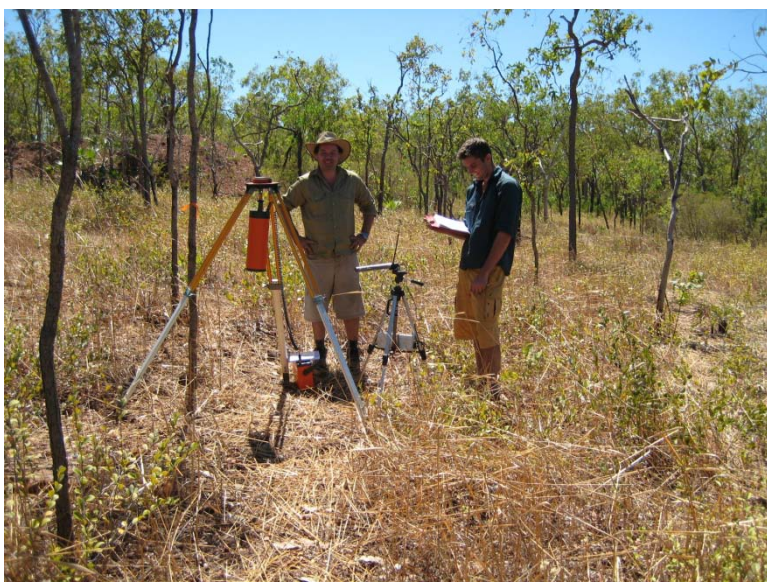


Figure 10 Set up of the GS-512 field gamma spectrometer.

A ^{137}Cs source located in the instrument is used to establish the position of the regions of interest for $e\text{U}$, $e\text{Th}$ and K by reference to the 661.6 keV gamma peak of ^{137}Cs . At locations with high uranium concentrations the instrument failed to stabilise the spectrum due to interference from lower energy peaks of ^{214}Bi with the location of the ^{137}Cs peak, and

Compton scattering originating from the decay of uranium series radionuclides, and no results were obtained.

The internal memory of the GS-512 allows to store 4300 readings of 4 window ROI data or 200 complete 512 channel spectra. After each day of measurements, the spectrum data were downloaded to a computer hard drive.

3.3.4.2 Laboratory soil activity concentration measurements

Soil samples were taken from the 25 locations where radon flux densities were determined in July 2009. At each flux density site (sites 1A to 25A), the top 2 cm of soil was sampled at 5 random locations within 1 m of the deployed radon cups and the 5 samples were combined in a plastic bag. Samples were then transported to Darwin for radionuclide analyses.

^{238}U , ^{226}Ra , ^{228}Ra , ^{228}Th , ^{210}Pb and ^{40}K activities in the samples were determined using the High Purity Germanium (HPGe) gamma detectors from the Environmental Radioactivity section at *eriss*. An in-house program is used for analysis of sample activity concentrations (Esparon & Pfitzner 2010, Pfitzner 2010). Details of the gamma spectrometry methods are described in Murray et al (1987) and Marten (1992). Procedures for sample collection, preparation and measurements of radionuclide activity concentrations via gamma spectroscopy at the Environmental Radioactivity laboratory are described in Marten (1992).

The stability and background of the detectors is checked weekly with a multi isotope standard containing radionuclides of the uranium and thorium decay chains and a blank matrix (empty container), respectively. Detection limits for soil samples using gamma spectrometry are dependent on sample size, detector efficiency and background count rates of the given nuclide, but were typically $\sim 3 \text{ Bq}\cdot\text{kg}^{-1}$ for ^{226}Ra for a one day count in the present study.

4 Results

4.1 1976 airborne gamma survey data

Figure 11 shows the results of the counts in the uranium channel over the whole of the 1976 AGS, overlaid on an aerial photo mosaic of Kakadu National Park from 2004. The locations of Ranger orebodies 1 and 3, and Anomaly 2 are clearly visible in the 1976 AGS data. A subset of the uranium channel data, only including count rates above 250 counts per second, is overlaid on the Ranger region photo in Figure 12 and on the Anomaly 2 photo in Figure 13.

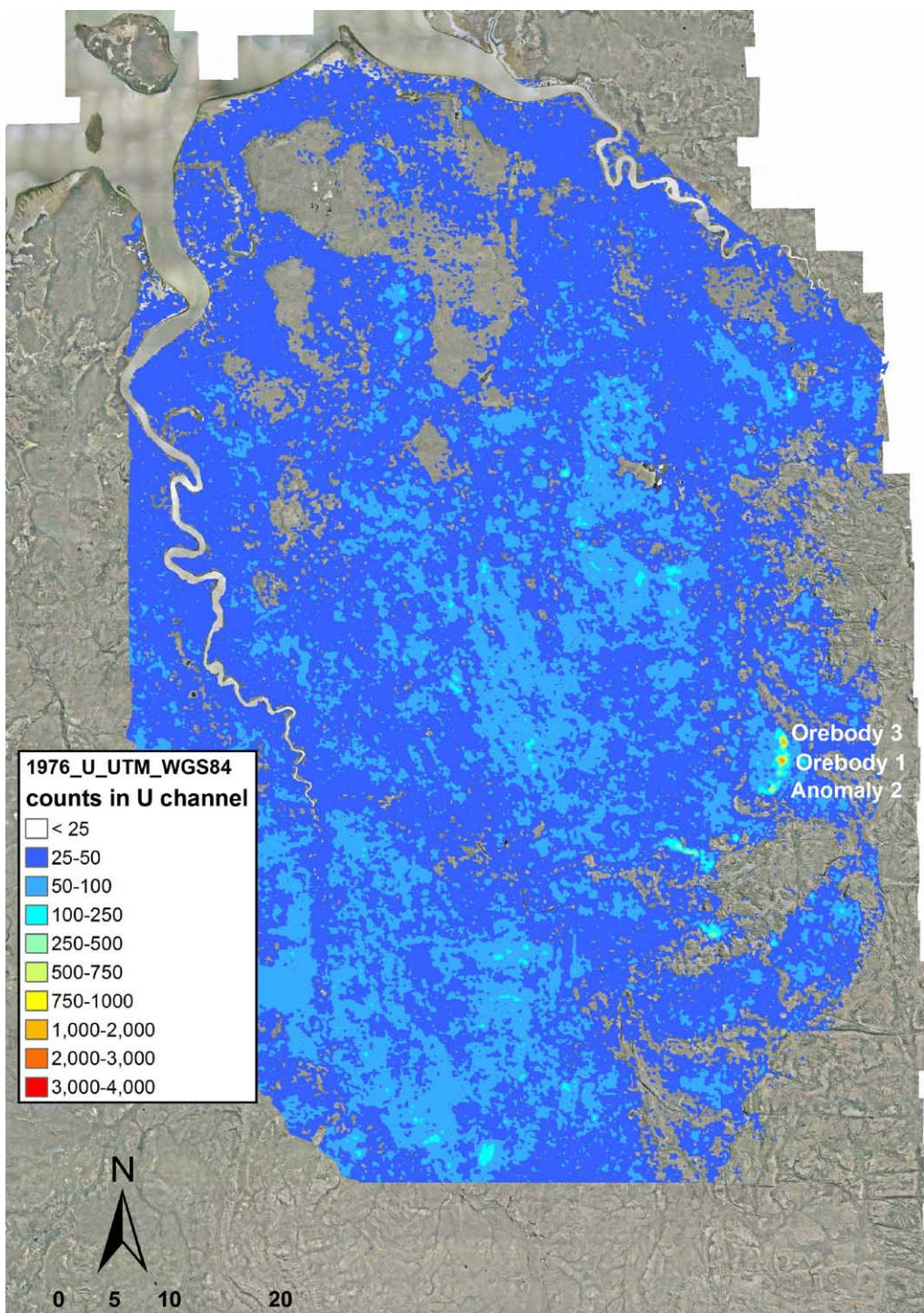


Figure 11 Counts (> 25 counts per sec) in the uranium channel of the 1976 AGS over the whole scene.

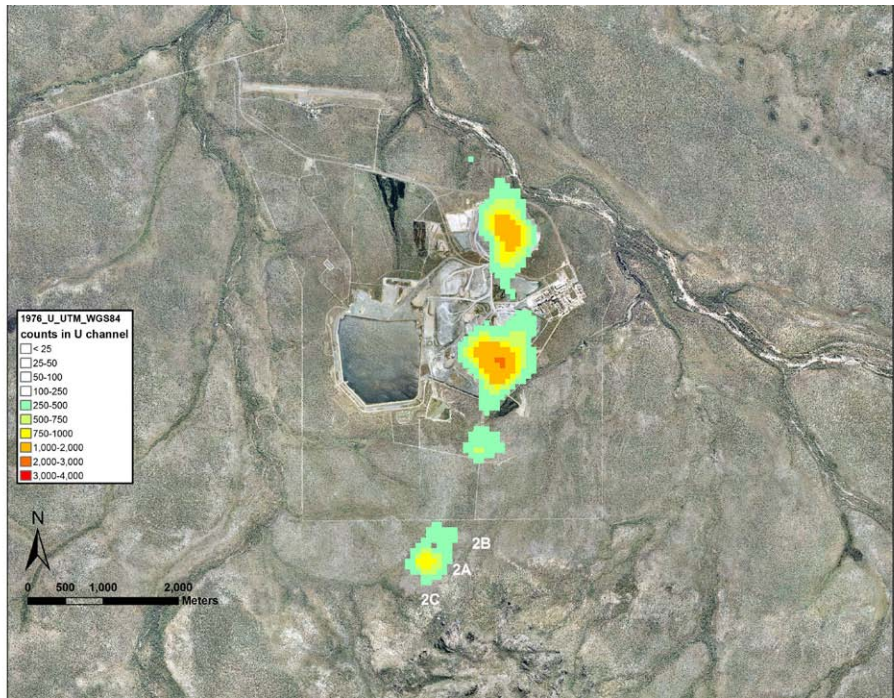


Figure 12 Counts (>250 counts per second) in the uranium channel of the 1976 AGS over the Ranger mine region.

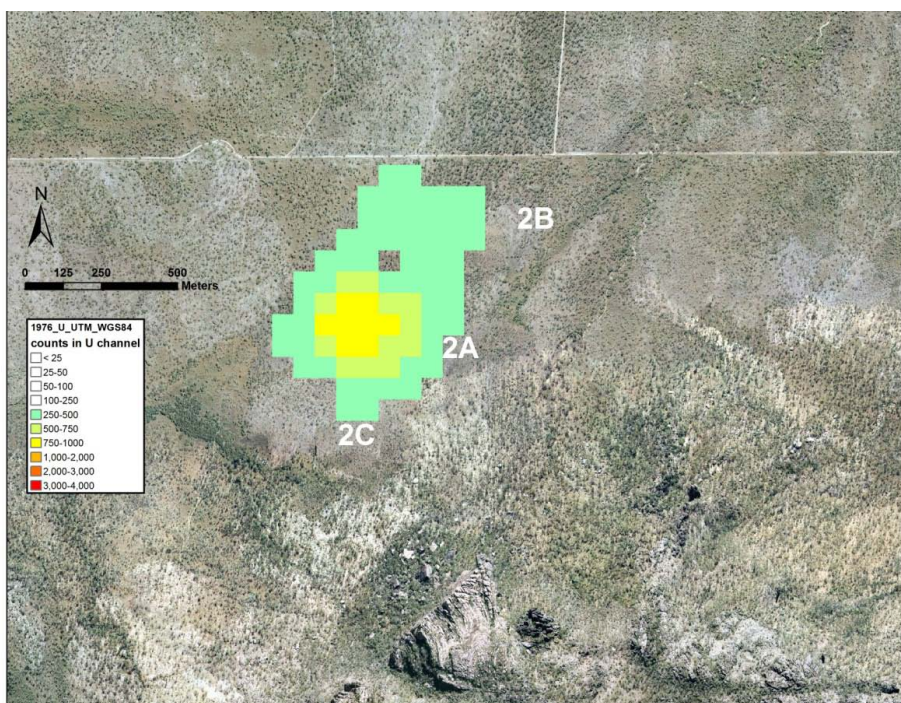


Figure 13 Counts (>250 counts per second) in the uranium channel of the 1976 AGS over Anomaly 2.

4.2 1997 airborne gamma survey

Figure 14 shows the results of the total counts measured south of the Ranger lease over Anomaly 2 during the 1997 AGS flown by Rio Tinto. It appears that an additional Anomaly is present (labelled Anomaly 2C) to the south of Anomalies 2A and 2B, in agreement with Hegge et al (1980) who stated that Anomaly 2 to the south of the Ranger lease is outcropping in places and characterised on ground by three strong separate radiometric anomalies.

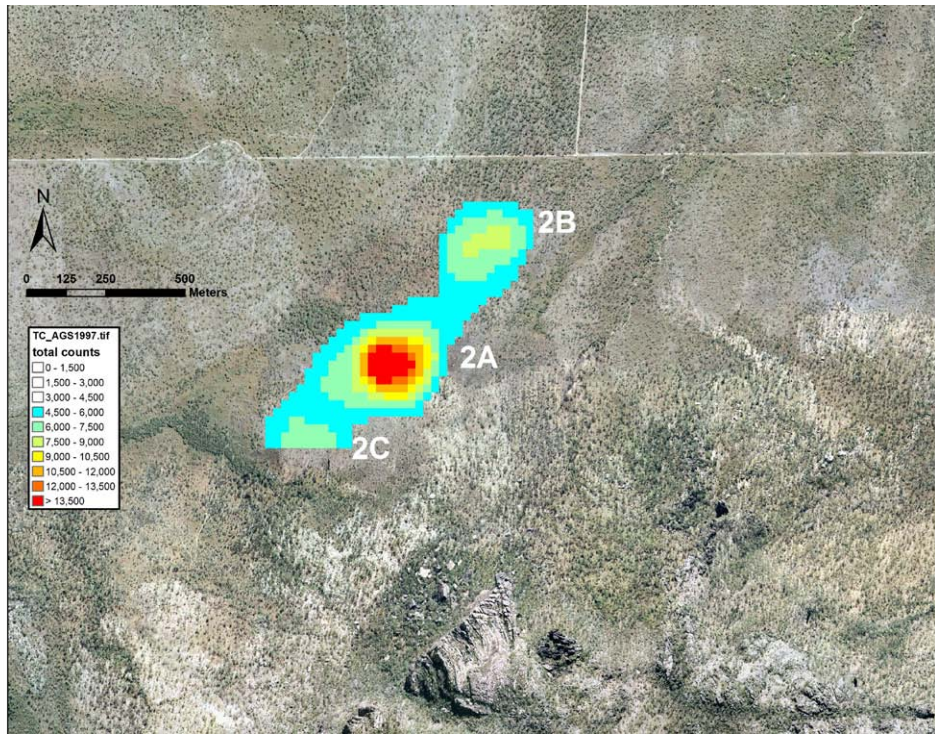


Figure 14 Counts (>4500 counts per second) in the TC channel of the 1997 AGS over Anomaly 2.

4.3 Gamma dose rates measured in the field

Figure 15 shows the results of the field gamma dose rates (in μGyhr^{-1}) measured in the region of Anomaly 2 between 2007 and 2009. The three separate radiation anomalies identified by AGS are clearly visible on the ground. Results are tabulated in Appendices A1–A4. Results of individual measurements are tabulated in Appendices A1–A4.

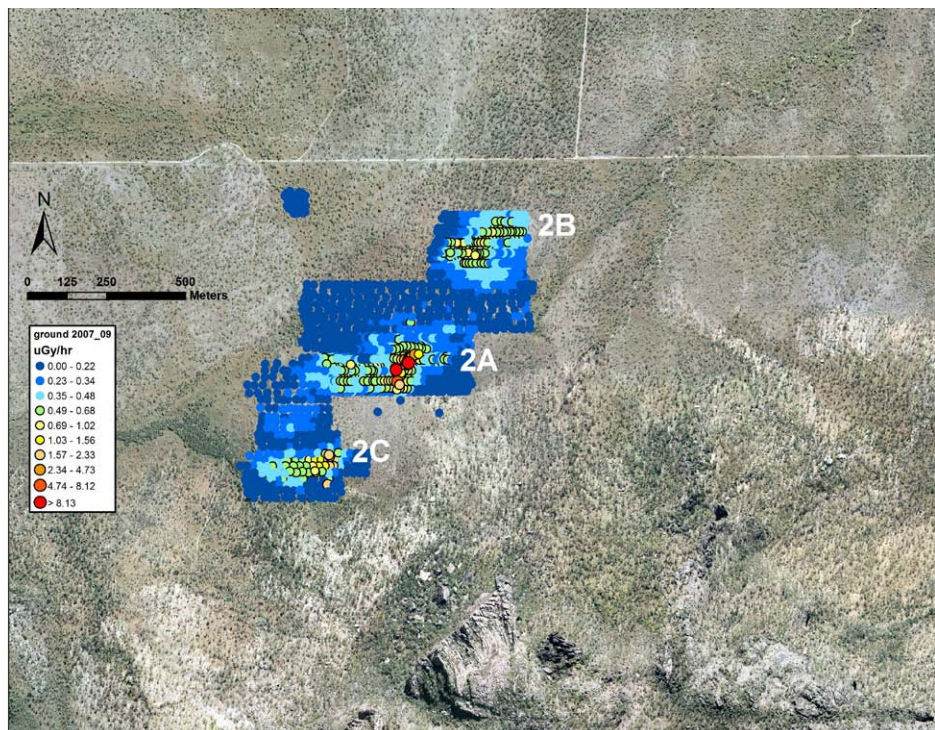


Figure 15 Field gamma dose rates measured over Anomaly 2 between 2007–09.

4.4 Radon

4.4.1 Radon flux densities

Figure 16 shows the geometric means of the three individual radon flux density measurements at sites 1A to 25A, colour-coded according to the magnitude of the calculated radon flux density (in $\text{mBq}\cdot\text{m}^{-2}\cdot\text{s}^{-1}$). Results for the individual sampling points and GPS locations of the sites are given in Appendix B.

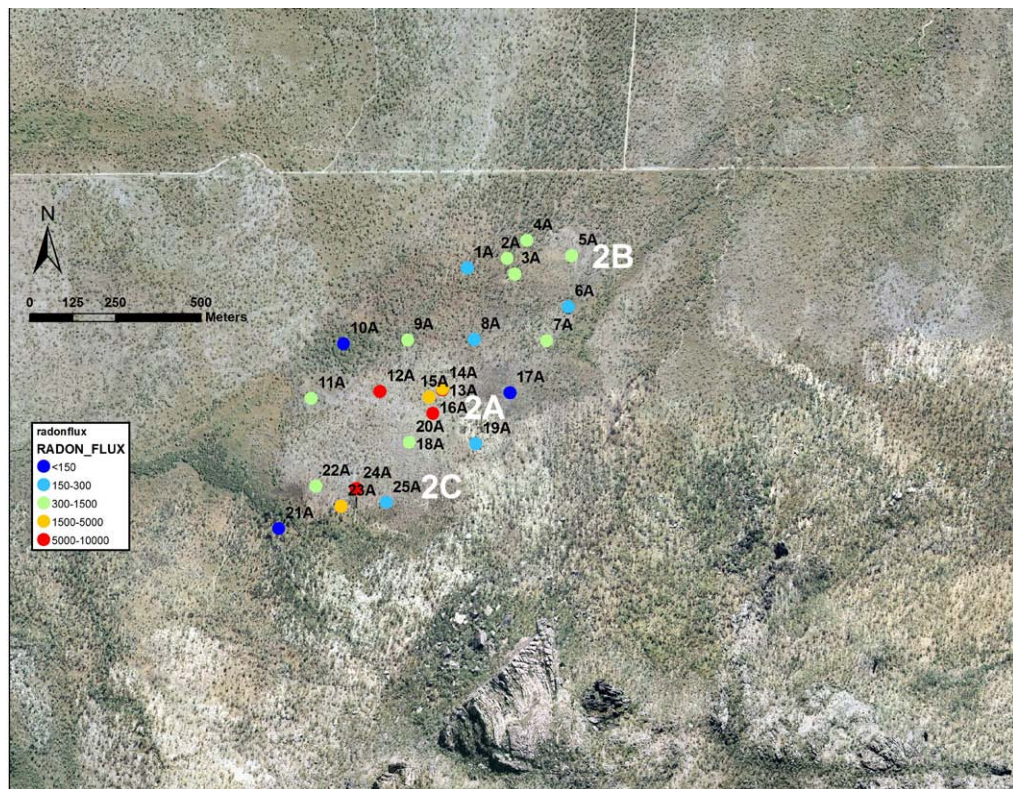


Figure 16 Radon flux densities measured over the Anomaly 2 area between 2007–09.

Higher radon flux densities were measured on top of the Anomalies, with the highest radon flux density of $\sim 10 \text{ Bq}\cdot\text{m}^{-2}\cdot\text{s}^{-1}$ measured at site 13A immediately on top of the Anomaly. This site is dominated by coarse gravel of a few centimetres thickness overlying rock strata. Similar soil morphology was encountered at sites 14A and 15A, where a relatively thin layer of gravel and sand, respectively, was overlying rocky terrain. Site 12A was located in a small depression, where fine gravel had accumulated, most likely erosion products from the nearby higher activity soil of Anomaly 2A.

4.4.2 Radon activity concentration in air

Typical uncertainties for individual radon activity concentration results provided by RDS are 40% (Kvasnicka, pers comm). Averages and standard deviations for the two radon activity concentration results per site were calculated. All calculated averages had a relative standard deviation of less than 100%, however, from a total of 37 averages calculated at Anomaly 2, 6 averages exhibited a relative standard deviation above 57% (which is the combined uncertainty of the individual measurements). Typical relative standard deviation of two track etch detectors deployed at the same site was 25%. Results of individual and site averaged radon activity concentrations are tabulated in Appendix C.

The maximum radon activity concentration in air 1.5 m above ground was 430 Bq·m⁻³ measured at site 14A in the immediate vicinity of Anomaly 2A. The next highest values at 332 and 331 Bq·m⁻³ were measured at sites 7A and 16A. Despite the high radon activity flux density at site 13A on top of Anomaly 2A (9532 mBqm^{-2·s⁻¹) it showed an activity concentration in air 1.5 m above ground of 220 Bq·m⁻³ only. Sites 17A (east of Anomaly 2A), 3A (close to Anomaly 2B) and 21A (southwest of Anomaly 2C) show radon activity concentrations of 160, 120 and 70 Bq·m⁻³. The remainder of the sites showed radon activity concentrations between 45 and ~200 Bq/m³.}

At 50 cm height above ground radon activity concentrations in air were highest (860–1550 Bq·m⁻³) at sites 14A, 15A and 13A in the immediate vicinity of Anomaly 2A, whereas sites 3A, 17A and 21A showed radon activity concentrations in air about 10 times lower (20–100 Bq·m⁻³). At 30 cm height above ground radon activity concentrations in air increase to up to 2000 Bq·m⁻³ on top of Anomaly 2A, whereas sites 3A, 17A and 21a exhibit radon activity concentrations in air of 100–200 Bq·m⁻³. Figure 17 summarises the results of the radon in air measurements.

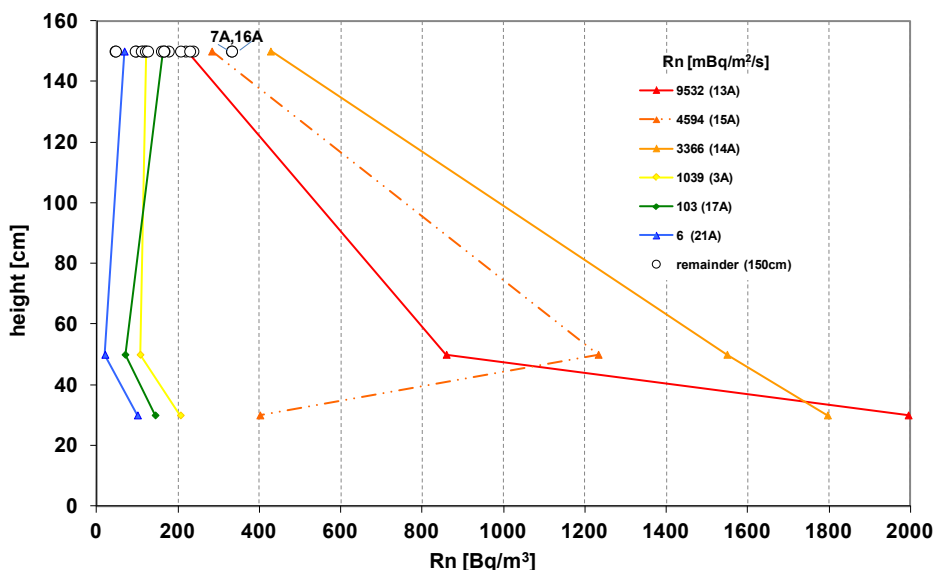


Figure 17 Radon activity concentrations measured in air at 30 cm, 50 cm and 150 cm above ground over the Anomaly 2 area for the dry season 2009.

4.5 Soil activity concentrations

4.5.1 Laboratory HPGe measurements

Surface soil radionuclide activity concentrations were measured in soil samples collected from radon exhalation measurement sites 1A-25A (Figure 17) using the *eriss* HPGe detectors in the Darwin laboratories. Results are given in Appendix D.

^{238}U activity concentrations were calculated from the contribution of ^{235}U to the 186 keV line in the gamma emission spectrum, and then multiplying the calculated ^{235}U activity concentration with the natural $^{238}\text{U}/^{235}\text{U}$ activity ratio of 21.7. ^{238}U activity concentrations can also be estimated from the ^{234}Th activities, assuming equilibrium between ^{238}U and ^{234}Th . Figure 18a shows the derived ^{238}U activity concentrations (ie calculated from the contribution of ^{235}U to the 186 keV line) plotted versus the measured ^{234}Th activity concentrations for activity concentrations between 40 and 40 000 Bq·kg⁻¹. The slope of the linear best fit to the measured values indicates that, on average, the ^{234}Th activity concentration was measured at

about 90% of the ^{238}U activity concentration. This slope is dominated by values above 10 000 $\text{Bq}\cdot\text{kg}^{-1}$, for values below 10 000 $\text{Bq}\cdot\text{kg}^{-1}$ the slope is approximately 1 (Figure 18b). ^{238}U activity concentrations given in Appendix D are the error weighted mean of the ^{238}U and ^{234}Th activity concentrations measured in a sample.

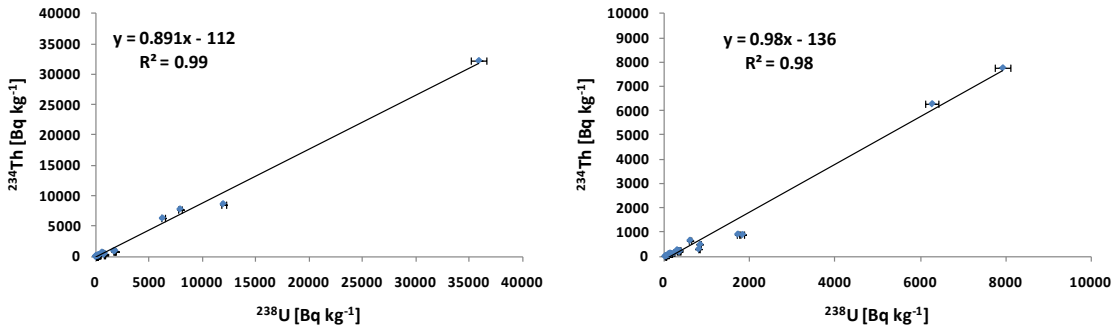


Figure 18 (a) Measured ^{234}Th activity concentration plotted against derived ^{238}U for sample activity concentrations between (a) 40 – 40 000 $\text{Bq}\cdot\text{kg}^{-1}$, and (b) 40 – 10 000 $\text{Bq}\cdot\text{kg}^{-1}$.

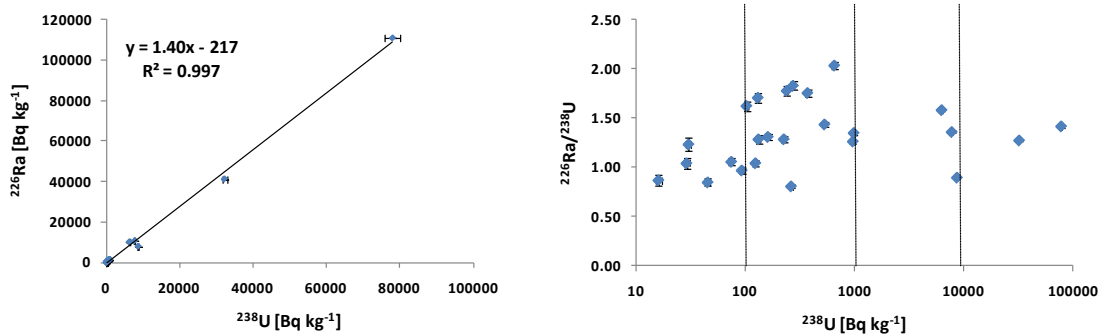


Figure 19 (a) ^{226}Ra activity concentration and (b) $^{226}\text{Ra}/^{238}\text{U}$ activity concentration ratio plotted against ^{238}U activity concentrations in samples from Anomaly 2.

Figures 19a and b show the activity concentration of ^{226}Ra and the $^{226}\text{Ra}/^{238}\text{U}$ activity concentration ratio plotted versus the ^{238}U activity concentration in the soil samples. ^{226}Ra activity concentrations measured in the lower activity samples is close to secular equilibrium with ^{238}U . However, $^{226}\text{Ra}/^{238}\text{U}$ activity concentration ratios vary between 0.8 and 2.0, and are higher especially in samples with activity concentrations of ^{238}U between 100 and 1000 $\text{Bq}\cdot\text{kg}^{-1}$. On average ^{226}Ra is approximately 40% higher than the activity concentrations of ^{238}U in the samples.

It is important to note that:

1. equivalent uranium concentrations (eU) measured with the in-situ NaI gamma spectrometer and given in Appendix A are not representative of the uranium concentration. Much rather the NaI gamma spectrometer determines the activity of ^{214}Bi in soil from its gamma emission line at 1.76 MeV. As ^{214}Bi can be assumed to be in radioactive equilibrium with ^{226}Ra in soil, the eU values measured using the hand held gamma spectrometer should be multiplied with 12.35 $\text{Bq}\cdot\text{kg}^{-1}$ per ppm_U to calculate and report activity concentrations of ^{226}Ra measured in situ.
2. ^{226}Ra activity concentration measured in surface scrapes in the laboratory may not be representative of the ^{226}Ra activity concentration in deeper sections of the soil profile.

To illustrate the importance of the second point, the expected terrestrial gamma dose rate (H_e) has been calculated from the soil activity concentrations at sites 1A – 25A measured using the laboratory HPGe detector:

$$H_e = a_1 \cdot {}^{238}\text{U} + a_2 \cdot {}^{232}\text{Th} + a_3 \cdot {}^{40}\text{K} \quad (2)$$

with the conversion factors a_i given in Table 5, assuming equilibrium between all members in the uranium and thorium decay chains, respectively (Saito & Jacob 1994), ie the measured ${}^{226}\text{Ra}$ was used as a proxy for ${}^{238}\text{U}$ activity concentrations.

Table 5 Conversion factors used to calculate ${}^{238}\text{U}$, ${}^{232}\text{Th}$ and ${}^{40}\text{K}$ activity concentrations and expected terrestrial gamma dose rates from given soil uranium, thorium and potassium concentrations.

	Uranium-238	Thorium-232	Potassium-40
a_i	0.462 (nGy·hr ⁻¹)/(Bq·kg ⁻¹)	0.604 (nGy·hr ⁻¹)/(Bq·kg ⁻¹)	0.0417 (nGy·hr ⁻¹)/(Bq·kg ⁻¹)
c_i	12.35 Bq _{U-238} /mg _U	4.07 Bq _{Th232} /mg _{Th}	31.6 Bq _{K40} /g _K

Figure 20a shows the terrestrial gamma dose rates as calculated from the activity concentrations measured in the surface soil scrapes, plotted versus the measured terrestrial gamma dose rate at sites 1A to 25A. A value of 0.066 $\mu\text{Gy}\cdot\text{hr}^{-1}$ has been subtracted from the measured values, as the contribution from cosmic radiation to the measured gamma dose rate in the field (Marten 1992).

The slope of this fit indicates that calculated terrestrial gamma dose rates using equation 2 are on average two times higher than measured terrestrial gamma dose rates. However, the correlation is dominated by the high terrestrial gamma dose rates calculated for sites 14 A and 15A, which are both located on top of Anomaly 2. These two samples had the highest ${}^{226}\text{Ra}$ soil activity concentrations measured in this study (see Appendix D). Figure 20b illustrates that data regression for calculated values are only about 5% higher than measured terrestrial gamma dose rates for sites excluding 14A and 15A, and also excluding site 24A, which was located on top of a rock pile and exhibited relatively smaller measured dose rates due to the geometry of the surface (the measurement was done on the pile crest) where the measurement was conducted.

Most of the gamma dose rate measured in air at a height of 1 m above the ground originates from radionuclides located in the top 0.5 m of the soil (ICRU 1994, Saito & Jacobs 1992). Hence, gamma dose rates calculated from radionuclide activity concentrations measured in surface soils (0 – ~5 cm) may over (or under) estimate the actual terrestrial gamma dose rate if soil activity concentrations are higher (or lower) at the soil surface. At sites 14A and 15A on top of Anomaly 2A it appears that activity concentrations of the surface soil scrapes collected are higher than the average activity concentrations throughout the top ~0.5 m of soil.

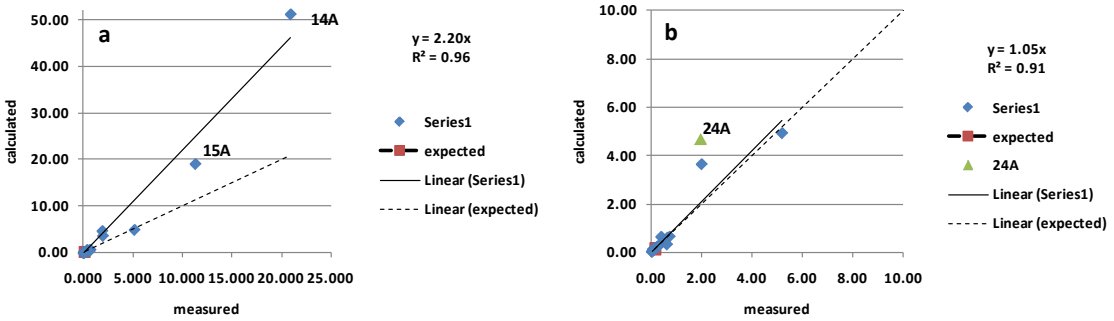


Figure 20 Calculated terrestrial gamma dose rates [$\mu\text{Gy}\cdot\text{hr}^{-1}$] from laboratory HPGe radionuclide activity concentration measurements plotted versus the measured terrestrial gamma dose rates at sites 1A-25A. a) entire range of dose rates measured, b) less than $10 \mu\text{Gy}\cdot\text{hr}^{-1}$.

4.5.2 In situ NaI measurements

Soil activity concentrations were also measured with a 512 channel portable NaI gamma detector (*Geofyzika*, now *SatisGeo*, model GS-512) during the August 2007 gamma survey at each gamma dose rate measurement point. Results are shown in Appendix A.

It is important to note that, similar to a dose rate meter, the signal measured by a portable NaI gamma detector at a height of 1 m above the ground originates from radionuclides located in the top ~ 0.5 m of the soil rather than the surface soil only. In addition, the footprints of both measurement methods are comparable. Thus, calculated (from NaI measurements) and measured terrestrial gamma dose rates should be more readily comparable than those using laboratory measurements of radionuclide activity concentration in surface soil scrapes.

The portable NaI gamma detector gives equivalent uranium (eU) and equivalent thorium (eTh) concentrations in ppm, potassium concentrations are given in %. These concentrations have been used to calculate soil ^{226}Ra , ^{232}Th and ^{40}K activity concentrations, using the conversion factors c_i shown in Table 4 (Figure 21).

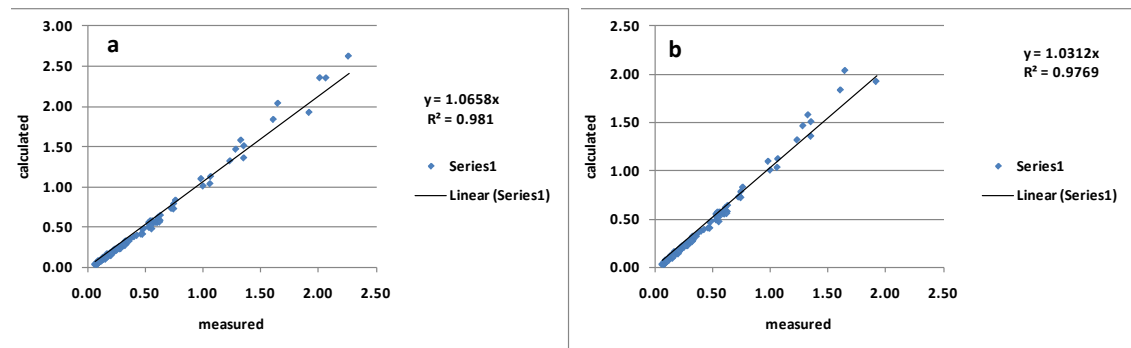


Figure 21 Calculated terrestrial gamma dose rates (using equation 2) in $\mu\text{Gy}\cdot\text{hr}^{-1}$ plotted versus measured terrestrial gamma dose rates performed in August 2007 using the NaI detector; a) entire range of dose rates measured, b) less than $2 \mu\text{Gy}\cdot\text{hr}^{-1}$.

Figure 21a shows a plot of calculated terrestrial gamma dose rates versus gamma dose rates measured in the field in August 2007. It shows a good agreement between calculated and measured values, with slightly higher calculated gamma dose rates. Figure 21b shows the calculated terrestrial gamma dose rates versus gamma dose rates measured in the field for gamma dose rates from $0-2 \mu\text{Gy}\cdot\text{hr}^{-1}$ (as the calibration for GM is strictly applicable for dose

rates from 0-2 $\mu\text{Gy}\cdot\text{hr}^{-1}$ only). The comparison shows good agreement between calculated and measured terrestrial dose rates.

5 Conversion factors

5.1 Terrestrial gamma dose rate to ^{226}Ra soil activity concentration

In Figure 22 the measured soil ^{226}Ra activity concentration is plotted against measured terrestrial gamma dose rates. This plot includes all laboratory measurements using the eriss HPGe detectors and also the in-situ NaI measurements. A fit to all ^{226}Ra data is shown, in addition to a fit to the NaI measurements only.

The yellow sample points in Figure 22 indicate scrape samples that were taken immediately on top of Anomaly 2 (sites 13A-15A, see Figure 17). Sites 14A and 15A are samples from rocky terrain and the substrate consisted of coarse gravel and some rocks. ^{226}Ra activity concentrations were higher than ^{238}U in these surface scrapes. Site 16A also consisted of gravel but ^{226}Ra and ^{238}U in this sample were close to equilibrium. As mentioned previously, the measurement of the gamma dose rate at site 24A was taken on top of a rock heap next to an old trench, which most likely lead to lower measured terrestrial gamma dose rates due to the change in surface geometry. Consequently, it is justified to omit these samples from the fit of terrestrial gamma dose rates to ^{226}Ra soil activity concentrations.

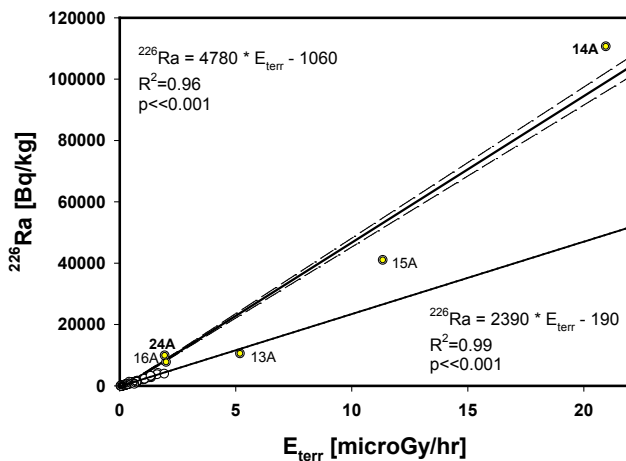


Figure 22 In situ and laboratory measured soil ^{226}Ra activity concentration plotted against the measured terrestrial gamma dose rates, all data shown. Filled symbols (yellow) indicate the results from laboratory measurements. In addition a fit to the NaI data only (open symbols) is shown.

Figure 23 shows the in-situ measured ^{226}Ra activity concentration plotted against the measured terrestrial dose rate, for dose rates between 0-2 $\mu\text{Gy}\cdot\text{hr}^{-1}$, and including the HPGe measurements in that range. A conversion factor of 2330 $\text{Bq}\cdot\text{kg}^{-1}$ per $\mu\text{Gy}\cdot\text{hr}^{-1}$ has been determined with a 95% confidence interval of (2280-2380) $\text{Bq}\cdot\text{kg}^{-1}$ per $\mu\text{Gy}\cdot\text{hr}^{-1}$. The value of the x-intercept ($y = 0$) is $(0.07 \pm 0.01) \mu\text{Gy}\cdot\text{hr}^{-1}$, which is only slightly higher, than the average terrestrial gamma dose rate calculated from the measured soil ^{232}Th and ^{40}K activity concentrations alone of $0.034 \pm 0.030 \mu\text{Gy}\cdot\text{hr}^{-1}$ (95% confidence) using equation (2) above.

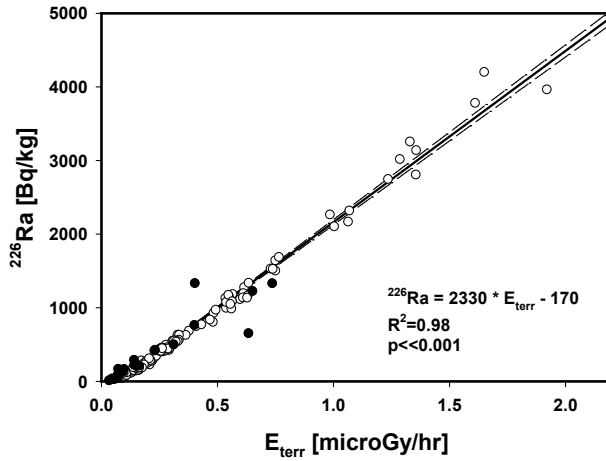


Figure 23 In situ (Nal) (o) and laboratory (HPGe) (•) measured soil ^{226}Ra activity concentration plotted against measured terrestrial gamma dose rates ($< 2 \mu\text{Gy} \cdot \text{hr}^{-1}$).

Using equation (3) we can convert terrestrial gamma dose rates measured 1 m above the ground to ^{226}Ra soil activity concentrations.

$$^{226}\text{Ra} \left[\frac{\text{Bq}}{\text{kg}} \right] = (2330 \pm 50) \frac{\text{Bq}/\text{kg}}{\mu\text{Gy}/\text{hr}} \cdot E_{\text{terr}} - (165 \pm 20) \left[\frac{\text{Bq}}{\text{kg}} \right] \quad (3)$$

5.2 ^{226}Ra soil activity concentration to ^{222}Rn flux density

Similar to the terrestrial gamma radiation, where most of the signal originates from the top approximately 50 cm of the soil (ICRU 1994), soil layers down to several metres can contribute to radon exhalation at the surface, with a typical diffusion length for ^{222}Rn of 1.5 m (Porstendorfer 1994). In addition, it has been shown that radon exhalation for different geomorphic sites, or soil types, can differ for similar ^{226}Ra activity concentration in the soil (Lawrence et al 2009). For example in the greater Ranger area barren compacted surfaces with no vegetation show a ^{226}Ra activity concentration to ^{222}Rn flux density conversion factor R_{E-R} of 0.27 $[(\text{mBq} \cdot \text{m}^{-2} \cdot \text{s}^{-1}) / (\text{Bq} \cdot \text{kg}^{-1})]$ whereas the conversion factor for non compacted material can be up to 10 times higher.

Figure 24 shows the geometric mean of the ^{222}Rn flux densities at each site plotted against the measured ^{226}Ra soil activity concentrations.

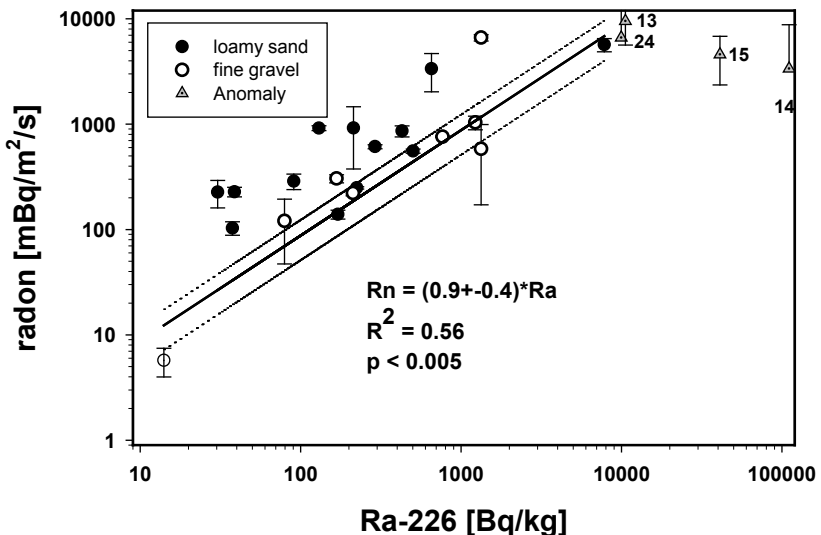


Figure 24 ^{222}Rn flux densities plotted against the measured (HPGe) ^{226}Ra soil activity concentrations. Only the loamy sand and fine gravel sample types are included in the line of best fit.

Equation (4) below can be used to calculate the expected ^{222}Rn flux density for loamy sands and gravel, if soil ^{226}Ra activity concentrations are known. This has been derived excluding data from sites 13A – 15A on top of Anomaly 2A, and site 24A, which was on top of a rockpile in the vicinity of Anomaly 2C, not representative of the general soil morphology in the area.

$$^{222}\text{Rn} \left[\frac{\text{mBq}}{\text{m}^2 \cdot \text{s}} \right] = (0.9 \pm 0.4) \frac{\frac{\text{m}^2 \cdot \text{s}}{\text{Bq}}}{\frac{\text{Bq}}{\text{kg}}} \cdot ^{226}\text{Ra} \left[\frac{\text{Bq}}{\text{kg}} \right] \quad (4)$$

For coarser material and rocks that can be found on top of the Anomalies it appears that, whereas ^{226}Ra activity concentration increases in these areas, the ^{222}Rn flux densities do not. This discrepancy may be due to the reduced surface area of the coarser gravel and rocks relative to the sand and gravel sites. Consequently, this equation does not apply immediately on top of Anomaly 2, and also most likely not immediately on top of the anomalies associated with orebodies 1 and 3 before mining started. The average ^{222}Rn flux density immediately on top of Anomaly 2A is $6000 \pm 2300 \text{ mBq} \cdot \text{m}^{-2} \cdot \text{s}^{-1}$, while the ^{226}Ra activity concentration varies by more than one order of magnitude.

5.3 Terrestrial gamma dose rate to ^{222}Rn flux density

Approximately 56% of the terrestrial gamma signal measured 1 m above the ground originate from a circle of about 2 m (IAEA 1989) and the measurement of the terrestrial gamma dose rate is more representative of the radioactivity in the top 50 cm of soil, rather than the surface soils only. The typical diffusion length for ^{222}Rn is about 1.5 m (Porstendorfer 1994) and in our study radon exhalation at the sites has been determined as the geometric mean of three individual radon cup results within a radius of approximately 1 m.

Hence, a conversion factor has also been calculated to determine ^{222}Rn flux density from the measured terrestrial gamma dose rates. Terrestrial gamma dose rates have been calculated by subtracting $0.066 \mu\text{Gyhr}^{-1}$ as the contribution from cosmic radiation from the gamma dose rate measured on ground (Marten 1992).

The plot of the geometric means of the radon flux densities at each site against the measured terrestrial gamma dose rates is shown in Figure 25. The line shows the best fit to the data

points, but excludes sites 13A, 14A and 15A directly on top of Anomaly 2A for the reasons mentioned above.

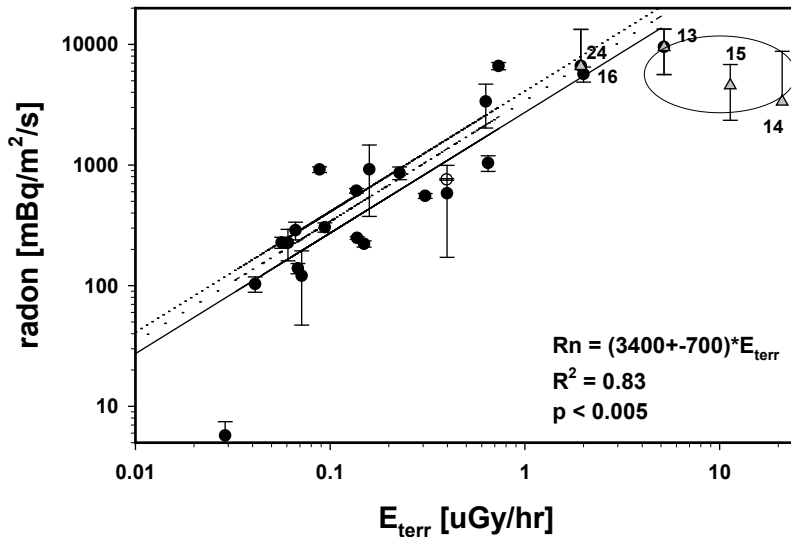


Figure 25 ^{222}Rn flux densities plotted against the measured (in situ) terrestrial gamma dose rates. The line of best fit has been drawn including loamy sand and fine gravel substrate types, but excluding measurements from directly on top of the Anomaly (circled) and sample 24.

The coefficient of determination R^2 between the averaged ^{222}Rn flux densities and the measured terrestrial dose rates in the field is significantly better than the correlation between ^{222}Rn flux densities and measured ^{226}Ra soil activity concentration in the surface scrapes (Figure 24). The variability in terrestrial gamma dose rates accounts for approximately 80% of the variability observed in radon activity flux densities, using a linear model. This is not surprising, due to the depth related effects discussed above.

The equation to convert terrestrial gamma dose rates into ^{222}Rn flux densities can thus be written as:

$$^{222}\text{Rn} \left[\frac{\text{Bq}}{\text{m}^2 \cdot \text{s}} \right] = (3.4 \pm 0.7) \frac{\text{Bq}}{\frac{\text{m}^2 \cdot \text{s}}{\text{uGy}}} \cdot E_{\text{terr}} \left[\frac{\text{uGy}}{\text{hr}} \right] \quad (5)$$

5.4 Converting the 1976 AGS U data to terrestrial dose rate in the field

Differences in survey parameters, height of the detector above ground, detector type and calibration do not allow direct comparison of spatial data from the two (ie 1976 and 1997) AGSs and the ground-based gamma dose rate survey, respectively. Upscaling of the ground-based survey is required to make the footprints of the ground-based survey and the AGSs comparable. Bollhöfer et al (2008) show a table which compares the typical footprints of AGSs with the footprint of ground-based surveys usually performed at 1 m above ground. This table is re-produced here (Table 6). Spatial referencing and data processing (which is largely unknown for the 1976 AGS) can furthermore complicate the process of upscaling the data.

Table 6 Comparison of typical footprints for ground-based and airborne gamma surveys.

	Altitude	Footprint, radius r	% signal from within r	Reference
Airborne gamma survey	120 m	180 m	50	Bierwirth et al 1996
Airborne gamma survey	50 m	50 m	40	Duval et al 1971
Airborne gamma survey	30 m	36 m	56	Billings & Hovgard 1999
Ground gamma survey	1 m	2 m	56	IAEA 1989

In this study, data from two AGSs were available over the greater Anomaly 2 area. One survey was flown by Rio Tinto in 1997, at a flying height above Anomaly 2 of approximately 50 m and a flight line spacing of 100 m. The other survey was flown in 1976 before mining started, at an unknown flying height and a line spacing of 300 m. In addition, the 1976 data have been processed and pixilated (70 m x 70 m) but processing algorithms are largely unknown.

Due to the better resolution of the 1997 AGS data it was decided that the upscaling of the gamma dose rates measured in the field to the $eU (s^{-1})$ data measured during the 1976 AGS should be performed via an intermediate step, using the $eU (Bq \cdot kg^{-1})$ line data above Anomaly 2 from the 1997 survey. The underlying assumption for the upscaling of our data is that between 1976 and the time of the groundtruthing, no changes that would significantly alter the radiological conditions at Anomaly 2 have occurred. This assumption appears reasonable, as Anomaly 2 has been excluded from the Ranger Project Area after recommendations made in the second Fox Report (RUEI, 1977), due to its close proximity to Mount Brockman and its Aboriginal sacred sites, Djidbidjidbi and Dadbe, sites of significant value to the Mirrar Aboriginal people.

5.4.1 Modelling the 1997 AGS line data to the field gamma dose rate data

The AGS data originally received from Rio Tinto as projected coordinates of the Australian geodetic datum 1984, were reprojected into the WGS84 map datum, UTM Zone 53S. A shapefile was then created, defined by the boundary of the 2007 to 2009 field data obtained for the Anomaly 2 area (Figures 15 and 26).

Airborne gamma survey points which lie within the boundary of the shapefile and have integer time records were then extracted. The basic assumption here is that all non-integer second data is interpolated based on the integer second records. The integer records were then given a unique id (ID_97) and the uranium (eU in $Bq \cdot kg^{-1}$) and total count (TC in s^{-1}) data was used for modeling purposes.

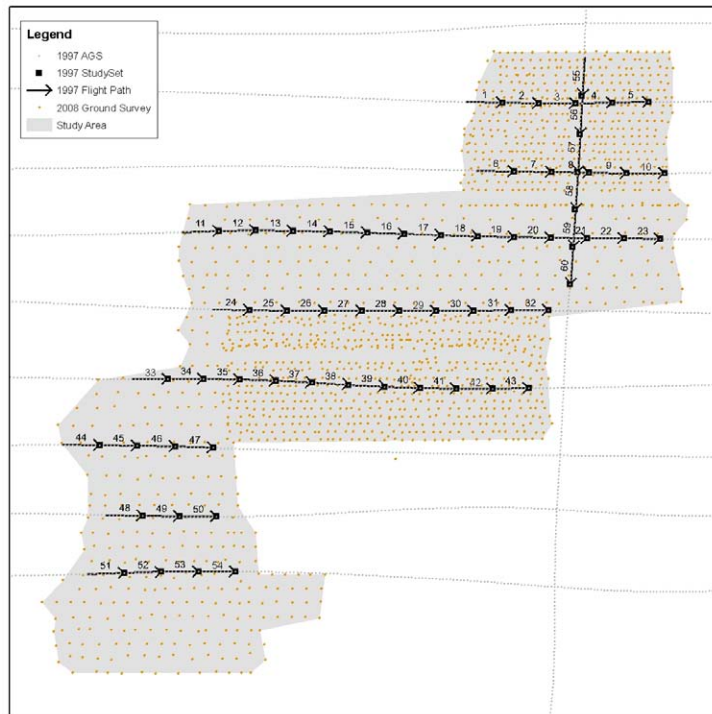


Figure 26 Shapefile created in ArcGIS for the 2007-2009 ground survey (grey), flight lines and flight line numbers (black arrows) and individual ground survey points (orange).

Lines were then created which represent the flight path for each of the records and each line adopted the TC and eU values from the integer time stamp of the AGS data file. In addition, the average altitude of the flight lines was calculated using the average altitude of the previous and current records.

Table 6 above illustrates the influence of survey height on the effective footprint for various AGS specifications. Consequently, the ground data need to be upscaled. A circular footprint is justified for a stationary plane, but the average distance the plane travels between individual measurements is 60 m. Consequently, a series of buffers of the shape shown in Figure 27 was created in ArcGIS and the buffer radius was varied.

The calculated mean gamma dose rates [μGy^{-1}] measured on ground within the chosen buffers for each line were then calculated for various buffer radii chosen. These averages were then plotted against airborne total counts (TC) of the respective flight lines to obtain the buffer radius giving the best correlation between averaged dose rates and TC measured on board of the plane.

Figure 28 shows the coefficient of determination R^2 obtained in the GIS analysis between averaged gamma dose rates on ground and total counts in the 1997 AGS for buffer radii ranging from 60 m – 130 m. The radii were varied in 5 m steps. Analysis of the data indicated that the best correlation between averaged gamma dose rates measured on ground and total counts measured on board the plane was gained for a buffer radius of 90 m.

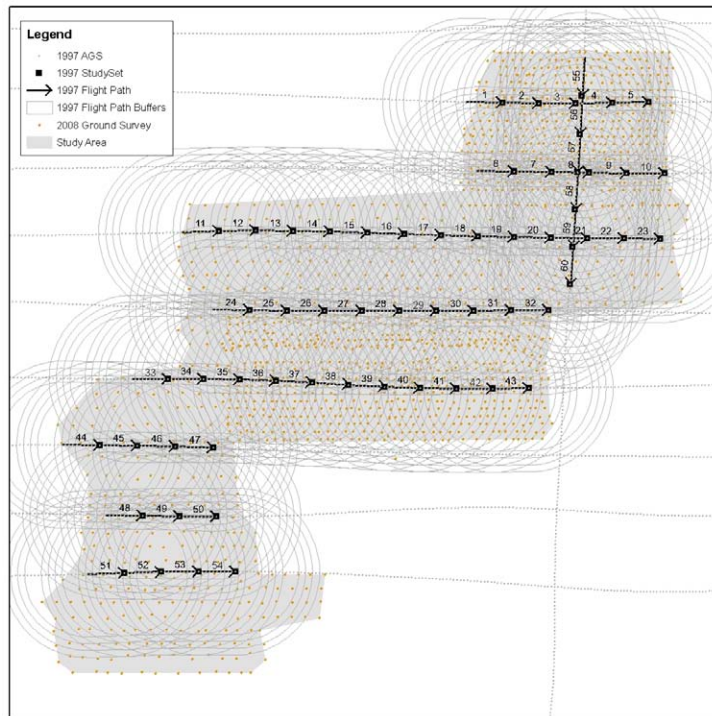


Figure 27 Variable buffers overlaid on shapefile created in ArcGIS for the 2007–2009 ground survey.

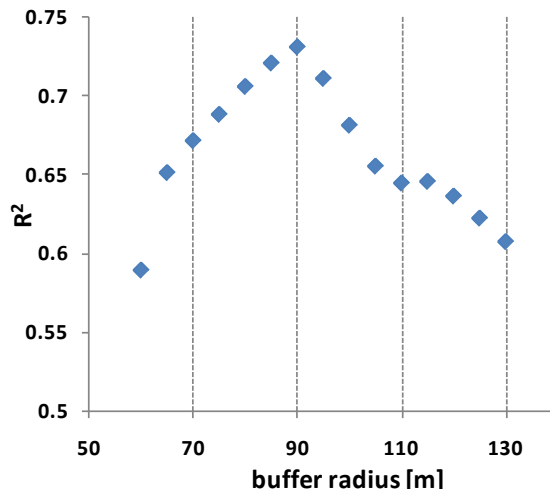


Figure 28 Coefficient of determination R^2 obtained between average ground gamma dose rates for varying buffer radii measured in the field and TC measured in 1997 on board the plane.

Figures 29 and 30 show the correlations between the averaged (buffer radius = 90 m; $n = 54$) terrestrial gamma dose rates and the TC (s^{-1}) and eU ($Bq \cdot kg^{-1}$) channels, respectively. Terrestrial gamma dose rates have been calculated by subtracting $0.066 \cdot hrGy^{-1}$ as the contribution from cosmic radiation from the gamma dose rate measured on ground (Marten 1992).

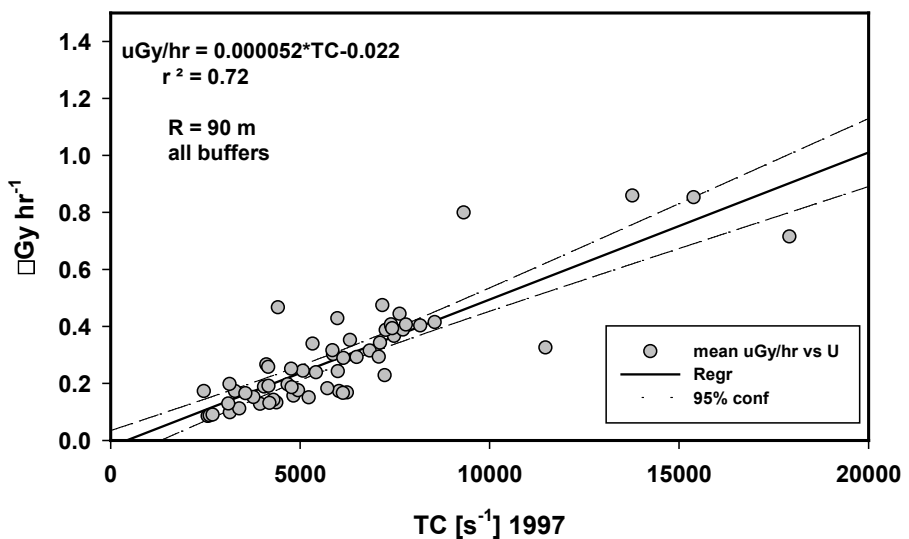


Figure 29 Correlation between averaged terrestrial gamma dose rates and the TC (s^{-1}) channel of the 1997 AGS. Buffer radius of 90 m, n=54.

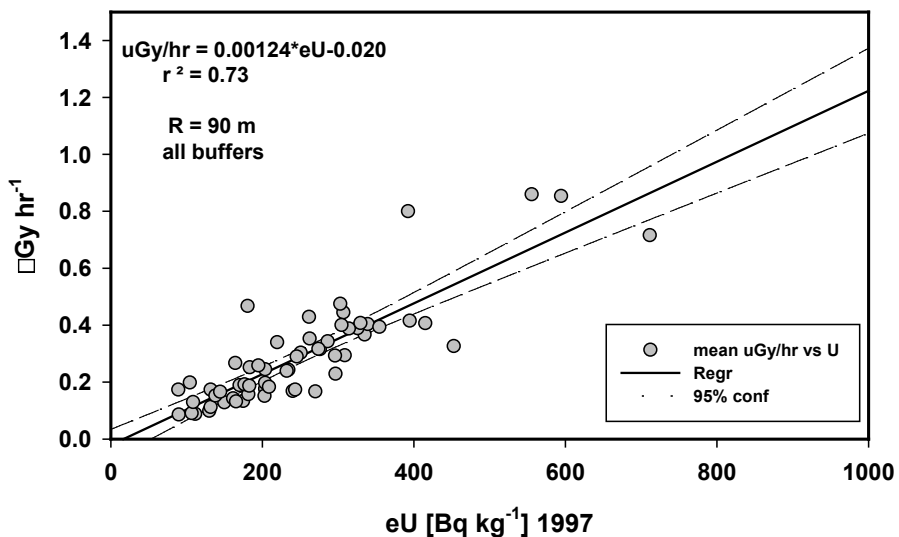


Figure 30 Correlation between averaged terrestrial gamma dose rates and eU ($Bq \cdot kg^{-1}$) channel of the 1997 AGS. Buffer radius $r=90$ m, n=54.

To ensure that results of the correlations were not affected by variations in ground sample spacing, only those buffers which have a consistent distribution of ground points within have been used. Figure 31 shows those buffers that have been selected out and were then used for further analysis. A total of 29 buffers were extracted.

Figures 32 and 33 show the correlations between the averaged (buffer radius = 90 m; n = 29) terrestrial gamma dose rates and the TC (s^{-1}) and eU ($Bq \cdot kg^{-1}$) channels, respectively. The equation to convert the eU data from the 1997 AGS into terrestrial dose rates measured in the field can thus be written as:

$$E_{terr} \left[\frac{\mu Gy}{hr} \right] = (0.00126 \pm 0.00028) \left[\frac{\mu Gy \cdot kg}{hr \cdot Bq} \right] \cdot eU_{1997} [Bq \cdot kg^{-1}] - (0.023 \pm 0.086) \left[\frac{\mu Gy}{hr} \right] \quad (6)$$

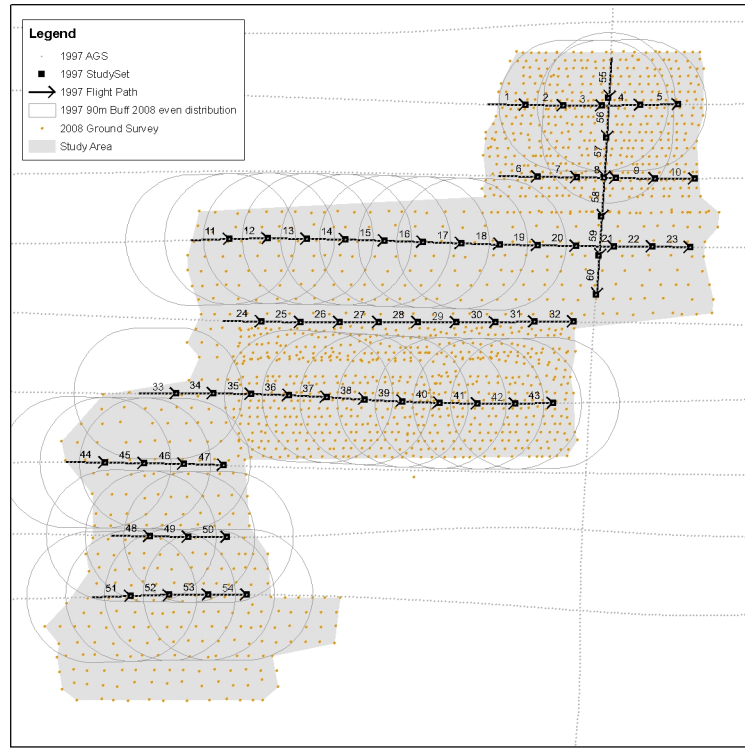


Figure 31 Buffers ($n=29$) with even distribution of ground survey points chosen to establish the correlation between the ground survey and the 1997 AGS data. Buffer radius $r=90$ m.

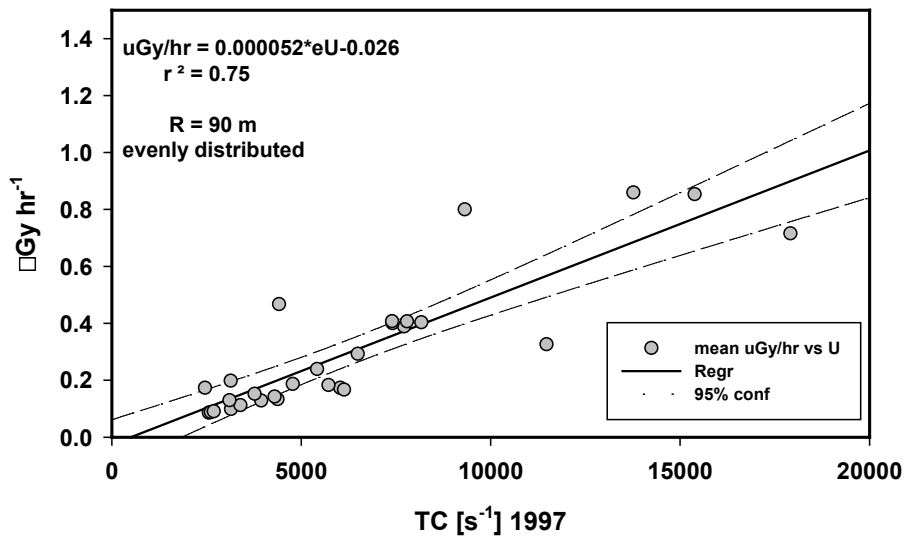


Figure 32 Correlation between averaged terrestrial gamma dose rates and the TC (s^{-1}) channel of the 1997 AGS for buffers with evenly distributed ground survey points only. $r = 90$ m, $n = 29$.

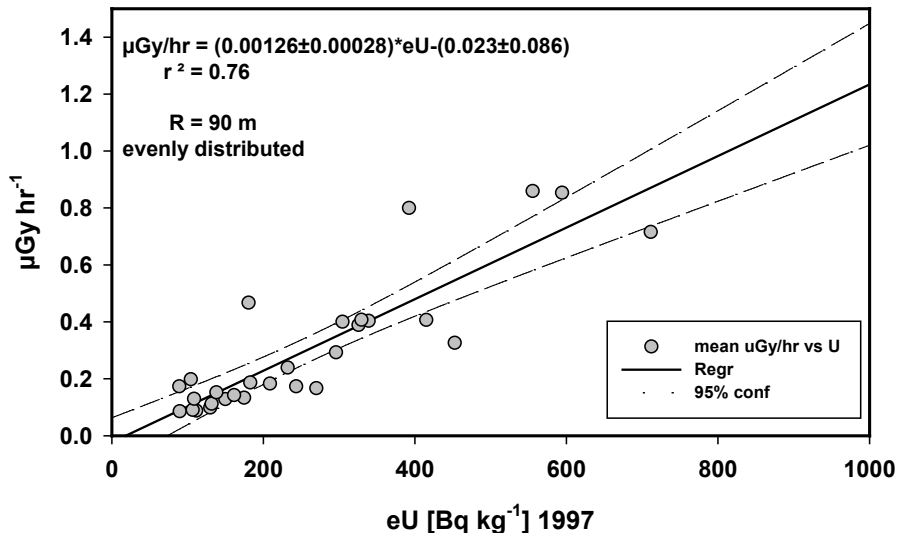


Figure 33 Correlation between averaged terrestrial gamma dose rates and eU ($\text{Bq}\cdot\text{kg}^{-1}$) channel of the 1997 AGS for buffers with evenly distributed ground survey points only. $r=90$ m, $n=29$.

5.4.2 Modelling the 1976 raster to the 1997 raster airborne gamma data

Both the 1976 (70 m x 70 m) and 1997 (25 m x 25 m) raster datasets were reprojected to WGS84 UTM53S and a subset of the raster data was created (Figure 34). Both the 1997 and 1976 data were then clipped to this subset. The subset includes the full extent of the 1997 raster imagery including Anomaly 2 at the southern edge of the dataset, but excludes the mine footprint. The assumption is, that apart from areas on site, radiation levels have not changed between 1976 and 1997.

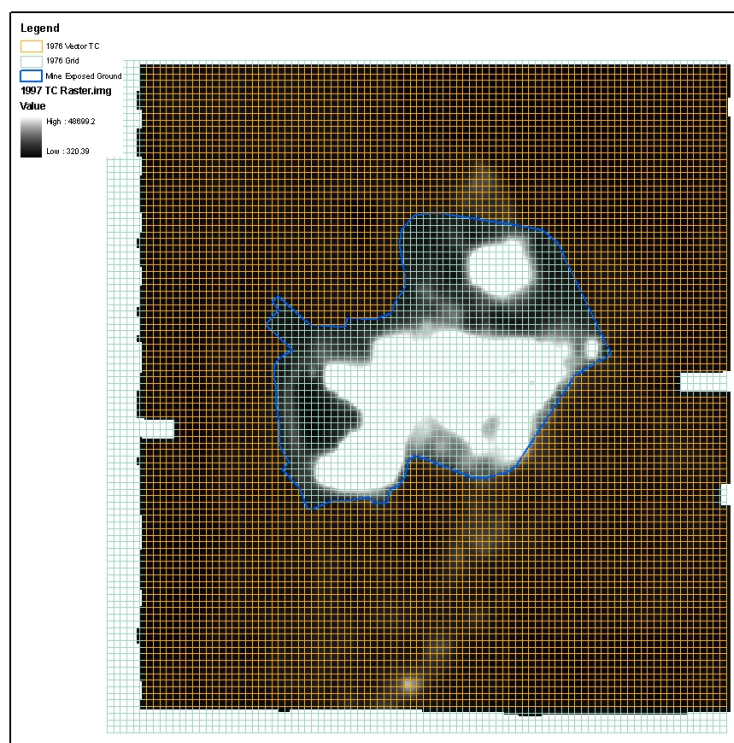


Figure 34 Full extent of the 1997 raster imagery. The total counts of the 1997 AGS are shown, with light colours indicating high values. The area within the blue outline was excluded and includes the disturbed footprint of the Ranger mine site.

A vector grid of the 1976 data was then created using the Hawth's Tool in ArcGIS. Each grid cell was populated with both the TC (s^{-1}) and eU (s^{-1}) values of the 1976 raster, with the centre of each grid cell taking on the respective values. The 1997 raster data (TC in s^{-1} and eU in $Bq\cdot kg^{-1}$) was then overlaid and the averages were calculated of those 1997 raster data that are completely contained within the respective 1976 vector grid cell using the Spatial Analyst Tool in ArcGIS. Using this method a total of 6916 records were obtained. Results of the correlation between averaged 1997 eU data and the values of the respective 1976 vector grid cell, and the R^2 are shown in Figure 35.

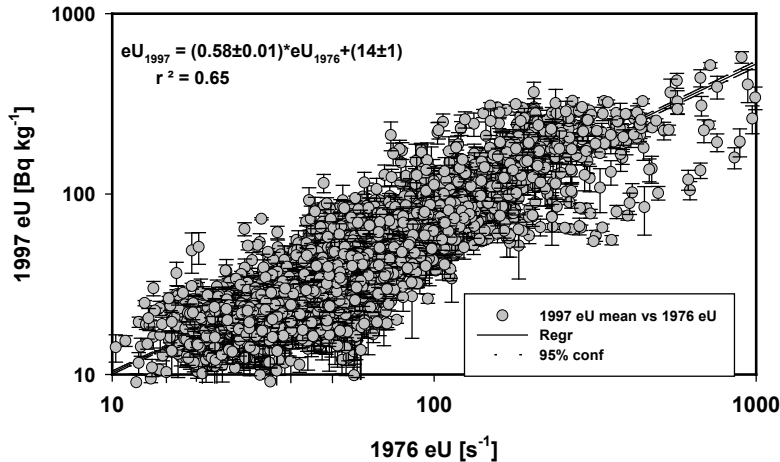


Figure 35 Averaged eU data ($Bq\cdot kg^{-1}$) from the 1997 AGS plotted versus the 1976 eU data (s^{-1}) of the respective grid cell.

The equation to convert the eU data (s^{-1}) from the 1976 AGS into averaged eU ($Bq\cdot kg^{-1}$) for the 1997 AGS can thus be written as:

$$eU_{1997}[Bq\ kg^{-1}] = (0.58 \pm 0.01)[Bq\ kg^{-1}\ s] \cdot eU_{1976}[s^{-1}] + (14 \pm 1)[Bq\ kg^{-1}] \quad (7)$$

5.4.3 Converting 1976 eU data to terrestrial gamma dose rates and radon flux densities

Combining equations (3), (5), (6) and (7) allows us to determine conversion equations and associated uncertainties (at the 95% confidence level) to determine terrestrial gamma dose rates, radon flux densities and ^{226}Ra soil activity concentrations from the count rates in the eU channel of the 1976 AGS.

Equation (8), (9) and (10) are the conversion equations and associated 95% confidence intervals to convert the 1976 eU data (s^{-1}) into terrestrial gamma dose rates measured 1m above ground (equation 8), radon flux densities (equation 9) and soil ^{226}Ra activity concentrations (equation 10), respectively.

1976 eU data to terrestrial gamma dose rates:

$$E_{terr} \left[\frac{\mu Gy}{hr} \right] = (0.00073 \pm 0.00016) \left[\frac{\mu Gy \cdot s}{hr} \right] \cdot eU_{1976}[s^{-1}] - (0.005 \pm 0.086) \left[\frac{\mu Gy}{hr} \right] \quad (8)$$

1976 eU data to radon flux densities:

$$^{222}\text{Rn} \left[\frac{mBq}{m^2 \cdot s} \right] = (2.48 \pm 0.76) \left[\frac{mBq}{m^2} \right] \cdot eU_{1976}[s^{-1}] - (20 \pm 290) \left[\frac{mBq}{m^2 \cdot s} \right] \quad (9)$$

1976 eU data to ^{226}Ra activity concentrations:

$$^{226}\text{Ra} \left[\frac{Bq}{kg} \right] = (1.70 \pm 0.38) \left[\frac{Bq \cdot s}{kg} \right] \cdot eU_{1976}[s^{-1}] - (160 \pm 200) \left[\frac{Bq}{kg} \right] \quad (10)$$

6 Discussion

6.1 Pre-mining external γ dose rates, radon flux densities and ^{226}Ra activity concentrations in the greater Ranger region

Equations 8, 9 and 10 above have been used to determine pre-mining terrestrial gamma dose rates, radon flux densities and soil ^{226}Ra activity concentrations in the greater Ranger region from the U counts (s^{-1}) of the 1976 AGS. For ease of comparison with measurements of gamma dose rates conducted in the field, the contribution from cosmic rays ($0.066 \mu\text{Gy}\cdot\text{hr}^{-1}$; Marten 1992b) has been added to the modelled terrestrial gamma dose rates.

Various shapefiles have been created in ArcGIS. For each of those shapefiles the sum of the counts per second in the eU channel of the 1976 AGS was determined using the Zonal Statistics tool in ArcGIS. This number was used in conversion equations 8-10, and the result divided by the number of pixels within the shapefile, to determine mean pre-mining gamma dose rates, ^{222}Rn flux densities and soil ^{226}Ra activity concentrations for those various areas. Results are shown in Table 7.

Table 7 Pre-mining mean (95% confidence intervals) external gamma dose rates $E [\mu\text{Gy}\cdot\text{hr}^{-1}]$ (including cosmic component), ^{222}Rn flux densities and soil ^{226}Ra activity concentrations in the Ranger area.

Infrastructure	Sum [s^{-1}]	n	Area [ha]	E_{ave} [$\mu\text{Gy}\cdot\text{hr}^{-1}$]	$^{226}\text{Ra}_{\text{ave}}$ [$\text{Bq}\cdot\text{g}^{-1}$]	Rn_{ave} [$\text{Bq}\cdot\text{m}^{-2}\cdot\text{s}^{-1}$]
1 - Pit 1	89599	81	40	0.87 ± 0.18	1.8 ± 0.4	2.7 ± 0.9
2 - Pit 3	81930	157	77	0.44 ± 0.09	0.88 ± 0.20	1.3 ± 0.4
3 - Anomaly 2	28458	77	38	0.33 ± 0.06	0.63 ± 0.14	0.92 ± 0.28
4 - Djalkmara LAA	3549	19	9	0.20 ± 0.03	0.31 ± 0.07	0.46 ± 0.14
5 - Corridor Ck LAAs	28316	284	139	0.14 ± 0.02	0.17 ± 0.04	0.25 ± 0.08
6 - Tailings Dam	14247	225	110	0.11 ± 0.01	0.11 ± 0.03	0.16 ± 0.05
7 - Magela LAAs	7823	114	56	0.12 ± 0.01	0.11 ± 0.03	0.17 ± 0.05
8 - RP1	1932	35	17	0.11 ± 0.01	0.09 ± 0.02	0.14 ± 0.04
9 - RP1 LAAs	4159	77	38	0.11 ± 0.01	0.09 ± 0.02	0.13 ± 0.04
10 - Djalkmara ex LAA	916	19	9	0.10 ± 0.01	0.07 ± 0.02	0.12 ± 0.04
11 - Jabiru East LAA	5308	103	50	0.10 ± 0.01	0.09 ± 0.02	0.13 ± 0.04
12 - Jabiru	34177	624	306	0.11 ± 0.01	0.09 ± 0.02	0.14 ± 0.04
Ranger Project Area	996080	16082	7881	0.11 ± 0.01	0.11 ± 0.02	0.15 ± 0.05

Figure 36 shows the shapefiles that were created, including the area of the township of Jabiru, overlaid on an aerial photo from 2004 of the region. In addition, the pixilated eU counts per second of the 1976 AGS over the same region are shown. Figure 37 shows the same two plots, but over the Ranger mine area only.

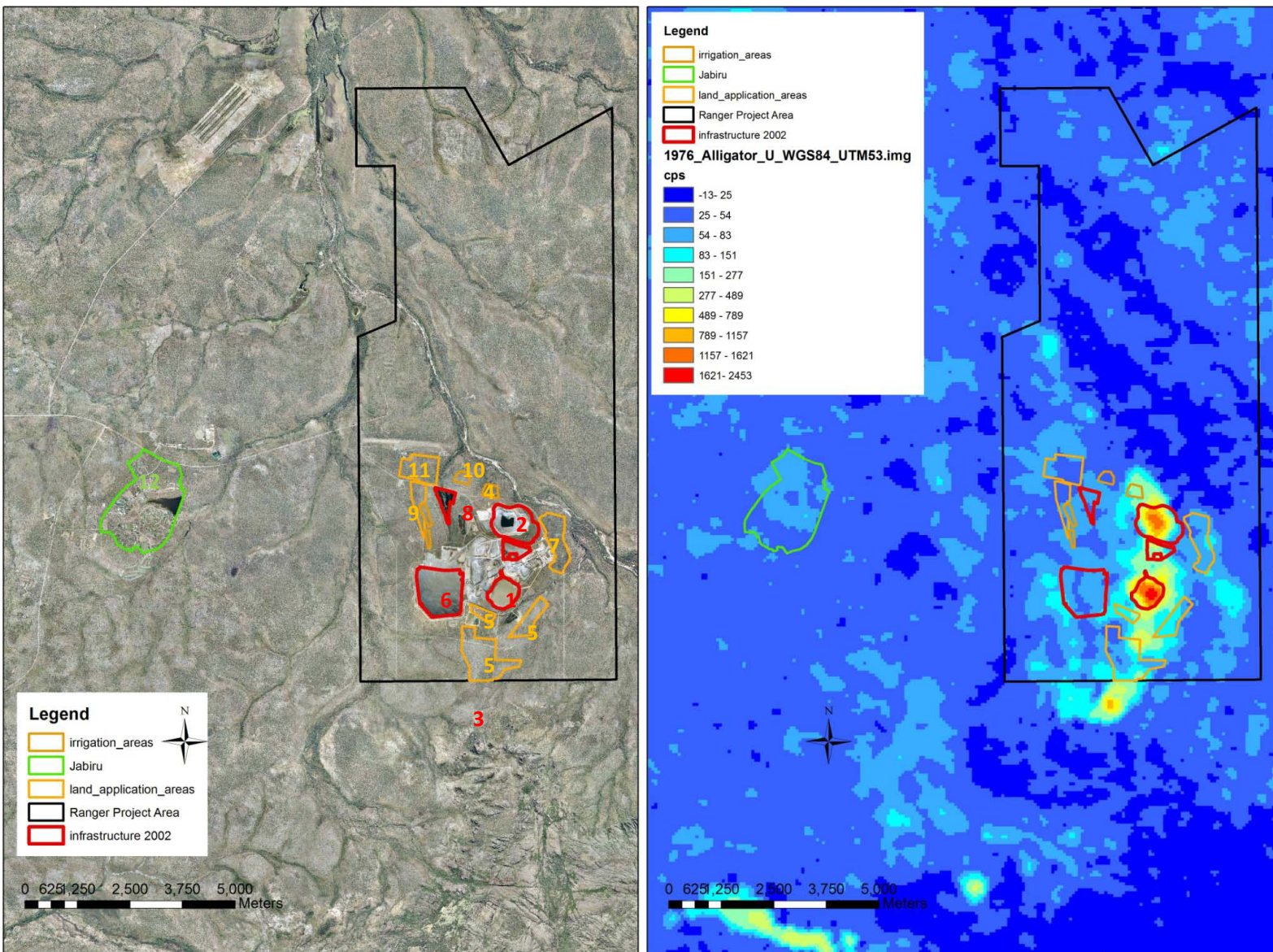


Figure 36 Shapefiles overlaid on aerial photo of the greater Ranger region (left) and on the counts in the eU channel of the 1976 AGS of the same extent (right). 1: Pit 1; 2: Pit 3; 3: Anomaly 2; 4: Djalkmara land application area (LAA); 5: Corridor Creek LAA; 6: Tailings Dam; 7: Magela LAAs; 8: Retention Pond 1; 9: Retention Pond 1 LAAs; 10: Djalkmara extension LAA; 11: Jabiru East LAA; 12: Jabiru.

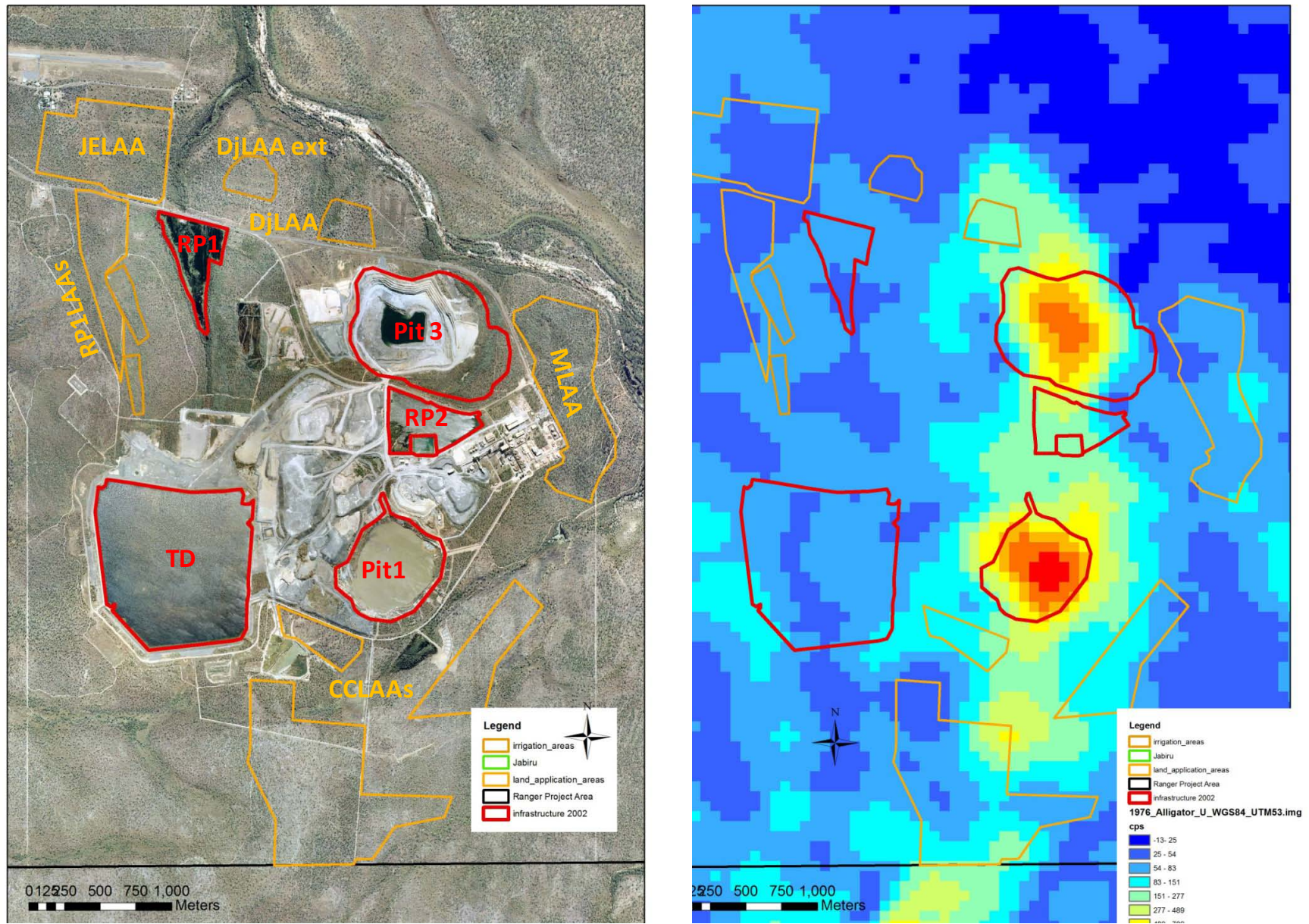


Figure 37 Shapefiles overlaid on aerial photo of Ranger only (left) and on the counts in the eU channel of the 1976 AGS of the same extent (right).

6.2 Orebody 1, Orebody 3 and Anomaly 2

6.2.1 Gamma dose rates and ^{226}Ra activity concentrations

Count rates in the eU channel of the 1976 AGS are highest over Orebody 1, Orebody 3 and Anomaly 2 (Figure 39) and thus these features exhibit the highest calculated external gamma dose rates, radon flux densities and soil ^{226}Ra activity concentrations. The average pre-mining external gamma dose rates calculated from the radiological GIS data for orebodies 1 and 3 and for the Anomaly 2 area are 0.87, 0.44 and 0.33 $\mu\text{Gy}\cdot\text{hr}^{-1}$, respectively (95% confidence intervals are given in Table 6). Average ^{226}Ra activity concentrations are 1900, 900 and 600 $\text{Bq}\cdot\text{kg}^{-1}$. The average has been determined in ArcGIS for the surface area (shapefile) of the two pits, rather than the surface area of the outcropping orebodies.

Kvasnicka (1993) and Kvasnicka & Auty (1994) have determined gamma dose rates for the two orebodies (see table 1). The terrestrial gamma dose rate on orebody 1 was 0.96 $\mu\text{Gy}\cdot\text{hr}^{-1}$ and on orebody 3 it was 0.58 $\mu\text{Gy}\cdot\text{hr}^{-1}$. Whereas the dose rate on top of orebody 3 was measured directly, dose rates on top of orebody 1 were estimated from radionuclide activity concentrations in drill core taken above the orebody. ^{226}Ra activity concentrations on top of the orebodies were estimated to 2230 and 1350 $\text{Bq}\cdot\text{kg}^{-1}$, respectively.

Differences in average values between our study and Kvasnicka and Auty (1994) most likely arise from the different areal extent of the anomalies investigated. The surface area of orebody 1 investigated by Kvasnicka and Auty (1994) was 44 ha, which is similar to the area used for averaging in our study, and average external gamma dose rates and ^{226}Ra soil activity concentrations agree well. In contrast, measurements of the gamma dose rates on top of orebody 3 were only taken over an area of 66 ha by Kvasnicka and Auty (1994) compared with an average calculated above 77 ha in our study. Most likely relatively more lower values at the outer edges of the orebody have been included in our average of the external gamma dose rate, leading to the difference observed between the two studies.

The average external gamma dose rates determined above Anomaly 2 using the GIS data is 0.33 $\mu\text{Gy}\cdot\text{hr}^{-1}$, whereas the average of all field measurements is 0.40 $\mu\text{Gy}\cdot\text{hr}^{-1}$. This translates to an average soil ^{226}Ra activity concentration of 600 $\text{Bq}\cdot\text{kg}^{-1}$ at Anomaly 2.

6.2.2 Radon flux density

The average pre-mining radon flux density calculated from the radiological GIS data for orebodies 1 and 3 and for the Anomaly 2 area are 2.7, 1.3 and 0.9 $\text{Bq}\cdot\text{m}^{-2}\cdot\text{s}^{-1}$, respectively

Kvasnicka & Auty (1994) also measured the radon flux density on top of orebody 3 at three locations and the average amounted to (4.4 ± 1.0 $\text{Bq}\cdot\text{m}^{-2}\cdot\text{s}^{-1}$). They furthermore use the measurements of radon flux densities and soil ^{226}Ra activity concentrations at those three locations to calculate a conversion factor of 1.85 ± 0.23 [$(\text{mBq}\cdot\text{m}^{-2}\cdot\text{s}^{-1})/(\text{Bq}\cdot\text{kg}^{-1})$] to determine the ^{222}Rn flux density for known soil ^{226}Ra activity concentrations across the two orebodies from the estimated average ^{226}Ra activity concentrations. Using this conversion factor, they estimate radon flux densities of 4.1 $\text{Bq}\cdot\text{m}^{-2}\cdot\text{s}^{-1}$ for orebody 1 and 2.5 $\text{Bq}\cdot\text{m}^{-2}\cdot\text{s}^{-1}$ for orebody 3, respectively. These values are higher but within the 95% confidence intervals determined in our study.

Some of the difference in radon exhalation flux densities for orebody 3 can be explained by the smaller areal extent of the orebody 3 study area compared to our study (see above). In addition, the conversion factor of 1.85 ± 0.23 [$(\text{mBq}\cdot\text{m}^{-2}\cdot\text{s}^{-1})/(\text{Bq}\cdot\text{kg}^{-1})$] used by Kvasnicka and Auty (1994) to calculate radon flux densities is much larger than the conversion factor estimated in our study from direct radon flux density measurements and ^{226}Ra measurements

in soil samples via HPGe gamma spectrometry (equation 4). The conversion factor determined in our study is 0.9 ± 0.4 ($\text{mBq} \cdot \text{m}^{-2} \cdot \text{s}^{-1}$) / ($\text{Bq} \cdot \text{kg}^{-1}$) similar to values published in Lawrence et al (2009) for vegetated woodland (0.61 ± 0.03). Kvasnicka and Auty's (1994) conversion factor may potentially be too high, due to radon potentially diffusing from deeper layers, with higher ^{226}Ra activity concentrations than the surface few centimetres of the soil. This may lead to higher estimated radon flux densities.

The terrestrial gamma dose rate to radon flux density conversion described by equation (5) provides a more reliable approach to convert ^{226}Ra activity concentrations to average radon flux densities. Using equation (3) a conversion factor of (1.4 ± 0.3) ($\text{mBq} \cdot \text{m}^{-2} \cdot \text{s}^{-1}$) / ($\text{Bq} \cdot \text{kg}^{-1}$) was calculated, which is in agreement with direct measurements. Using this conversion factor, radon flux densities for orebodies 1 and 3 from Kvasnicka & Auty (1994) amount to $3.2 \text{ mBq} \cdot \text{m}^{-2} \cdot \text{s}^{-1}$ and $1.9 \text{ mBq} \cdot \text{m}^{-2} \cdot \text{s}^{-1}$, similar to the averages determined in our study.

The average radon flux density determined from measurement in the field above Anomaly 2 were $2.2 \text{ Bq} \cdot \text{m}^{-2} \cdot \text{s}^{-1}$ compared to $0.9 \text{ Bq} \cdot \text{m}^{-2} \cdot \text{s}^{-1}$ determined using the radiological GIS data. This difference is due to the over-representation of radon exhalation measurements on top of the radiation anomalies (Figure 9) compared to other areas. Repeated measurements on high radon flux areas will skew the average value of the field measurements towards a higher value. The typical radon flux density, ie the geometric mean of all individual field measurements taken above the Anomaly, is $0.7 \text{ Bq} \cdot \text{m}^{-2} \cdot \text{s}^{-1}$, similar to the average determined using the GIS model.

6.2.3 Airborne radon activity concentration

Airborne radon activity concentrations were measured at 1.5 m height on Anomaly 2 in the dry season 2009. Figure 41 shows the measured radon activity concentrations at various heights (30 cm, 50 cm and 150 cm) above ground (from Bollhöfer et al 2011) and its dependence on ^{226}Ra soil activity concentrations at the sites.

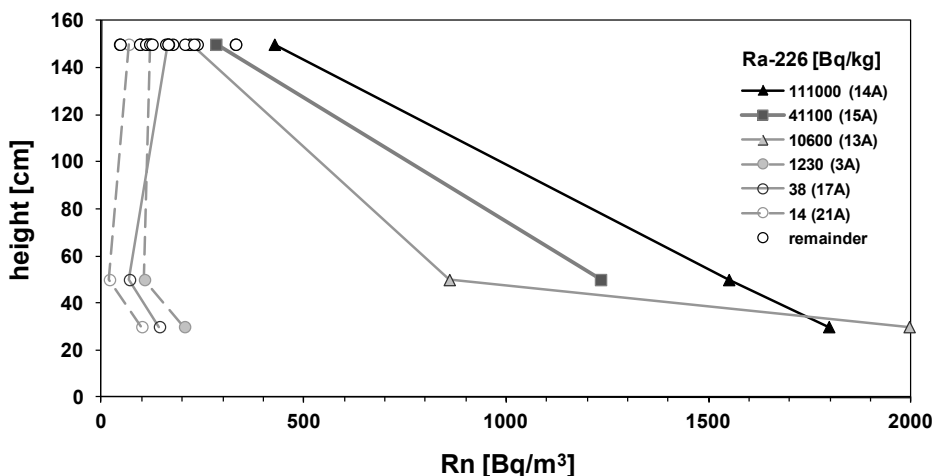


Figure 38 Radon activity concentrations measured in air at 30 cm, 50 cm and 150 cm above ground over the Anomaly 2 area for the dry season 2009. Also given are soil ^{226}Ra activity concentrations.

Whereas the soil activity concentrations vary by almost 4 orders of magnitude ($14 - 111\,000 \text{ Bq} \cdot \text{kg}^{-1}$) radon activities in air at 1.5 m height vary much less ($45 - 427 \text{ Bq} \cdot \text{m}^{-3}$). This indicates rapid aerial dispersion of radon and effective mixing at this height. The typical dry season radon concentration (ie the geometric mean of the measured values) 1.5 m above the area investigated is $\sim 150 \text{ Bq} \cdot \text{m}^{-3}$ (the arithmetic average is $175 \text{ Bq} \cdot \text{m}^{-3}$). This is about 2.5 times higher than the dry season radon concentration measured at Jabiru East of $60 \text{ Bq} \cdot \text{m}^{-3}$ (Akber &

Pfitzner 1994) and about 6 times higher than annual average radon concentration measured at Jabiru of $24 \text{ Bq}\cdot\text{m}^3$ (Akber et al 1992).

There is a positive correlation between the radon concentration at 1.5 m height and the ^{226}Ra activity concentrations in the underlying soil ($p < 0.005$; $R^2 = 0.4$), but radon concentration only increases slightly above the $150 \text{ Bq}\cdot\text{m}^3$, rising by $\sim 1 \text{ Bq}\cdot\text{m}^3$ for every $370 \text{ Bq}\cdot\text{kg}^{-1}$ increase in soil ^{226}Ra activity concentration. Wet season radon concentrations in air will generally be lower than the values cited above, which has previously been shown at other areas in the Alligator Rivers Region (Martin et al 2004).

Figure 40 illustrates that at areas away from ‘hot spots’, radon concentration is relatively uniform vertically, but concentrations are higher when sitting or lying in close vicinity to the outcropping uranium anomalies that exhibit elevated ^{226}Ra activity concentrations. This potential exposure route and its dependence on height needs to be factored into the broader land use requirements of local indigenous people when assessing potential radiation doses to humans that accessed the sites prior to mining and after rehabilitation.

No attempt has been made in our study to model the radon activity concentrations in air to the counts in the uranium channel of the 1997 or 1976 AGSs. Atmospheric dispersion does not allow concentrations in air to be correlated directly with radon exhalation or ^{226}Ra activity concentrations in the underlying soil. Rather, the measured radon activity concentration values will be used to validate atmospheric transport models used to calculate radon activity concentrations in air close to sources of known radon activity fluxes.

6.2 Djalkmara and Corridor Creek Land Application Areas

The Djalkmara and Corridor Creek land application areas are located on top of natural radiation anomalies, as can be seen in Figure 39. The Djalkmara LAA lies on top of radiation Anomaly 4, whereas parts of the Corridor Creek land application areas lie on top of radiation Anomaly 5 (Ryan 1972; Eupene et al 1975). These anomalies are smaller in intensity and size than anomalies 1, 2 and 3, but both external gamma dose rates and radon flux densities are somewhat higher than the values for the surrounding areas. The average pre-mining values for the external gamma dose rate, radon activity flux and ^{226}Ra activity concentration estimated from our study for the Djalkmara LAA are $0.2 \mu\text{Gy}\cdot\text{hr}^{-1}$, $0.45 \text{ Bq}\cdot\text{m}^{-2}\cdot\text{s}^{-1}$ and $310 \text{ Bq}\cdot\text{kg}^{-1}$ respectively. For the Corridor Creek land application areas the averages are $0.13 \mu\text{Gy}\cdot\text{hr}^{-1}$, $0.23 \text{ Bq}\cdot\text{m}^{-2}\cdot\text{s}^{-1}$ and $160 \text{ Bq}\cdot\text{kg}^{-1}$.

The slightly higher than background external dose rates and radon flux densities measured in the Djalkmara and Corridor Creek land application areas are in agreement with measurements performed recently within these areas, as part of a project to determine the radiological status of the Ranger land application areas. The average external gamma dose rate determined for the Djalkmara LAA was $0.29 \pm 0.09 \mu\text{Gy}\cdot\text{hr}^{-1}$ excluding the contribution from applied radionuclides, and $0.21 \pm 0.06 \mu\text{Gy}\cdot\text{hr}^{-1}$ for the Corridor Creek LAA (Akber et al 2011a). The average radon flux density at the Djalkmara LAA was $0.66 \text{ Bq}\cdot\text{m}^{-2}\cdot\text{s}^{-1}$ and most of this radon exhalation was attributed to the existing radiation anomaly rather than applied radionuclides (Akber et al 2011b). The Corridor Creek average was $0.28 \text{ Bq}\cdot\text{m}^{-2}\cdot\text{s}^{-1}$, in good agreement with the values determined using the GIS model.

6.3 Environmental background

There are many data published on environmental background dose rates in the Alligator Rivers Region and close to Ranger uranium mine. Akber et al (2011) report background

external gamma dose rates for Jabiru East and the South Alligator Ranger Station of 0.09 and 0.07 $\mu\text{Gy}\cdot\text{hr}^{-1}$, respectively. Storm and Martin (1995) also measured background external gamma dose rates at Jabiru East and report values between 0.12 and 0.13 $\mu\text{Gy}\cdot\text{hr}^{-1}$. Lawrence (2005) measured external gamma dose rates (unpublished data) at Jabiru Water Tower, Jabiru East and the Mudginberri radon station and values there amounted to 0.14, 0.12 and 0.21 $\mu\text{Gy}\cdot\text{hr}^{-1}$, respectively.

In the Draft Jabiluka Environmental Impact Statement (ERA 1996) gamma dose rates are given for a 300m x 300m area covering parts of the Jabiluka evaporation pond and infrastructure, before works commenced. Assuming that the values reported are given in $\mu\text{Gy}\cdot\text{hr}^{-1}$ (rather than $\text{mGy}\cdot\text{hr}^{-1}$, see Table 9.5 in Main Report) the average at Jabiluka is 0.05 $\mu\text{Gy}\cdot\text{hr}^{-1}$, with a range of 0.035-0.083 $\mu\text{Gy}\cdot\text{hr}^{-1}$. These values are generally in agreement with the magnitude of background dose rates determined using our GIS data, which provides around 0.10 $\mu\text{Gy}\cdot\text{hr}^{-1}$ for Jabiru and Jabiru East, 0.08 $\mu\text{Gy}\cdot\text{hr}^{-1}$ for the South Alligator Ranger Station and 0.08 $\mu\text{Gy}\cdot\text{hr}^{-1}$ for Jabiluka.

Radon flux densities for environmental background sites calculated using the conversion factors above (equation 9) and assuming about 35 counts per second (typical for environmental background) up to 55 counts per second (determined for the Jabiru area) amount to 0.06 – 0.12 $\text{Bq}\cdot\text{m}^{-2}\cdot\text{s}^{-1}$. This is in agreement with values reported previously for the area (Lawrence 2005; Todd et al 1994).

7 Conclusions

Pre-mining radiological conditions have been determined from historic AGS data by groundtruthing an undisturbed radiological anomaly and extrapolating to the whole extent of the AGS including the unmined Ranger Project Area. The minimum footprint area that can be assessed is set by the optimum buffer radius determined when up-scaling the external gamma dose rates measured on the ground to the AGS data. For the current case this is approximately 4 ha. Thus, the correlation models developed allow estimates to be made of the pre-mining baseline gamma dose rates, ^{226}Ra soil activity concentrations and ^{222}Rn fluxes for any selected area larger than 4 ha covered by the 1976 AGS over the greater Ranger area.

Comparison with published data on external gamma dose rates, ^{226}Ra activity concentrations and ^{222}Rn flux densities measured in the greater Ranger region shows that our model estimates are in good agreement with radiation levels estimated previously via direct measurement on top of orebody 3, and from previous environmental radiation surveys. It has thus been shown that the model can reliably estimate the pre-mining radiological conditions at Ranger mine. Whereas the gamma dose rates, ^{226}Ra soil activity concentrations and ^{222}Rn fluxes for the Ranger Project Area as a whole (7881 ha) are on average not different from typical backgrounds measured in the region, there are areas, notably orebodies 1 (40 ha) and 3 (77 ha) and Anomaly 2 (38 ha), that exhibited gamma dose rates 3 to 9 times higher, and ^{226}Ra soil activity concentrations and ^{222}Rn flux densities, respectively, 7 to 20 times higher than typical environmental background. This needs to be taken into account when estimating pre-mining radiation doses that may have been received by indigenous people accessing the area around the orebodies before mining started.

The GIS model will also allow an estimate of pre-mining uptake of uranium series radionuclides into biota over the footprint of the Ranger mine, assuming secular equilibrium of the radionuclides in soils and using concentration ratios determined for bush Tucker in the region (eg Martin et al 1998; Ryan et al 2003) or from the BRUCE database (Doering et al in prep). This will facilitate the calculation of pre mining ingestion doses from the consumption of traditional foods harvested on site, in addition to an estimate of the internal and external radiation doses to humans and the environment.

References

- Akber RA & Pfitzner JL 1994. *Atmospheric concentrations of radon and radon daughters in Jabiru East*. Technical memorandum 45, Supervising Scientist for the Alligator Rivers Region, AGPS, Canberra.
- Akber R, Pfitzner J & Johnston A 1992. Radon transport from Ranger Uranium Mine: a review of the public radiation dose estimates. *Radiation Protection in Australia* 10, 41–46.
- Akber R, Lu P & Bollhöfer A 2011. ^{222}Rn in the land application areas. Energy Resources of Australia Ltd, Darwin.
- Australian Atomic Energy Commission (AAEC) 1963. Rum Jungle Project. A report on the uranium mining and treatment industry established by the Commonwealth Government at Rum Jungle, and its contribution to the development of the Northern Territory of Australia.
- Australian Radiation Protection and Nuclear Safety Agency (ARPANSA), 2005. Code of Practice and Safety Guide for Radiation Protection and Radioactive Waste Management in Mining and Mineral Processing. Radiation Protection Series Publication No 9.
- Australian Radiation Protection and Nuclear Safety Agency (ARPANSA) 2002. Recommendations for limiting exposure to ionizing radiation (1995) (Guidance note [NOHSC:3022(1995)]) and National standard for limiting occupational exposure to ionizing radiation [NOHSC:1013(1995)], Radiation Protection Series Publication No 1, Republished March 2002.
- Berkman DA 1968. The geology of the Rum Jungle uranium deposits. In *Uranium in Australia: symposium at Rum Jungle NT, June 16–21, 1968*. Australasian Institute of Mining and Metallurgy, Darwin Branch, 12–31.
- Bollhöfer A, Ryan B, Pfitzner K, Martin P & Iles M 2002. A radiation dose estimate for visitors of the South Alligator River valley, Australia, from remnants of uranium mining and milling activities. In *Uranium mining and hydrogeology III*, eds BJ Merkel, B Planer-Friedrich & C Wolkersdorfer. Technical University, Bergakademie Freiberg, 931–940.
- Bollhöfer A, Storm J, Martin P & Tims S 2005. Geographic variability in radon exhalation at a rehabilitated uranium mine in the Northern Territory, Australia. *Environmental Monitoring and Assessment* 114, 313–330.
- Bollhöfer A, Pfitzner K, Ryan B & Fawcett M 2007a. Ground truthing of an airborne gamma survey and assessment of the radiological conditions of the Sleinbeck mine area. Internal Report 526, June, Supervising Scientist, Darwin. Unpublished paper.
- Bollhöfer A, Pfitzner K, Ryan B, Espanon A, Brazier J & Jones D 2007b. Radiological assessment of Rum Jungle mine, Northern Territory. Report to the Department of Regional Development, Primary Industry, Fisheries and Resources, Northern Territory Government, Darwin.
- Bollhöfer A, Pfitzner K, Ryan B, Martin P, Fawcett M & Jones DR 2008. Airborne gamma survey of the historic Sleinbeck mine area in the Northern Territory, Australia, and its use for site rehabilitation planning. *Journal of Environmental Radioactivity* 99, 1770–1774.

- Bollhöfer A, Esparon A & Pfitzner K 2011. Pre-mining radiological conditions at Ranger mine. In *eriss research summary 2009–2010*. eds Jones DR & Webb A, Supervising Scientist Report 202, Supervising Scientist, Darwin NT, 101–106.
- Coetzee H, Wade P & Winde F 2006, Understanding environmental geophysical anomalies - An interdisciplinary case study from the West Rand. *South African Journal of Geology* 109, 495–502.
- Commonwealth of Australia, 1999. Environmental Requirements of the Commonwealth of Australia for the Operation of Ranger Uranium Mine.
- Conway NF, Davy DR, Giles MS, Newton PJF & Pollard DA 1974. *The Alligator Rivers Area Fact Finding Study*. Four Reports by the Australian Atomic Energy Commission (AAEC).
- Darnley AG 1972. Airborne gamma-ray survey techniques. In *Proceedings of a NATO sponsored Advanced Study Institute on Methods of Prospecting for Uranium Minerals*, eds Bowie SHU, Davis M & Ostle D, London Inst. Min. Metall, 174–211.
- Dickson BL & Snelling AA 1980. Movemenets of uranium and daughter isotopes in the Koongarra uranium deposit. In *Uranium in the Pine Creek Geosyncline. Proceedings of the International Uranium Symposium on the Pine Creek Geosyncline*. International Atomic Energy Agency, Vienna, 499–508.
- Durrani SA & Ilic R (eds) 1997. *Radon measurements by etched track detectors: Applications in radiation protection, earth sciences, and the environment*. World Scientific, Singapore.
- Esparon A, Pfitzner K, Bollhöfer A, Ryan B 2009. Pre-mining radiological conditions at Ranger mine. In *eriss research summary 2007–2008*. eds Jones DR & Webb A, Supervising Scientist Report 200, Supervising Scientist, Darwin NT, 111–116.
- Esparon A & Pfitzner J 2010. Visual gamma: *eriss* gamma analysis technical manual. Internal Report 539, December, Supervising Scientist, Darwin.
- Eupene GS, Fee PH & Colville RG 1975. Ranger 1 uranium deposits. In: *Economic geology of Australia and Papua New Guinea. 1. Metals*. ed Knight CL, Australasian Institute of Mining & Metallurgy; Monograph 5, 308–317.
- Foy MF & Pedersen CP 1975. Koongarra uranium deposit. In *Economic geology of Australia and Papua New Guinea. 1. Metals*. ed Knight CL, Australasian Institute of Mining & Metallurgy; Monograph 5, 317–321.
- Giblin A 2004. Alligator Rivers Uranium Deposits (Koongarra, Nabarlek and Ranger One) Northern Territory. CRC LEME, CSIRO Exploration and Mining.
- Hegge MR, Mosher DV, Eupene GS & Anthony PJ 1980. Geologic setting of the East Alligator uranium deposits and prospects. In *Uranium in the Pine Creek Geosyncline. Proceedings of the International Uranium Symposium on the Pine Creek Geosyncline*. International Atomic Energy Agency, Vienna, 259–272.
- International Atomic Energy Agency (IAEA) 1989. *Construction and use of calibration facilities for radiometric field equipment*. Technical Reports Series No 309, International Atomic Energy Agency, Vienna.
- International Commission on Radiation Units and Measurements (ICRU) 1994. *Gamma-ray spectrometry in the environment*. ICRU Report 53.

- International Commission on Radiological Protection (ICRP) 2000. *Radiation protection recommendations as applied to the disposal of long-lived solid radioactive waste*. ICRP Publication 81, Pergamon Press, Oxford.
- Knoll GF 1979. *Radiation detection and measurement*. 2nd edn, John Wiley & Sons, New York.
- Kvasnicka J & Auty RF 1994. Assessment of background radiation exposures at Ranger Uranium Mine. *Radiation Protection in Australia* October 12(4), 126–134.
- Lawrence CE 2005. Measurement of ²²²Rn exhalation rates and ²¹⁰Pb deposition rates in a tropical environment. PhD thesis. Queensland University of Technology, Brisbane.
- Lawrence CE, Akber RA, Bollhöfer A & Martin P 2009. Radon-222 exhalation from open ground on and around a uranium mine in the wet-dry tropics. *Journal of Environmental Radioactivity* 100, 1–8.
- Marten R 1992. External gamma dose rate survey of the Ranger Uranium Mine land application plot. In: *Proceedings of the Workshop on Land Application of Effluent Water from Uranium Mines in the Alligator Rivers Region*. Supervising Scientist for the Alligator Rivers Region, AGPS, Canberra.
- Marten R 1992. Procedures for routine analysis of naturally occurring radionuclides in environmental samples by gamma-ray spectrometry with HPGe detectors. Internal report 76, Supervising Scientist for the Alligator Rivers Region, Canberra. Unpublished paper.
- Martin P, Tims S, Ryan B & Bollhöfer A 2004. A radon and meteorological measurement network for the Alligator Rivers Region, Australia. *Journal of Environmental Radioactivity* 76, 35–49.
- Martin P, Tims S, McGill A, Ryan B & Pfitzner K 2006. Use of airborne γ -ray spectrometry for environmental assessment of the rehabilitated Nabarlek uranium mine, northern Australia. *Environmental Monitoring and Assessment* 115, 531–553.
- Murray AS, Marten R, Johnston A & Martin P 1987. Analysis for naturally occurring radionuclides at environmental concentrations by gamma spectrometry. *Journal of Radioanalytical and Nuclear Chemistry, Articles* 115, 263–288.
- Northern Territory Geological Survey (NTGS) 2007. MODAT, mineral occurrence database [electronic resource (CD)], Darwin. ISSN 1445-5358.
- Pfitzner J 2010. *eriss* HPGe detector calibration. Internal Report 576, October, Supervising Scientist, Darwin. Unpublished paper.
- Pfitzner K & Martin P 2000. Airborne gamma survey of the South Alligator River valley: First report. Internal Report 353, Supervising Scientist, Darwin. Unpublished paper.
- Pfitzner K & Martin P 2003. An assessment of radiation anomalies in the Alligator Rivers Region – a review. Internal Report 446, July, Supervising Scientist, Darwin. Unpublished paper.
- Pfitzner K, Martin P & Ryan B 2001a. Airborne gamma survey of the upper South Alligator River valley: Second Report. Internal Report 377, Supervising Scientist, Darwin. Unpublished paper.
- Pfitzner K, Ryan B, Bollhöfer & Martin P 2001b. Airborne gamma survey of the upper South Alligator River valley: Third Report. Internal Report 383, Supervising Scientist, Darwin. Unpublished paper.

- Pfitzner K, Ryan B & Martin P 2003. Airborne gamma survey of the Sleinbeck mine area. Internal Report 400, January, Supervising Scientist, Darwin. Unpublished paper.
- Porstendorfer J 1994. Properties and behaviour of radon and thoron and their decay products in the air. *Journal of Aerosol Science* 25(2), 219–263.
- Ryan GR 1972. Ranger 1: a case study. In *Proceedings of a NATO sponsored Advanced Study Institute on Methods of Prospecting for Uranium Minerals*, eds Bowie SHU, Davis M & Ostle D, London Institute of Mining and Metallurgy, 296–400.
- Saito K & Jacob P 1995. Gamma ray fields in the air due to sources in the ground. *Radiat. Prot. Dosim.* 58(1), 29–45.
- Snelling AA 1980. Uraninite and its alteration products, Koongarra uranium deposit. In *Uranium in the Pine Creek Geosyncline. Proceedings of the International Uranium Symposium on the Pine Creek Geosyncline*. International Atomic Energy Agency, Vienna, 487–498.
- Spehr W & Johnston A 1983. The measurement of radon exhalation rates using activated charcoal. *Radiation Protect. Australia* 1(3), 113–116.
- Tipper DB & Lawrence G 1972. The Nabarlek area, Arnhemland, Australia: a case history. In *Proceedings of a NATO sponsored Advanced Study Institute on Methods of Prospecting for Uranium Minerals*, eds Bowie SHU, Davis M & Ostle D, London Inst. Min. Metall., 301–305.
- Todd R, Akber RA & Martin P 1998. ^{222}Rn and ^{220}Rn activity flux from the ground in the vicinity of Ranger Uranium Mine. Internal report 279, Supervising Scientist, Canberra. Unpublished paper.
- Tucker DH, Stuart DC, Hone IG & Sampath N 1980. The characteristics and interpretation of regional gravity, magnetic and radiometric surveys in the Pine Creek Geosyncline. In *Uranium in the Pine Creek Geosyncline. Proceedings of the International Uranium Symposium on the Pine Creek Geosyncline*. International Atomic Energy Agency, Vienna, 101–140.
- Winkelmann I, Thomas M & Vogl K 2001. Aerial measurements on uranium ore mining, milling and processing areas in Germany. *Journal of Environmental Radioactivity* 53, 301–311.

Appendix A Results of external gamma dose rate and in-situ soil activity concentration measurements

Appendix A1 γ dose rates and in-situ γ -spectrometry results from Anomaly 2 survey (4 pixels at 70 m x 70 m each) conducted 21–24 August 2007. GM tube 1 was used for dose rate measurements, a GS-512 hand held NaI gamma spectrometer (*Geofyzika*, now *SatisGeo*) was used for in-situ γ -spectrometry.

line	pos	UTM easting	UTM northing	counts/100s	uGy/hr meas	uGy/hr calc	+-	K %	U ppm	Th ppm
37-16	1	272510.41	8593989	249	0.15	0.160	0.010	0.2	5.4	8.5
37-0	2	272519.43	8593993	245	0.175	0.158	0.010	0.1	7.8	9.2
37-39	3	272503.26	8593978	203	0.1	0.132	0.009	0.1	3.4	6.6
37-24	4	272515.9	8593982	250	0.14	0.161	0.010	0.2	6.1	8.2
37-14	5	272512.35	8593972	238	0.15	0.153	0.010	0.1	4.2	5.1
37-27	6	272519.57	8593976	223	0.125	0.144	0.009	0.1	4.9	6.1
37-02	7	272528.78	8593956	234	0.125	0.151	0.009	0.1	4.7	5.9
37-09	8	272528.72	8593963	245	0.14	0.158	0.010	0.3	5.3	7
37-06	9	272514.25	8593961	229	0.125	0.148	0.009	0.2	4.3	7
37-03	10	272528.78	8593956	249	0.14	0.160	0.010	0.1	6.2	6.2
37-33	11	272536.08	8593949	250	0.15	0.161	0.010	0.2	5.6	7.9
37-32	12	272528.86	8593947	225	0.14	0.145	0.009	0.2	5.4	7.1
37-35	13	272510.75	8593947	233	0.15	0.150	0.009	0.2	4	6.7
37-05	14	272516.24	8593939	230	0.125	0.149	0.009	0.2	4	5.8
37-11	15	272523.51	8593936	233	0.125	0.150	0.009	0.2	4.6	6.8
37-17	16	272530.77	8593934	223	0.125	0.144	0.009	0.2	3.8	6
37-20	17	272534.36	8593938	240	0.14	0.155	0.010	0.3	3.6	6.6
37-10	18	272539.87	8593928	235	0.15	0.152	0.010	0.1	4.4	6.8
37-15	19	272534.48	8593923	223	0.125	0.144	0.009	0	5.2	6.5
37-13	20	272541.72	8593923	235	0.14	0.152	0.010	0.1	4.8	6.4
37-34	21	272547.14	8593925	225	0.125	0.145	0.009	0.1	5	7.1
37-07	22	272543.46	8593932	249	0.13	0.160	0.010	0.2	4.3	5.7
37-08	23	272559.81	8593925	259	0.15	0.166	0.010	0.2	5.2	7.6
37-18	24	272567.03	8593929	242	0.1	0.156	0.010	0.1	7.5	7.8
37-29	25	272563.37	8593932	244	0.15	0.157	0.010	0.2	6.3	7.3
37-26	26	272568.69	8593947	279	0.14	0.179	0.010	0.2	8.5	8.3
37-04	27	272564.99	8593956	289	0.15	0.185	0.011	0.2	11.7	7.7
37-38	28	272543.31	8593951	237	0.14	0.153	0.010	0.1	6.1	5.7
37-30	29	272539.62	8593960	239	0.15	0.154	0.010	0.1	6.4	5.6
37-12	30	272555.91	8593960	289	0.16	0.185	0.011	0.3	8.8	7.5
37-31	31	272563.12	8593964	304	0.175	0.194	0.011	0.2	9.5	8.7
37-36	32	272543.21	8593964	232	0.14	0.150	0.009	0.2	6.2	7.9
37-28	33	272552.23	8593967	268	0.125	0.172	0.010	0.2	8	7.6
37-22	34	272537.72	8593971	255	0.14	0.164	0.010	0.1	6.3	7.5
37-21	35	272539.48	8593976	239	0.13	0.154	0.010	0.2	7	6.6
37-25	36	272535.85	8593978	254	0.15	0.163	0.010	0.2	6	6.3
37-19	37	272552.13	8593980	271	0.14	0.174	0.010	0.3	6.9	6.8
37-37	38	272568.42	8593980	315	0.15	0.201	0.011	0.2	11.5	10.4
37-01	39	272559.32	8593986	272	0.15	0.175	0.010	0.2	9.8	9.1
37-23	40	272550.23	8593991	252	0.15	0.162	0.010	0.2	9.4	10.1
266-99	1	273064	8593658	325	0.15	0.207	0.011	0.3	12.7	12.6
266-101	2	273063.5	8593658	322	0.15	0.206	0.011	0.3	12.7	12.4

line	pos	UTM easting	UTM northing	counts/ 100s	uGy/hr meas	uGy/hr calc	+-	K %	U ppm	Th ppm
266-92	3	273076.13	8593663	335	0.18	0.214	0.011	0.4	11.8	15.1
266-114	4	273083.39	8593662	346	0.16	0.220	0.012	0.2	14	12.6
266-81	5	273092.52	8593653	353	0.2	0.225	0.012	0.2	14.2	13.3
266-94	6	273085.35	8593643	334	0.175	0.213	0.011	0.2	12.5	11.3
266-112	7	273074.49	8593643	352	0.2	0.224	0.012	0.1	13.4	13.3
266-117	8	273101.6	8593649	323	0.2	0.206	0.011	0.1	13.6	12.1
266-107	9	273116.13	8593644	323	0.19	0.206	0.011	0.2	12.3	10.4
266-95	10	273123.34	8593647	354	0.19	0.225	0.012	0.2	12.3	10.7
266-100	11	273123.27	8593656	364	0.16	0.232	0.012	0.2	15.1	12.4
266-108	12	273108.77	8593658	368	0.2	0.234	0.012	0.3	14.5	12.2
266-97	13	273114.17	8593662	356	0.21	0.227	0.012	0.2	16.3	14
266-83	14	273106.87	8593669	346	0.2	0.220	0.012	0.3	14.3	12.8
266-102	15	273101.47	8593666	319	0.2	0.204	0.011	0.1	15.6	13.6
266-85	16	273094.25	8593662	362	0.19	0.230	0.012	0.2	13.7	13.3
266-105	17	273117.7	8593673	432	0.21	0.274	0.013	0.3	18.6	13.7
266-110	18	273124.9	8593679	392	0.2	0.249	0.012	0.2	20	15.4
266-104	19	273119.45	8593680	450	0.2	0.285	0.013	0.1	22.9	14.4
266-103	20	273115.79	8593686	374	0.25	0.238	0.012	0.3	22.9	13
266-89	21	273108.53	8593688	447	0.25	0.283	0.013	0.3	22.6	13.6
266-119	22	273103.17	8593678	406	0.21	0.258	0.012	0.2	21.3	13.1
266-116	23	273099.54	8593680	414	0.2	0.263	0.013	0.2	20.1	13
266-111	24	273104.88	8593691	411	0.21	0.261	0.013	0.1	21.9	12.9
266-115	25	273117.55	8593691	566	0.23	0.357	0.015	0.2	34.5	15.3
266-80	26	273126.53	8593701	573	0.24	0.361	0.015	0.2	38	15.7
266-96	27	273113.83	8593704	549	0.24	0.346	0.015	0.2	34.9	15.1
266-93	28	273108.41	8593702	483	0.24	0.305	0.014	0.4	32.1	15.1
266-86	29	273092.19	8593693	448	0.24	0.284	0.013	0.3	24.7	14.5
266-90	30	273090.41	8593689	406	0.22	0.258	0.012	0.2	21.9	12.9
266-84	31	273088.53	8593699	468	0.22	0.296	0.013	0.3	26.8	14.3
266-98	32	273081.27	8593700	477	0.25	0.302	0.014	0	28.1	13.7
266-87	33	273081.34	8593691	438	0.25	0.277	0.013	0.3	23.5	16.9
266-109	34	273081.37	8593688	390	0.19	0.248	0.012	0.2	19.7	15.4
266-118	35	273075.87	8593697	428	0.21	0.271	0.013	0	25.3	16.8
266-91	36	273075.78	8593708	533	0.23	0.336	0.014	0.3	33.3	16.6
266-82	37	273068.7	8593687	393	0.21	0.250	0.012	0.2	18.4	12.7
266-88	38	273061.5	8593682	379	0.18	0.241	0.012	0.3	15.2	13.8
266-113	39	273070.58	8593678	349	0.2	0.222	0.012	0.4	16.4	13.7
266-106	40	273076.02	8593678	360	0.2	0.229	0.012	0.2	15.2	12.7
267	1	273158	8593807	705	0.4	0.443	0.016	0.4	55.7	12
267	2	273161	8593793	545	0.35	0.344	0.014	0.3	40.3	9.6
267	3	273141	8593821	1089	0.6	0.681	0.020	0.7	103.6	9.3
267	4	273188	8593804	503	0.3	0.318	0.014	0.4	35.9	5.1
267	5	273162	8593840	654	0.4	0.411	0.016	0.4	50.1	10.7
267	6	273165	8593808	626	0.35	0.394	0.016	0.3	51.2	9.8
267	7	273153	8593814	683	0.4	0.429	0.016	0.7	51	8.7
267	8	273154	8593800	637	0.45	0.401	0.016	0.7	51.3	10.4
267	9	273157	8593800	596	0.35	0.375	0.015	0.3	43.2	8.2
267	10	273166	8593820	546	0.3	0.344	0.014	0.5	36.1	7.3
267	11	273174	8593806	552	0.25	0.348	0.015	0.3	37.4	6.1
267	12	273191	8593806	464	0.25	0.294	0.013	0.3	33.9	5.1
267	13	273197	8593803	591	0.4	0.372	0.015	0.5	43.7	5.6
267	14	273181	8593807	508	0.25	0.321	0.014	0.3	35.7	6.3

line	pos	UTM easting	UTM northing	counts/ 100s	uGy/hr meas	uGy/hr calc	+-	K %	U ppm	Th ppm
267	15	273185	8593816	517	0.3	0.326	0.014	0.2	37.1	6.7
267	16	273181	8593822	635	0.3	0.400	0.016	0.3	45.8	5.5
267	17	273177	8593825	628	0.3	0.395	0.016	0.4	44.2	5
267	18	273171	8593824	591	0.35	0.372	0.015	0.2	44.7	5.8
267	19	273156	8593821	755	0.35	0.474	0.017	0.5	60.7	10.8
267	20	273139	8593812	1120	0.6	0.700	0.021	0.6	108.4	7.3
267	21	273142	8593807	876	0.6	0.549	0.018	1	75.2	11.5
267	22	273135	8593803	1061	0.7	0.664	0.020	0.7	90.4	13.3
267	23	273131	8593794	958	0.6	0.600	0.019	0.5	91.7	11.4
267	24	273139	8593787	891	0.5	0.558	0.019	0.6	78.8	9.1
267	25	273150	8593790	607	0.35	0.382	0.015	0.4	44.9	8.3
267	26	273158	8593786	570	0.25	0.359	0.015	0.6	36.4	7.2
267	27	273158	8593783	495	0.25	0.313	0.014	0.4	33.8	7
267	29	273171	8593784	522	0.35	0.330	0.014	0.6	36.8	8.8
267	28	273156	8593821	549	0.35	0.346	0.015	0.3	41.5	10
267	30	273180	8593792	559	0.3	0.352	0.015	0.3	36	7.5
267	31	273184	8593791	514	0.3	0.325	0.014	0.4	36.9	7.9
267	32	273190	8593784	601	0.35	0.379	0.015	0.3	44.8	10.4
267	33	273186	8593782	614	0.35	0.387	0.015	0.4	43.7	10.7
267	34	273194	8593786	513	0.3	0.324	0.014	0.3	32.7	9.3
267	35	273195	8593785	511	0.3	0.323	0.014	0	33.5	8
267	36	273194	8593808	519	0.275	0.328	0.014	0.4	36.4	6.2
267	37	273181	8593849	1008	0.5	0.631	0.020	0.7	96.1	7.9
267	38	273155	8593844	1305	0.85	0.815	0.022	0.8	133.1	7.2
267	39	273144	8593848	986	0.6	0.617	0.019	0.6	92.4	4.9
267	40	273151	8593852	1273	0.7	0.795	0.022	0.8	124	5.9
720	1	272874	8593490	1083	0.6	0.677	0.020	1.2	97	10.2
720	2	272866	8593493	872	0.55	0.547	0.018	1.1	65.4	8.8
720	3	272864	8593499	1115	0.55	0.697	0.021	1.2	94.4	10.3
720	4	272856	8593492	851	0.45	0.534	0.018	0.5	67.9	7.2
720	5	272859	8593482	963	0.5	0.603	0.019	0.8	80.9	9.5
720	6	272855	8593476	963	0.55	0.603	0.019	1	87.3	8.4
720	7	272868	8593477	2282	1.4	1.421	0.030	2.2	227.5	13.3
720	8	272876	8593473	2171	1.4	1.352	0.029	2.8	244.5	14.7
720	9	272862	8593467	1685	1.25	1.051	0.025	1.9	183.6	11.6
720	10	272860	8593461	1330	0.85	0.831	0.023	2.2	136.8	9.9
720	11	272865	8593460	5578	3.5	3.464	0.046			
720	12	272863	8593454	5474	3.5	3.400	0.046			
720	13	272866	8593444	17184	11	10.660	0.081			
720	14	272866	8593437	19151	13	11.880	0.086			
720	15	272871	8593444	13092	8	8.123	0.071			
720	16	272878	8593448	3742	2.5	2.326	0.038	5.4	431.8	37.4
720	17	272872	8593454	3343	2	2.079	0.036	4.6	388.8	31.7
720	18	272874	8593463	2757	1.15	1.715	0.033	3.2	340.4	22.4
720	19	272884	8593454	3429	2	2.132	0.036	3.9	392	27.2
720	hot	272886	8593455	22015	15	13.655	0.092			
720	20	272891	8593457	12906	8	8.008	0.070			
720	21	272889	8593445	1811	1	1.129	0.026	1.2	175.7	7.9
720	22	272908	8593444	1306	0.7	0.816	0.022	1.1	121.9	5.9
720	23	272917	8593441	1000	0.6	0.626	0.020	0.7	80.1	3.9
720	24	272918	8593452	1715	1.1	1.069	0.026	1.4	170.5	7.5
720	25	272900	8593457	8129	5	5.046	0.056			

line	pos	UTM easting	UTM northing	counts/ 100s	uGy/hr meas	uGy/hr calc	+-	K %	U ppm	Th ppm
720	27	272915	8593466	2694	1.5	1.676	0.032	3.2	306.3	19.8
720	28	272904	8593470	5224	3.5	3.245	0.045			
720	26	272906	8593462	6893	4.5	4.280	0.051			
720	29	272898	8593471	2089	1.3	1.301	0.028	1.8	222.5	11.9
720	30	272889	8593467	3193	2	1.986	0.035	3.1	321.1	21.6
720	31	272906	8593479	1820	1	1.134	0.026	2.1	187.9	11.3
720	32	272911	8593486	2284	1.4	1.422	0.030	1.8	254.3	14.3
720	33	272918	8593489	2241	1.25	1.395	0.029	2.3	263.8	18.6
720	34	272913	8593491	1288	0.8	0.804	0.022	0.4	123.7	10.5
720	35	272906	8593493	979	0.6	0.613	0.019	0.7	95.1	10
720	36	272904	8593498	1080	0.6	0.676	0.020	0.7	92.3	8.5
720	37	272899	8593490	1005	0.5	0.629	0.020	1.1	88.1	8.5
720	38	272898	8593501	993	0.55	0.622	0.020	0.8	85.1	8.9
720	39	272886	8593487	1109	0.65	0.693	0.021	1.2	92.1	7.8
720	40	272873	8593501	792	0.5	0.497	0.017	1	62.7	9.8

Appendix A2 γ dose rate results from Anomaly 2A survey conducted 21-24 July 2008. Measured values were read off the analogue dial in the field, calculated values used the calibration equation.

UTM Easting	UTM Northing	counts/ 100s	uGy/hr meas	uGy/hr calc	+-
272628.29	8593516.04	348	0.2	0.18	0.01
272642.76	8593518	346	0.2	0.18	0.01
272653.62	8593518.08	319	0.175	0.17	0.01
272660.86	8593518.14	379	0.2	0.20	0.01
272669.9	8593520.06	391	0.2	0.21	0.01
272680.76	8593520.15	356	0.2	0.19	0.01
272686.22	8593516.5	376	0.2	0.20	0.01
272693.46	8593516.56	317	0.175	0.17	0.01
272707.96	8593514.83	334	0.2	0.18	0.01
272720.64	8593514.93	381	0.25	0.20	0.01
272733.31	8593515.04	399	0.25	0.21	0.01
272747.79	8593515.15	428	0.25	0.23	0.01
272756.86	8593513.38	467	0.25	0.25	0.01
272769.5	8593517.17	509	0.25	0.27	0.01
272782.18	8593517.27	518	0.25	0.28	0.01
272794.81	8593522.91	665	0.35	0.36	0.01
272803.84	8593524.82	613	0.3	0.33	0.01
272809.31	8593521.18	637	0.35	0.34	0.01
272823.8	8593519.45	733	0.4	0.40	0.02
272836.51	8593515.87	744	0.4	0.40	0.02
272851.01	8593514.14	673	0.4	0.36	0.01
272858.25	8593514.2	623	0.35	0.34	0.01
272865.49	8593514.25	855	0.5	0.47	0.02
272874.54	8593514.33	826	0.45	0.45	0.02
272887.22	8593514.43	787	0.45	0.43	0.02
272905.29	8593518.26	624	0.4	0.34	0.01
272917.95	8593520.21	648	0.4	0.35	0.01
272925.22	8593516.58	609	0.4	0.33	0.01
272937.87	8593520.37	650	0.4	0.35	0.01
272950.54	8593520.47	558	0.35	0.30	0.01
272961.42	8593518.71	614	0.35	0.33	0.01
272975.92	8593516.99	794	0.45	0.43	0.02
272990.39	8593518.95	593	0.35	0.32	0.01
273004.87	8593519.06	457	0.25	0.24	0.01
273012.13	8593517.28	578	0.35	0.31	0.01
273021.19	8593515.51	519	0.3	0.28	0.01
273032.09	8593511.9	482	0.3	0.26	0.01
273046.57	8593512.02	386	0.25	0.20	0.01
273061.05	8593512.14	463	0.3	0.25	0.01
273070.11	8593512.21	454	0.3	0.24	0.01
273081	8593508.61	472	0.3	0.25	0.01
273091.86	8593508.7	473	0.3	0.25	0.01
273077.59	8593482.76	338	0.175	0.18	0.01
273064.9	8593484.5	470	0.3	0.25	0.01
273053.99	8593489.95	432	0.25	0.23	0.01
273041.3	8593491.69	481	0.3	0.26	0.01
273032.28	8593487.93	547	0.35	0.29	0.01
273021.39	8593491.53	664	0.4	0.36	0.01

UTM Eastings	UTM Northing	counts/ 100s	uGy/hr meas	uGy/hr calc	+-
273010.51	8593493.29	486	0.3	0.26	0.01
272996.01	8593495.02	454	0.25	0.24	0.01
272986.94	8593496.79	491	0.3	0.26	0.01
272976.06	8593498.54	581	0.35	0.31	0.01
272961.58	8593498.43	716	0.4	0.39	0.01
272947.1	8593498.31	1222	0.7	0.67	0.02
272936.23	8593498.22	1164	0.7	0.64	0.02
272925.4	8593494.45	1325	0.8	0.73	0.02
272910.95	8593490.64	2261	1	1.25	0.03
272896.43	8593494.22	1027	0.6	0.56	0.02
272878.31	8593495.91	1242	0.7	0.68	0.02
272865.64	8593495.81	948	0.5	0.52	0.02
272856.57	8593497.58	932	0.5	0.51	0.02
272843.88	8593499.33	829	0.5	0.45	0.02
272834.85	8593497.41	712	0.4	0.39	0.01
272820.35	8593499.14	530	0.3	0.28	0.01
272813.12	8593497.23	516	0.3	0.28	0.01
272796.83	8593497.1	642	0.35	0.35	0.01
272778.68	8593502.49	562	0.35	0.30	0.01
272764.21	8593500.53	501	0.3	0.27	0.01
272755.14	8593502.3	480	0.3	0.26	0.01
272742.48	8593500.36	379	0.25	0.20	0.01
272731.62	8593500.27	414	0.25	0.22	0.01
272717.13	8593500.15	325	0.2	0.17	0.01
272708.05	8593503.77	271	0.15	0.14	0.01
272699.01	8593501.85	279	0.15	0.14	0.01
272684.56	8593498.05	299	0.15	0.16	0.01
272668.24	8593501.6	377	0.25	0.20	0.01
272655.59	8593497.81	338	0.25	0.18	0.01
272644.73	8593497.72	411	0.25	0.22	0.01
272633.91	8593492.1	447	0.25	0.24	0.01
272626.67	8593492.05	406	0.2	0.22	0.01
272630.63	8593449.66	1109	0.7	0.61	0.02
272639.67	8593451.58	1137	0.7	0.62	0.02
272654.17	8593449.85	1022	0.6	0.56	0.02
272674.07	8593451.85	863	0.5	0.47	0.02
272690.38	8593450.14	899	0.5	0.49	0.02
272697.6	8593452.04	857	0.5	0.47	0.02
272708.47	8593452.13	1164	0.6	0.64	0.02
272715.71	8593452.19	1572	0.9	0.87	0.02
272726.59	8593450.43	1085	0.6	0.60	0.02
272739.25	8593452.38	962	0.5	0.53	0.02
272753.74	8593450.65	487	0.3	0.26	0.01
272764.59	8593452.58	403	0.2	0.21	0.01
272773.66	8593450.81	593	0.35	0.32	0.01
272788.13	8593452.77	1031	0.6	0.57	0.02
272802.63	8593451.04	576	0.3	0.31	0.01
272813.49	8593451.13	789	0.4	0.43	0.02
272824.35	8593451.22	844	0.5	0.46	0.02
272840.65	8593451.35	960	0.5	0.53	0.02

UTM Easting	UTM Northing	counts/ 100s	uGy/hr meas	uGy/hr calc	+-
272847.89	8593451.41	1215	0.7	0.67	0.02
272856.94	8593451.48	2135	1.25	1.18	0.03
272867.82	8593449.72	10834	6	6.06	0.06
272880.48	8593451.67	3291	2	1.83	0.03
272889.53	8593451.74	29049	15	16.26	0.10
272896.77	8593451.8	2391	1.5	1.33	0.03
272904.03	8593450.01	1688	1	0.93	0.02
272913.07	8593451.93	2125	1.25	1.18	0.03
272923.93	8593452.02	1030	0.5	0.56	0.02
272940.23	8593452.15	638	0.4	0.35	0.01
272958.33	8593452.29	661	0.4	0.36	0.01
272972.83	8593450.57	513	0.3	0.28	0.01
272980.07	8593450.63	563	0.35	0.30	0.01
272999.97	8593452.63	709	0.4	0.39	0.01
273009.04	8593450.86	854	0.5	0.47	0.02
273025.33	8593450.99	470	0.3	0.25	0.01
273039.82	8593451.11	339	0.2	0.18	0.01
273052.48	8593453.05	300	0.2	0.16	0.01
273063.35	8593451.29	277	0.15	0.14	0.01
273079.65	8593451.43	223	0.15	0.11	0.01
273088.7	8593451.5	241	0.15	0.12	0.01
273079.91	8593418.23	229	1	0.12	0.01
273072.66	8593420.02	209	0.1	0.11	0.01
273059.98	8593419.91	213	0.1	0.11	0.01
273047.31	8593419.81	212	0.1	0.11	0.01
273034.64	8593419.71	233	0.15	0.12	0.01
273023.79	8593417.78	245	0.15	0.13	0.01
273011.1	8593419.52	271	0.15	0.14	0.01
272998.44	8593417.58	284	0.15	0.15	0.01
272982.13	8593419.29	377	0.2	0.20	0.01
272973.08	8593419.22	388	0.2	0.21	0.01
272953.18	8593417.21	496	0.3	0.27	0.01
272936.87	8593418.92	575	0.35	0.31	0.01
272929.63	8593418.87	728	0.4	0.40	0.02
272916.94	8593420.61	908	0.5	0.50	0.02
272906.09	8593418.68	1224	0.6	0.67	0.02
272895.21	8593420.43	895	0.5	0.49	0.02
272880.75	8593418.47	1443	0.7	0.80	0.02
272864.45	8593418.34	12714	7.5	7.11	0.06
272857.21	8593418.28	21443	12.5	12.00	0.08
272842.73	8593418.17	870	0.5	0.48	0.02
272826.43	8593418.04	1224	0.7	0.67	0.02
272810.12	8593419.75	1211	0.7	0.67	0.02
272792.02	8593419.6	926	0.5	0.51	0.02
272782.96	8593419.53	848	0.5	0.46	0.02
272770.29	8593419.43	876	0.5	0.48	0.02
272754	8593419.3	774	0.4	0.42	0.02
272743.13	8593419.21	868	0.5	0.47	0.02
272734.08	8593419.14	822	0.4	0.45	0.02
272725.03	8593419.07	881	0.5	0.48	0.02

UTM Eastings	UTM Northings	counts/ 100s	uGy/hr meas	uGy/hr calc	+-
272708.73	8593418.93	1000	0.6	0.55	0.02
272699.68	8593418.86	839	0.5	0.46	0.02
272692.44	8593418.8	834	0.4	0.46	0.02
272679.77	8593418.7	806	0.4	0.44	0.02
272667.09	8593418.6	807	0.5	0.44	0.02
272654.42	8593418.5	725	0.4	0.39	0.02
272643.56	8593418.41	690	0.4	0.37	0.01
272632.68	8593420.17	646	0.4	0.35	0.01
272621.83	8593418.24	631	0.4	0.34	0.01
272629.32	8593386.94	683	0.4	0.37	0.01
272642	8593387.04	749	0.5	0.41	0.02
272647.44	8593385.24	900	0.5	0.49	0.02
272660.12	8593385.35	847	0.5	0.46	0.02
272669.17	8593385.42	966	0.5	0.53	0.02
272683.65	8593385.54	1627	0.9	0.90	0.02
272696.33	8593385.64	1130	0.6	0.62	0.02
272707.19	8593385.72	965	0.5	0.53	0.02
272721.67	8593385.84	756	0.45	0.41	0.02
272732.54	8593385.93	695	0.4	0.38	0.01
272745.21	8593386.03	784	0.5	0.43	0.02
272761.51	8593386.16	956	0.5	0.52	0.02
272775.99	8593386.28	1048	0.6	0.57	0.02
272788.66	8593386.38	1209	0.6	0.67	0.02
272801.34	8593386.48	1448	0.8	0.80	0.02
272810.39	8593386.55	1689	1	0.93	0.02
272819.44	8593386.63	1682	1	0.93	0.02
272830.3	8593386.72	1684	1	0.93	0.02
272844.79	8593386.83	2102	1.25	1.17	0.03
272861.1	8593385.12	10891	6	6.09	0.06
272875.58	8593385.23	2621	1.25	1.46	0.03
272884.63	8593385.31	1489	0.9	0.82	0.02
272895.5	8593385.39	871	0.5	0.48	0.02
272908.17	8593385.5	627	0.35	0.34	0.01
272924.46	8593385.63	430	0.25	0.23	0.01
272938.95	8593385.74	426	0.25	0.23	0.01
272953.43	8593385.86	304	0.2	0.16	0.01
272964.29	8593385.95	285	0.175	0.15	0.01
272975.16	8593386.04	234	0.125	0.12	0.01
272991.45	8593386.17	236	0.125	0.12	0.01
273000.5	8593386.24	212	0.125	0.11	0.01
273013.18	8593386.34	214	0.125	0.11	0.01
273025.85	8593386.44	220	0.125	0.11	0.01
273038.52	8593386.54	195	0.1	0.10	0.01
273053.02	8593384.82	208	0.125	0.10	0.01
273063.87	8593386.75	230	0.15	0.12	0.01
273080.17	8593386.88	216	0.125	0.11	0.01
273094.65	8593387	216	0.15	0.11	0.01
273080.34	8593364.75	199	0.125	0.10	0.01
273065.86	8593364.63	190	0.125	0.09	0.01
273056.81	8593364.56	198	0.125	0.10	0.01

UTM Eastings	UTM Northing	counts/ 100s	uGy/hr meas	uGy/hr calc	+-
273045.94	8593364.47	198	0.125	0.10	0.01
273038.7	8593364.41	218	0.125	0.11	0.01
273027.84	8593364.33	212	0.125	0.11	0.01
273004.3	8593364.14	223	0.125	0.11	0.01
272986.2	8593363.99	212	0.125	0.11	0.01
272966.28	8593363.83	220	0.125	0.11	0.01
272946.37	8593363.67	274	0.15	0.14	0.01
272937.32	8593363.6	291	0.15	0.15	0.01
272926.45	8593363.51	343	0.2	0.18	0.01
272911.97	8593363.4	389	0.25	0.21	0.01
272893.86	8593363.25	557	0.35	0.30	0.01
272879.38	8593363.13	849	0.5	0.46	0.02
272868.5	8593364.89	850	0.5	0.46	0.02
272854.03	8593362.93	658	0.4	0.36	0.01
272839.55	8593362.81	579	0.35	0.31	0.01
272828.67	8593364.57	533	0.3	0.29	0.01
272817.81	8593364.48	505	0.3	0.27	0.01
272806.95	8593364.4	447	0.3	0.24	0.01
272790.65	8593364.26	413	0.25	0.22	0.01
272779.79	8593364.18	458	0.25	0.24	0.01
272772.55	8593364.12	518	0.3	0.28	0.01
272761.68	8593364.03	416	0.25	0.22	0.01
272743.58	8593363.89	428	0.25	0.23	0.01
272727.28	8593363.75	423	0.25	0.22	0.01
272718.23	8593363.68	675	0.4	0.37	0.01
272709.18	8593363.61	550	0.3	0.30	0.01
272696.49	8593365.35	476	0.3	0.25	0.01
272685.64	8593363.42	473	0.25	0.25	0.01
272672.97	8593363.32	427	0.25	0.23	0.01
272662.09	8593365.07	543	0.3	0.29	0.01
272645.81	8593363.1	445	0.25	0.24	0.01
272627.69	8593364.8	468	0.25	0.25	0.01
272629.9	8593540.02	286	0.13	0.16	0.01
272646.2	8593540.16	290	0.16	0.16	0.01
272655.25	8593540.23	329	0.18	0.19	0.01
272666.11	8593540.32	355	0.20	0.20	0.01
272673.37	8593538.53	343	0.18	0.20	0.01
272684.22	8593540.46	366	0.22	0.21	0.01
272700.53	8593538.75	340	0.20	0.19	0.01
272709.57	8593540.67	345	0.17	0.20	0.01
272725.87	8593538.95	344	0.20	0.20	0.01
272734.94	8593537.18	377	0.18	0.22	0.01
272745.81	8593537.27	433	0.26	0.25	0.01
272760.27	8593539.23	469	0.28	0.27	0.01
272769.31	8593541.15	567	0.29	0.33	0.01
272781.97	8593543.09	540	0.28	0.32	0.01
272798.28	8593541.38	546	0.29	0.32	0.01
272812.78	8593539.65	450	0.25	0.26	0.01
272830.88	8593539.8	435	0.28	0.25	0.01
272845.38	8593538.07	466	0.28	0.27	0.01

UTM Eastings	UTM Northings	counts/ 100s	uGy/hr meas	uGy/hr calc	+-
272863.47	8593540.06	664	0.33	0.39	0.01
272877.96	8593540.18	502	0.29	0.29	0.01
272888.82	8593540.26	541	0.30	0.32	0.01
272897.89	8593538.49	520	0.32	0.30	0.01
272906.97	8593534.88	477	0.28	0.28	0.01
272925.03	8593540.55	557	0.30	0.33	0.01
272941.31	8593542.53	460	0.25	0.27	0.01
272955.81	8593540.8	468	0.25	0.27	0.01
272963.05	8593540.86	512	0.28	0.30	0.01
272975.72	8593540.96	491	0.28	0.29	0.01
272988.38	8593542.91	504	0.30	0.29	0.01
273002.88	8593541.18	503	0.27	0.29	0.01
273017.37	8593541.3	422	0.22	0.24	0.01
273031.86	8593539.57	409	0.23	0.24	0.01
273044.55	8593537.83	351	0.15	0.20	0.01
273055.4	8593539.76	370	0.20	0.21	0.01
273064.47	8593537.99	483	0.27	0.28	0.01
273073.51	8593539.9	396	0.22	0.23	0.01
273089.8	8593540.03	435	0.25	0.25	0.01
273079.2	8593506.75	371	0.18	0.21	0.01
273062.91	8593506.62	416	0.24	0.24	0.01
273044.8	8593506.47	443	0.28	0.26	0.01
273037.56	8593506.42	448	0.23	0.26	0.01
273026.7	8593506.33	488	0.25	0.28	0.01
273012.2	8593508.06	443	0.24	0.26	0.01
273003.15	8593507.98	424	0.28	0.25	0.01
272994.1	8593507.91	421	0.25	0.24	0.01
272985.06	8593505.99	431	0.23	0.25	0.01
272975.99	8593507.77	419	0.22	0.24	0.01
272961.51	8593507.65	552	0.32	0.32	0.01
272945.21	8593507.52	627	0.35	0.37	0.01
272934.35	8593507.43	848	0.45	0.50	0.02
272921.68	8593507.33	715	0.37	0.42	0.01
272907.19	8593507.21	889	0.52	0.53	0.02
272890.9	8593507.08	842	0.47	0.50	0.02
272885.47	8593507.04	888	0.51	0.53	0.02
272876.41	8593506.97	957	0.52	0.57	0.02
272865.55	8593506.88	818	0.49	0.49	0.02
272856.5	8593506.81	1350	0.85	0.81	0.02
272842.01	8593506.69	787	0.40	0.47	0.02
272831.15	8593506.6	665	0.35	0.39	0.01
272820.29	8593506.51	440	0.28	0.26	0.01
272811.24	8593506.44	443	0.29	0.26	0.01
272802.18	8593506.37	439	0.23	0.25	0.01
272787.68	8593508.1	632	0.32	0.37	0.01
272767.78	8593506.09	444	0.24	0.26	0.01
272758.72	8593507.86	454	0.28	0.26	0.01
272747.87	8593505.93	458	0.22	0.27	0.01
272731.57	8593505.8	295	0.14	0.17	0.01
272713.45	8593507.5	235	0.14	0.13	0.01

UTM Eastings	UTM Northings	counts/ 100s	uGy/hr meas	uGy/hr calc	+-
272691.73	8593507.32	288	0.16	0.16	0.01
272680.86	8593507.24	286	0.16	0.16	0.01
272668.19	8593507.14	321	0.18	0.18	0.01
272648.28	8593506.97	346	0.18	0.20	0.01
272631.98	8593506.84	317	0.16	0.18	0.01
272634.06	8593473.66	719	0.45	0.43	0.02
272653.97	8593473.82	716	0.38	0.42	0.01
272668.46	8593473.94	580	0.30	0.34	0.01
272675.7	8593474	505	0.28	0.30	0.01
272684.75	8593474.07	433	0.22	0.25	0.01
272699.24	8593474.19	406	0.20	0.23	0.01
272708.29	8593474.26	443	0.27	0.26	0.01
272720.96	8593474.36	361	0.18	0.21	0.01
272733.64	8593474.46	297	0.17	0.17	0.01
272744.5	8593474.55	275	0.15	0.15	0.01
272762.6	8593474.7	240	0.14	0.13	0.01
272775.28	8593474.8	312	0.13	0.18	0.01
272789.76	8593474.92	296	0.15	0.17	0.01
272802.45	8593473.17	539	0.22	0.32	0.01
272813.31	8593473.26	680	0.41	0.40	0.01
272829.61	8593473.39	476	0.24	0.28	0.01
272840.47	8593473.48	719	0.43	0.43	0.02
272851.33	8593473.57	839	0.42	0.50	0.02
272864.01	8593473.67	1113	0.65	0.67	0.02
272880.3	8593473.8	1289	0.67	0.77	0.02
272894.78	8593473.92	1603	0.95	0.97	0.02
272907.46	8593474.02	2225	1.20	1.34	0.03
272916.51	8593474.09	2648	1.60	1.60	0.03
272927.37	8593474.18	2800	1.50	1.70	0.03
272947.29	8593474.34	1270	0.68	0.76	0.02
272958.15	8593474.42	687	0.38	0.41	0.01
272969.02	8593474.51	593	0.38	0.35	0.01
272985.31	8593474.64	600	0.34	0.35	0.01
272996.19	8593472.89	498	0.30	0.29	0.01
273005.24	8593472.96	611	0.30	0.36	0.01
273014.29	8593473.03	898	0.54	0.53	0.02
273026.95	8593474.98	786	0.44	0.47	0.02
273037.83	8593473.22	487	0.27	0.28	0.01
273052.3	8593475.18	391	0.19	0.23	0.01
273063.18	8593473.42	397	0.18	0.23	0.01
273075.85	8593473.53	334	0.16	0.19	0.01
273084.9	8593473.6	332	0.18	0.19	0.01
273077.91	8593442.19	194	0.09	0.11	0.01
273065.25	8593440.24	191	0.09	0.10	0.01
273047.13	8593441.94	269	0.13	0.15	0.01
273032.65	8593441.83	289	0.15	0.16	0.01
273021.79	8593441.74	378	0.19	0.22	0.01
273009.11	8593441.64	449	0.30	0.26	0.01
272992.82	8593441.51	593	0.29	0.35	0.01
272978.33	8593441.39	843	0.42	0.50	0.02

UTM Eastings	UTM Northings	counts/ 100s	uGy/hr meas	uGy/hr calc	+-
272965.66	8593441.29	543	0.30	0.32	0.01
272952.99	8593441.19	601	0.28	0.35	0.01
272943.93	8593441.11	723	0.36	0.43	0.02
272931.26	8593441.01	667	0.38	0.39	0.01
272922.21	8593440.94	784	0.38	0.47	0.02
272907.73	8593440.82	1391	0.62	0.84	0.02
272896.86	8593440.73	1578	0.85	0.95	0.02
272887.81	8593440.66	1452	0.72	0.87	0.02
272878.76	8593440.59	1700	0.95	1.02	0.02
272864.27	8593440.47	17808	10.20	10.85	0.07
272849.79	8593440.36	1863	1.00	1.12	0.02
272831.68	8593440.21	848	0.42	0.50	0.02
272819.01	8593440.11	664	0.32	0.39	0.01
272804.51	8593441.84	1261	0.65	0.76	0.02
272797.27	8593441.78	1553	0.85	0.93	0.02
272786.41	8593441.69	1304	0.62	0.78	0.02
272771.92	8593441.57	918	0.53	0.55	0.02
272757.44	8593441.46	910	0.50	0.54	0.02
272744.77	8593441.36	839	0.44	0.50	0.02
272726.66	8593441.21	962	0.45	0.57	0.02
272717.61	8593441.14	1284	0.72	0.77	0.02
272710.37	8593441.08	1007	0.60	0.60	0.02
272701.31	8593441.01	998	0.45	0.60	0.02
272688.64	8593440.9	967	0.50	0.58	0.02
272677.78	8593440.82	938	0.55	0.56	0.02
272663.29	8593440.7	884	0.46	0.53	0.02
272656.05	8593440.64	891	0.42	0.53	0.02
272645.19	8593440.56	764	0.46	0.45	0.02
272628.89	8593440.42	911	0.50	0.54	0.02
272630.96	8593409.09	726	0.45	0.43	0.02
272641.82	8593409.17	724	0.43	0.43	0.02
272656.3	8593409.29	479	0.30	0.28	0.01
272667.18	8593407.53	689	0.40	0.41	0.01
272679.86	8593407.64	799	0.45	0.47	0.02
272694.34	8593407.75	962	0.54	0.57	0.02
272707.01	8593407.86	1157	0.62	0.69	0.02
272714.25	8593407.91	1097	0.63	0.66	0.02
272723.31	8593407.99	963	0.57	0.57	0.02
272739.6	8593408.12	834	0.45	0.50	0.02
272748.65	8593408.19	821	0.49	0.49	0.02
272763.14	8593408.31	807	0.50	0.48	0.02
272775.81	8593408.41	878	0.47	0.52	0.02
272790.3	8593408.52	838	0.48	0.50	0.02
272799.35	8593408.6	939	0.50	0.56	0.02
272806.59	8593408.66	1051	0.58	0.63	0.02
272817.47	8593406.9	1325	0.83	0.80	0.02
272833.75	8593408.87	1735	0.94	1.05	0.02
272846.42	8593408.98	1293	0.63	0.78	0.02
272862.73	8593407.26	2415	1.40	1.46	0.03
272875.4	8593407.36	1525	0.88	0.92	0.02

UTM Eastings	UTM Northings	counts/ 100s	uGy/hr meas	uGy/hr calc	+-
272882.65	8593407.42	1161	0.73	0.70	0.02
272898.94	8593407.55	1040	0.58	0.62	0.02
272917.04	8593407.7	1021	0.50	0.61	0.02
272931.53	8593407.82	731	0.38	0.43	0.02
272947.82	8593407.95	489	0.30	0.29	0.01
272960.5	8593408.05	334	0.18	0.19	0.01
272974.98	8593408.17	311	0.16	0.18	0.01
272993.08	8593408.31	258	0.14	0.14	0.01
273000.33	8593408.37	259	0.14	0.14	0.01
273011.19	8593408.46	253	0.13	0.14	0.01
273023.86	8593408.56	244	0.13	0.14	0.01
273032.92	8593408.63	210	0.12	0.12	0.01
273049.21	8593408.76	189	0.15	0.10	0.01
273063.69	8593408.88	214	0.16	0.12	0.01
273070.94	8593408.94	206	0.12	0.11	0.01
273083.61	8593409.04	211	0.13	0.12	0.01
273082.08	8593373.98	217	0.10	0.12	0.01
273071.22	8593373.9	214	0.13	0.12	0.01
273054.91	8593375.61	234	0.14	0.13	0.01
273044.05	8593375.52	205	0.10	0.11	0.01
273027.75	8593375.39	184	0.11	0.10	0.01
273018.7	8593375.32	200	0.11	0.11	0.01
273009.65	8593375.25	222	0.12	0.12	0.01
272995.16	8593375.13	210	0.10	0.12	0.01
272980.68	8593375.01	204	0.12	0.11	0.01
272960.76	8593374.85	244	0.13	0.14	0.01
272948.09	8593374.75	266	0.15	0.15	0.01
272933.61	8593374.64	300	0.18	0.17	0.01
272924.55	8593374.56	302	0.17	0.17	0.01
272910.07	8593374.45	376	0.21	0.22	0.01
272899.21	8593374.36	655	0.36	0.39	0.01
272890.15	8593374.29	941	0.49	0.56	0.02
272879.29	8593374.2	1520	0.75	0.91	0.02
272866.6	8593375.94	2809	1.80	1.70	0.03
272850.32	8593373.97	3510	2.00	2.13	0.03
272835.82	8593375.69	1487	0.82	0.89	0.02
272824.96	8593375.61	1143	0.62	0.68	0.02
272808.67	8593375.48	834	0.43	0.50	0.02
272797.8	8593375.39	700	0.38	0.41	0.01
272783.32	8593375.27	712	0.37	0.42	0.01
272772.46	8593375.18	937	0.50	0.56	0.02
272759.78	8593375.08	644	0.37	0.38	0.01
272754.35	8593375.04	585	0.30	0.34	0.01
272738.06	8593374.91	617	0.31	0.36	0.01
272725.38	8593374.81	652	0.35	0.38	0.01
272709.09	8593374.67	707	0.37	0.42	0.01
272692.8	8593374.54	754	0.46	0.45	0.02
272680.12	8593374.44	864	0.50	0.51	0.02
272663.83	8593374.31	748	0.40	0.44	0.02
272656.57	8593376.1	755	0.38	0.45	0.02

UTM Easting	UTM Northing	counts/ 100s	uGy/hr meas	uGy/hr calc	+-
272647.53	8593374.18	627	0.35	0.37	0.01
272631.22	8593375.89	517	0.30	0.30	0.01
272631.8	8593528.97	329	0.12	0.19	0.01
272642.67	8593529.06	281	0.07	0.16	0.01
272649.89	8593530.96	280	0.1	0.16	0.01
272658.93	8593532.88	304	0.1	0.17	0.01
272667.98	8593532.95	292	0.1	0.16	0.01
272682.5	8593529.38	337	0.1	0.19	0.01
272695.16	8593531.33	353	0.11	0.20	0.01
272706	8593533.26	310	0.12	0.18	0.01
272716.87	8593533.35	306	0.09	0.17	0.01
272729.56	8593531.6	245	0.09	0.14	0.01
272738.64	8593527.99	290	0.1	0.16	0.01
272747.69	8593528.06	365	0.11	0.21	0.01
272758.52	8593531.84	420	0.15	0.24	0.01
272767.56	8593533.75	390	0.12	0.22	0.01
272782.06	8593532.03	592	0.22	0.35	0.01
272794.75	8593530.28	622	0.23	0.37	0.01
272809.25	8593528.56	574	0.22	0.34	0.01
272818.28	8593530.47	568	0.21	0.33	0.01
272832.75	8593532.43	538	0.2	0.31	0.01
272847.25	8593530.71	489	0.19	0.28	0.01
272854.51	8593528.92	465	0.16	0.27	0.01
272865.39	8593527.16	903	0.42	0.54	0.02
272876.24	8593529.1	714	0.3	0.42	0.01
272885.3	8593527.32	704	0.3	0.42	0.01
272892.51	8593531.07	565	0.23	0.33	0.01
272899.76	8593531.13	562	0.2	0.33	0.01
272914.23	8593533.09	561	0.28	0.33	0.01
272926.91	8593531.35	540	0.23	0.32	0.01
272939.56	8593535.14	610	0.26	0.36	0.01
272948.6	8593537.05	577	0.3	0.34	0.01
272959.49	8593533.45	553	0.22	0.32	0.01
272972.18	8593531.71	601	0.25	0.35	0.01
272981.23	8593531.78	713	0.3	0.42	0.01
272992.09	8593531.87	575	0.25	0.34	0.01
273004.75	8593533.82	503	0.23	0.29	0.01
273013.79	8593535.73	431	0.17	0.25	0.01
273026.49	8593532.15	451	0.16	0.26	0.01
273037.37	8593530.39	358	0.13	0.21	0.01
273053.66	8593530.52	326	0.17	0.19	0.01
273062.72	8593530.59	350	0.1	0.20	0.01
273071.75	8593532.51	389	0.1	0.22	0.01
273082.66	8593527.07	533	0.15	0.31	0.01
273077.48	8593495.67	379	0.12	0.22	0.01
273068.41	8593497.44	443	0.15	0.26	0.01
273055.77	8593493.65	372	0.15	0.21	0.01
273041.26	8593497.22	543	0.22	0.32	0.01
273030.36	8593500.83	462	0.21	0.27	0.01
273021.31	8593500.75	408	0.17	0.24	0.01

UTM Eastings	UTM Northings	counts/ 100s	uGy/hr meas	uGy/hr calc	+-
273012.24	8593502.52	418	0.16	0.24	0.01
272999.57	8593502.42	464	0.17	0.27	0.01
272983.28	8593502.29	428	0.18	0.25	0.01
272974.24	8593500.37	454	0.2	0.26	0.01
272965.19	8593500.3	545	0.22	0.32	0.01
272957.94	8593500.24	676	0.25	0.40	0.01
272950.72	8593498.34	868	0.35	0.52	0.02
272936.22	8593500.07	906	0.4	0.54	0.02
272927.15	8593501.84	933	0.42	0.56	0.02
272914.48	8593501.74	1047	0.49	0.62	0.02
272901.77	8593505.32	985	0.28	0.59	0.02
272889.09	8593507.07	869	0.45	0.52	0.02
272878.22	8593506.98	938	0.47	0.56	0.02
272865.61	8593499.5	933	0.38	0.56	0.02
272856.57	8593497.58	1000	0.37	0.60	0.02
272843.91	8593495.64	897	0.4	0.53	0.02
272834.85	8593497.41	586	0.28	0.34	0.01
272818.55	8593497.28	434	0.19	0.25	0.01
272807.72	8593493.5	633	0.23	0.37	0.01
272798.65	8593495.27	594	0.24	0.35	0.01
272785.98	8593495.17	560	0.26	0.33	0.01
272778.72	8593496.96	547	0.23	0.32	0.01
272767.86	8593496.87	436	0.14	0.25	0.01
272755.18	8593496.77	569	0.17	0.33	0.01
272753.34	8593500.44	394	0.18	0.23	0.01
272742.51	8593496.67	340	0.17	0.19	0.01
272733.46	8593496.59	437	0.15	0.25	0.01
272724.42	8593494.68	326	0.13	0.19	0.01
272711.72	8593498.26	283	0.13	0.16	0.01
272699.04	8593498.16	321	0.08	0.18	0.01
272680.95	8593496.17	295	0.07	0.17	0.01
272670.06	8593499.77	292	0.07	0.16	0.01
272659.2	8593499.69	351	0.1	0.20	0.01
272646.54	8593497.74	328	0.11	0.19	0.01
272635.69	8593495.81	306	0.1	0.17	0.01
272623.02	8593495.71	309	0.12	0.18	0.01
272630.53	8593462.57	894	0.12	0.53	0.02
272643.19	8593464.51	978	0.33	0.58	0.02
272654.05	8593464.6	1090	0.57	0.65	0.02
272668.5	8593468.41	691	0.41	0.41	0.01
272679.37	8593468.49	643	0.31	0.38	0.01
272693.89	8593463.08	772	0.38	0.46	0.02
272704.74	8593465.01	651	0.33	0.38	0.01
272715.61	8593465.1	609	0.29	0.36	0.01
272724.66	8593465.17	555	0.31	0.33	0.01
272735.54	8593463.41	589	0.12	0.35	0.01
272746.38	8593465.35	327	0.13	0.19	0.01
272764.49	8593465.49	247	0.09	0.14	0.01
272771.75	8593463.7	274	0.13	0.15	0.01
272786.21	8593465.67	805	0.29	0.48	0.02

UTM Eastings	UTM Northings	counts/ 100s	uGy/hr meas	uGy/hr calc	+-
272795.27	8593465.74	744	0.42	0.44	0.02
272806.13	8593465.83	707	0.27	0.42	0.01
272818.79	8593467.77	709	0.3	0.42	0.01
272829.67	8593466.01	619	0.31	0.36	0.01
272840.54	8593464.26	710	0.26	0.42	0.01
272849.57	8593468.02	862	0.35	0.51	0.02
272860.44	8593466.26	1175	0.52	0.70	0.02
272873.15	8593462.68	2688	1.3	1.63	0.03
272884.01	8593462.76	6285	2.9	3.82	0.04
272898.48	8593464.72	11192	8.1	6.81	0.06
272905.72	8593464.78	5804	4	3.52	0.04
272920.19	8593466.74	2916	1.4	1.76	0.03
272931.08	8593463.14	1323	0.62	0.79	0.02
272943.76	8593463.24	1048	0.5	0.63	0.02
272951	8593463.3	621	0.28	0.37	0.01
272956.4	8593467.03	764	0.32	0.45	0.02
272972.71	8593465.32	858	0.38	0.51	0.02
272985.38	8593465.42	491	0.22	0.29	0.01
273001.69	8593463.71	588	0.22	0.35	0.01
273008.92	8593465.61	1083	0.5	0.65	0.02
273019.8	8593463.85	953	0.4	0.57	0.02
273030.68	8593462.1	442	0.28	0.26	0.01
273043.33	8593464.04	389	0.16	0.22	0.01
273061.39	8593469.72	356	0.17	0.20	0.01
273072.32	8593462.43	247	0.12	0.14	0.01
273081.35	8593464.35	278	0.07	0.16	0.01
273079.83	8593429.29	175	0.06	0.09	0.01
273063.53	8593429.16	221	0.08	0.12	0.01
273050.86	8593429.06	237	0.07	0.13	0.01
273039.97	8593432.66	245	0.09	0.14	0.01
273027.31	8593430.72	244	0.07	0.14	0.01
273016.44	8593430.63	279	0.1	0.16	0.01
273005.58	8593430.54	310	0.11	0.18	0.01
272992.91	8593430.44	520	0.22	0.30	0.01
272978.42	8593430.32	491	0.14	0.29	0.01
272963.94	8593430.21	473	0.2	0.28	0.01
272953.08	8593430.12	522	0.22	0.31	0.01
272936.78	8593429.99	572	0.22	0.34	0.01
272924.09	8593431.73	686	0.26	0.40	0.01
272915.06	8593429.82	696	0.28	0.41	0.01
272904.19	8593429.73	897	0.4	0.53	0.02
272893.33	8593429.64	1400	0.85	0.84	0.02
272882.47	8593429.55	1039	0.5	0.62	0.02
272867.97	8593431.28	5151	2.8	3.13	0.04
272853.48	8593431.16	9071	8	5.51	0.05
272844.43	8593431.09	962	0.4	0.57	0.02
272833.58	8593429.16	673	0.26	0.40	0.01
272817.29	8593429.03	496	0.19	0.29	0.01
272797.36	8593430.71	732	0.28	0.43	0.02
272782.89	8593428.75	942	0.33	0.56	0.02

UTM Eastings	UTM Northing	counts/ 100s	uGy/hr meas	uGy/hr calc	+-
272777.44	8593430.55	957	0.32	0.57	0.02
272764.77	8593430.45	885	0.38	0.53	0.02
272750.29	8593430.33	782	0.32	0.46	0.02
272739.42	8593430.25	802	0.35	0.48	0.02
272724.94	8593430.13	1004	0.42	0.60	0.02
272714.09	8593428.2	942	0.35	0.56	0.02
272705.02	8593429.97	817	0.33	0.48	0.02
272692.35	8593429.87	842	0.35	0.50	0.02
272683.3	8593429.8	842	0.36	0.50	0.02
272672.42	8593431.55	801	0.32	0.48	0.02
272661.56	8593431.47	812	0.36	0.48	0.02
272654.32	8593431.41	733	0.28	0.43	0.02
272643.45	8593431.32	618	0.21	0.36	0.01
272630.79	8593429.37	611	0.28	0.36	0.01
272621.74	8593429.3	622	0.23	0.37	0.01
272629.25	8593396.16	748	0.31	0.44	0.02
272647.36	8593396.31	731	0.3	0.43	0.02
272660.01	8593398.26	436	0.17	0.25	0.01
272665.46	8593396.45	734	0.42	0.43	0.02
272679.93	8593398.42	841	0.4	0.50	0.02
272689	8593396.64	1014	0.5	0.60	0.02
272703.48	8593396.76	1014	0.52	0.60	0.02
272712.53	8593396.83	954	0.51	0.57	0.02
272723.4	8593396.92	798	0.38	0.47	0.02
272734.26	8593397.01	731	0.39	0.43	0.02
272743.31	8593397.08	768	0.33	0.45	0.02
272754.17	8593397.17	842	0.33	0.50	0.02
272766.85	8593397.27	884	0.39	0.53	0.02
272783.14	8593397.4	1012	0.42	0.60	0.02
272790.38	8593397.46	920	0.5	0.55	0.02
272808.49	8593397.61	1118	0.52	0.67	0.02
272819.35	8593397.69	1335	0.58	0.80	0.02
272830.22	8593397.78	1427	0.75	0.86	0.02
272839.27	8593397.85	1409	0.8	0.85	0.02
272848.32	8593397.93	1603	0.75	0.96	0.02
272861.01	8593396.18	6078	2.9	3.69	0.04
272870.06	8593396.26	2358	1.05	1.42	0.03
272879.11	8593396.33	1598	0.8	0.96	0.02
272891.79	8593396.43	1182	0.6	0.71	0.02
272902.65	8593396.52	846	0.41	0.50	0.02
272918.94	8593396.65	771	0.29	0.46	0.02
272927.98	8593398.57	680	0.32	0.40	0.01
272946.09	8593398.71	479	0.21	0.28	0.01
272960.59	8593396.98	366	0.14	0.21	0.01
272971.45	8593397.07	286	0.12	0.16	0.01
272982.31	8593397.16	265	0.08	0.15	0.01
272991.36	8593397.23	264	0.09	0.15	0.01
273002.21	8593399.16				0.00
273002.23	8593397.32	241	0.07	0.13	0.01
273009.47	8593397.38	222	0.06	0.12	0.01

UTM Easting	UTM Northing	counts/ 100s	uGy/hr meas	uGy/hr calc	+-
273027.57	8593397.52	197	0.05	0.11	0.01
273043.87	8593397.65	204	0.05	0.11	0.01
273056.54	8593397.75	202	0.06	0.11	0.01
273067.4	8593397.84	209	0.04	0.11	0.01
273076.47	8593396.07	215	0.07	0.12	0.01
273090.94	8593398.03	168	0.04	0.09	0.01
272891.31	8593455.44	6032	4	3.66	0.04
272900.29	8593464.74	7790	5	4.73	0.05
272903.82	8593475.83	2120	1	1.28	0.03
272914.66	8593479.61	5603	3.5	3.40	0.04
272927.31	8593481.55	2300	1.1	1.39	0.03
272893.2	8593446.24	1611	0.9	0.97	0.02
272873.47	8593422.1	2578	1.3	1.56	0.03
272861.02	8593394.34	8348	5	5.07	0.05
272859.42	8593368.51	1198	0.7	0.72	0.02
272870	8593336	290	0.15	0.16	0.01

Appendix A3 γ dose rate results from Anomaly 2B survey (northeast of Anomaly 2A) conducted 1–5 September 2008.

UTM Eastings	UTM Northing	counts/ 100s	uGy/hr meas	uGy/hr calc	+-
273050.63	8593908.58	407	0.26	0.22	0.01
273063.3	8593908.68	471	0.25	0.25	0.01
273077.79	8593908.8	475	0.28	0.25	0.01
273090.46	8593908.9	539	0.29	0.29	0.01
273099.51	8593908.97	596	0.34	0.32	0.01
273108.56	8593909.04	728	0.39	0.40	0.01
273119.44	8593907.29	732	0.39	0.40	0.01
273130.29	8593909.22	734	0.48	0.40	0.02
273139.34	8593909.29	708	0.41	0.38	0.02
273153.83	8593909.41	742	0.41	0.40	0.02
273161.07	8593909.46	751	0.44	0.41	0.02
273170.08	8593915.07	853	0.45	0.47	0.02
273177.36	8593909.6	769	0.42	0.42	0.02
273179.17	8593909.61	813	0.48	0.44	0.02
273197.28	8593909.76	853	0.52	0.47	0.02
273213.57	8593909.89	637	0.39	0.34	0.02
273220.82	8593909.94	781	0.44	0.43	0.02
273229.88	8593908.17	721	0.45	0.39	0.02
273246.18	8593908.3	691	0.38	0.37	0.01
273262.46	8593910.28	740	0.42	0.40	0.02
273260.93	8593875.22	839	0.5	0.46	0.02
273250.05	8593876.98	910	0.51	0.50	0.02
273233.76	8593876.85	866	0.52	0.47	0.02
273217.48	8593874.88	955	0.55	0.52	0.02
273204.79	8593876.62	923	0.48	0.50	0.02
273192.11	8593876.52	1075	0.65	0.59	0.02
273179.44	8593876.41	1219	0.65	0.67	0.02
273166.77	8593876.31	1057	0.65	0.58	0.02
273150.47	8593876.18	968	0.6	0.53	0.02
273141.42	8593876.11	996	0.6	0.55	0.02
273126.94	8593875.99	851	0.5	0.46	0.02
273112.45	8593875.88	767	0.43	0.42	0.02
273101.59	8593875.79	712	0.4	0.39	0.01
273083.48	8593875.64	686	0.4	0.37	0.02
273067.19	8593875.51	564	0.35	0.30	0.01
273056.33	8593875.43	440	0.2	0.23	0.01
273047.26	8593877.2	363	0.2	0.19	0.01
273054.78	8593842.22	1091	0.65	0.60	0.02
273065.64	8593842.3	800	0.55	0.44	0.02
273078.33	8593840.56	1071	0.6	0.59	0.02
273083.74	8593844.29	904	0.5	0.49	0.02
273090.99	8593842.51	969	0.55	0.53	0.02
273103.65	8593844.45	1110	0.65	0.61	0.02
273112.7	8593844.53	1163	0.7	0.64	0.02
273123.58	8593842.77	1190	0.75	0.65	0.02
273134.43	8593844.7	953	0.6	0.52	0.02
273150.74	8593842.99	1237	0.7	0.68	0.02
273159.79	8593843.06	957	0.6	0.52	0.02
273176.09	8593843.19	827	0.45	0.45	0.02
273194.19	8593843.34	696	0.4	0.38	0.02

UTM Eastings	UTM Northing	counts/ 100s	uGy/hr meas	uGy/hr calc	+-
273203.24	8593843.41	626	0.3	0.34	0.01
273214.11	8593843.5	723	0.4	0.39	0.01
273226.78	8593843.6	906	0.45	0.50	0.01
273235.83	8593843.67	940	0.5	0.51	0.02
273253.94	8593843.82	698	0.45	0.38	0.02
273264.8	8593843.9	642	0.35	0.35	0.01
273243.36	8593808.69	516	0.3	0.28	0.01
273230.67	8593810.43	548	0.3	0.29	0.01
273219.82	8593808.5	611	0.35	0.33	0.01
273208.94	8593810.26	763	0.45	0.42	0.02
273196.27	8593810.15	596	0.3	0.32	0.01
273189.03	8593810.1	519	0.33	0.28	0.01
273179.97	8593810.02	511	0.32	0.27	0.01
273165.49	8593809.91	547	0.33	0.29	0.01
273154.63	8593809.82	689	0.4	0.37	0.02
273143.76	8593809.73	888	0.5	0.49	0.02
273131.09	8593809.63	1159	0.7	0.64	0.02
273112.98	8593809.49	1708	1	0.94	0.02
273098.49	8593811.21	1247	0.8	0.69	0.02
273082.19	8593811.08	1357	0.8	0.75	0.02
273073.15	8593809.17	1306	0.8	0.72	0.02
273058.67	8593809.05	1119	0.65	0.61	0.02
273049.6	8593810.82	1090	0.5	0.60	0.02
273033.57	8593777.5	785	0.45	0.43	0.02
273044.44	8593777.58	770	0.45	0.42	0.02
273051.68	8593777.64	783	0.45	0.43	0.02
273057.11	8593777.68	792	0.45	0.43	0.02
273067.97	8593777.77	1092	0.5	0.60	0.02
273078.85	8593776.02	1136	0.65	0.62	0.02
273100.56	8593778.03	1035	0.55	0.57	0.02
273109.62	8593778.11	1025	0.6	0.56	0.02
273122.3	8593776.36	1100	0.65	0.60	0.02
273131.36	8593776.44	1031	0.55	0.57	0.02
273140.39	8593778.35	892	0.45	0.49	0.02
273153.07	8593778.46	573	0.35	0.31	0.01
273162.14	8593776.68	563	0.3	0.30	0.01
273169.38	8593776.74	547	0.28	0.29	0.01
273183.86	8593776.86	651	0.33	0.35	0.01
273192.91	8593776.93	643	0.3	0.35	0.01
273203.78	8593777.02	584	0.3	0.32	0.01
273216.45	8593777.12	524	0.3	0.28	0.01
273227.31	8593777.21	505	0.25	0.27	0.01
273238.18	8593777.29	579	0.3	0.31	0.01
273256.55	8593744.24	456	0.3	0.24	0.01
273249.31	8593744.19	508	0.3	0.27	0.01
273240.25	8593744.11	538	0.3	0.29	0.01
273227.58	8593744.01	468	0.3	0.25	0.01
273216.72	8593743.92	494	0.3	0.26	0.01
273209.47	8593743.87	554	0.35	0.30	0.01
273198.61	8593743.78	688	0.4	0.37	0.02
273191.37	8593743.72	653	0.4	0.35	0.02
273180.51	8593743.63	678	0.4	0.37	0.02

UTM Eastings	UTM Northings	counts/ 100s	uGy/hr meas	uGy/hr calc	+-
273167.83	8593743.53	771	0.4	0.42	0.01
273153.35	8593743.42	850	0.5	0.46	0.02
273140.68	8593743.31	850	0.5	0.46	0.02
273129.81	8593743.23	795	0.45	0.43	0.02
273118.95	8593743.14	699	0.45	0.38	0.02
273106.26	8593744.88	736	0.48	0.40	0.02
273097.22	8593742.97	704	0.4	0.38	0.02
273088.16	8593744.74	677	0.4	0.37	0.02
273079.1	8593744.66	745	0.4	0.41	0.01
273062.81	8593744.53	694	0.4	0.38	0.02
273046.5	8593746.25	653	0.4	0.35	0.02
273032.03	8593744.29	543	0.35	0.29	0.02
273022.98	8593744.21	465	0.25	0.25	0.01
273012.11	8593744.13	487	0.22	0.26	0.01
272993.99	8593745.82	369	0.2	0.19	0.01
272979.53	8593743.86	396	0.2	0.21	0.01
272968.66	8593743.78	371	0.2	0.20	0.01
272982.97	8593766.02	369	0.15	0.19	0.01
272995.64	8593766.13	444	0.17	0.24	0.01
273004.69	8593766.2	517	0.25	0.28	0.01
273021	8593764.48	577	0.35	0.31	0.01
273026.44	8593764.53	578	0.3	0.31	0.01
273037.3	8593764.62	697	0.4	0.38	0.02
273037.2	8593777.52	808	0.4	0.44	0.01
273020.9	8593777.39	763	0.4	0.42	0.01
273008.23	8593777.29	628	0.35	0.34	0.01
272995.57	8593775.35	482	0.25	0.26	0.01
272984.69	8593777.1	401	0.2	0.21	0.01
272973.83	8593777.02	345	0.2	0.18	0.01
272964.76	8593778.79	292	0.15	0.15	0.01
272971.93	8593788.07	309	0.17	0.16	0.01
272975.53	8593789.94	353	0.2	0.19	0.01
272984.6	8593788.17	487	0.22	0.26	0.01
272999.09	8593788.28	676	0.4	0.37	0.02
273008.05	8593799.42	905	0.5	0.49	0.02
272995.36	8593801.16	490	0.25	0.26	0.01
272980.89	8593799.2	478	0.25	0.26	0.01
272977.26	8593801.02	368	0.2	0.19	0.01
272968.2	8593800.95	263	0.14	0.14	0.01
272968.13	8593810.17	325	0.17	0.17	0.01
272982.61	8593810.28	368	0.2	0.19	0.01
272993.48	8593810.37	418	0.25	0.22	0.01
273006.16	8593808.63	541	0.3	0.29	0.01
273017.03	8593808.72	833	0.5	0.45	0.02
273026.09	8593806.94	1063	0.6	0.58	0.02
273051.16	8593842.19	860	0.45	0.47	0.02
273034.85	8593843.9	866	0.45	0.47	0.02
273022.19	8593841.95	582	0.35	0.31	0.01
273013.14	8593841.88	506	0.3	0.27	0.01
273002.28	8593841.79	312	0.2	0.16	0.01
272991.4	8593843.55	309	0.17	0.16	0.01
272989.32	8593876.73	282	0.15	0.15	0.01

UTM Eastings	UTM Northing	counts/ 100s	uGy/hr meas	uGy/hr calc	+-
273000.18	8593876.82	262	0.15	0.13	0.01
273020.1	8593876.98	331	0.2	0.17	0.01
273036.4	8593877.11	351	0.22	0.18	0.01
273037.95	8593908.48	378	0.22	0.20	0.01
273023.47	8593908.36	339	0.18	0.18	0.01
273012.61	8593908.27	289	0.18	0.15	0.01
273001.74	8593908.19	272	0.15	0.14	0.01
273010.69	8593921.17	266	0.14	0.14	0.01
273051.00	8593919.00	390	0.16	0.22	0.01
273066.00	8593919.00	458	0.22	0.27	0.01
273066.00	8593920.00	440	0.20	0.26	0.01
273089.00	8593920.00	541	0.25	0.32	0.01
273100.00	8593919.00	547	0.25	0.32	0.01
273115.00	8593920.00	560	0.22	0.33	0.01
273134.00	8593920.00	670	0.28	0.40	0.01
273142.00	8593920.00	736	0.35	0.44	0.01
273158.00	8593921.00	633	0.29	0.37	0.01
273173.00	8593920.00	637	0.29	0.38	0.01
273189.00	8593919.00	626	0.30	0.37	0.01
273202.00	8593921.00	612	0.30	0.36	0.01
273207.00	8593920.00	600	0.21	0.35	0.01
273218.00	8593920.00	561	0.20	0.33	0.01
273230.00	8593920.00	646	0.28	0.38	0.01
273242.00	8593920.00	643	0.28	0.38	0.01
273253.00	8593920.00	640	0.24	0.38	0.01
273263.00	8593920.00	645	0.30	0.38	0.01
273258.00	8593887.00	746	0.26	0.44	0.01
273247.00	8593888.00	768	0.29	0.46	0.01
273235.00	8593887.00	765	0.31	0.45	0.01
273224.00	8593887.00	902	0.33	0.54	0.01
273211.00	8593888.00	914	0.38	0.54	0.01
273201.00	8593888.00	858	0.40	0.51	0.01
273192.00	8593887.00	933	0.38	0.56	0.01
273181.00	8593887.00	1065	0.43	0.64	0.01
273166.00	8593887.00	1054	0.42	0.63	0.01
273154.00	8593887.00	932	0.39	0.56	0.01
273143.00	8593887.00	871	0.30	0.52	0.01
273129.00	8593887.00	758	0.35	0.45	0.01
273116.00	8593887.00	734	0.31	0.43	0.01
273100.00	8593887.00	640	0.28	0.38	0.01
273081.00	8593887.00	650	0.22	0.38	0.01
273068.00	8593887.00	500	0.20	0.29	0.01
273058.00	8593887.00	438	0.15	0.25	0.01
273043.00	8593888.00	335	0.12	0.19	0.01
273061.65	8593888.38	338	0.21	0.19	0.01
273045.37	8593886.40	332	0.17	0.19	0.01
273029.08	8593886.27	298	0.10	0.17	0.01
273020.01	8593888.04	285	0.12	0.16	0.01
273009.43	8593852.92	355	0.11	0.20	0.01
273025.71	8593854.89	306	0.16	0.17	0.01
273036.57	8593854.98	423	0.19	0.25	0.01
273049.26	8593853.24	433	0.23	0.25	0.01

UTM Eastings	UTM Northing	counts/ 100s	uGy/hr meas	uGy/hr calc	+-
273058.31	8593853.31	419	0.20	0.24	0.01
273070.99	8593853.41	584	0.19	0.34	0.01
273080.03	8593855.33	768	0.25	0.46	0.01
273087.28	8593853.54	795	0.39	0.47	0.01
273098.15	8593853.63	778	0.28	0.46	0.01
273109.01	8593853.72	843	0.32	0.50	0.01
273116.25	8593853.78	1003	0.42	0.60	0.01
273128.92	8593853.88	1428	0.61	0.86	0.02
273137.96	8593855.79	1088	0.52	0.65	0.02
273145.22	8593854.01	1289	0.49	0.77	0.01
273152.46	8593854.07	1213	0.55	0.73	0.02
273161.51	8593854.14	1334	0.49	0.80	0.01
273174.19	8593854.24	1031	0.44	0.62	0.01
273185.05	8593854.33	847	0.35	0.50	0.01
273195.91	8593854.42	940	0.38	0.56	0.01
273204.97	8593854.49	818	0.29	0.49	0.01
273215.83	8593854.58	777	0.22	0.46	0.01
273230.31	8593854.69	817	0.28	0.49	0.01
273244.81	8593852.96	1134	0.47	0.68	0.01
273257.47	8593854.91	834	0.31	0.50	0.01
273266.52	8593854.98	734	0.28	0.43	0.01
273261.37	8593819.90	543	0.18	0.32	0.01
273252.31	8593821.67	583	0.21	0.34	0.01
273241.44	8593821.58	586	0.23	0.34	0.01
273230.58	8593821.50	684	0.18	0.40	0.01
273219.72	8593821.41	720	0.22	0.43	0.01
273205.23	8593821.29	664	0.24	0.39	0.01
273190.75	8593821.18	593	0.16	0.35	0.01
273181.70	8593821.10	586	0.27	0.34	0.01
273167.21	8593820.99	616	0.19	0.36	0.01
273156.35	8593820.90	657	0.22	0.39	0.01
273149.11	8593820.84	840	0.30	0.50	0.01
273134.62	8593820.73	1114	0.38	0.67	0.01
273118.31	8593822.44	1479	0.65	0.89	0.02
273100.22	8593820.45	1098	0.60	0.66	0.02
273087.55	8593820.35	1119	0.60	0.67	0.02
273080.29	8593822.13	1248	0.50	0.75	0.01
273064.01	8593820.16	1496	0.65	0.90	0.02
273054.94	8593821.93	1089	0.50	0.65	0.02
273042.29	8593819.98	1321	0.57	0.79	0.02
273029.60	8593821.73	1037	0.50	0.62	0.02
273016.92	8593821.63	820	0.38	0.49	0.01
273004.25	8593821.52	639	0.37	0.38	0.01
272991.58	8593821.42	420	0.20	0.24	0.01
272978.90	8593821.32	365	0.21	0.21	0.01
273028.05	8593788.52	944	0.55	0.56	0.02
273044.35	8593788.65	759	0.44	0.45	0.02
273055.23	8593786.89	874	0.49	0.52	0.02
273064.26	8593788.81	830	0.52	0.49	0.02
273075.13	8593788.90	964	0.55	0.58	0.02
273082.37	8593788.95	1014	0.58	0.61	0.02
273096.85	8593789.07	1597	0.77	0.96	0.02

UTM Eastings	UTM Northing	counts/ 100s	uGy/hr meas	uGy/hr calc	+-
273107.73	8593787.31	1164	0.60	0.70	0.02
273120.40	8593787.41	918	0.47	0.55	0.02
273131.27	8593787.50	1021	0.60	0.61	0.02
273142.13	8593787.59	874	0.51	0.52	0.02
273154.80	8593787.69	610	0.29	0.36	0.01
273163.86	8593787.76	595	0.38	0.35	0.02
273171.10	8593787.82	523	0.28	0.31	0.01
273183.77	8593787.92	524	0.29	0.31	0.01
273198.26	8593788.04	484	0.29	0.28	0.01
273210.93	8593788.14	566	0.28	0.33	0.01
273219.98	8593788.21	430	0.23	0.25	0.01
273230.85	8593788.30	460	0.26	0.27	0.01
273245.33	8593788.42	480	0.25	0.28	0.01
273254.38	8593788.49	475	0.26	0.28	0.01
273258.27	8593755.32	505	0.25	0.30	0.01
273252.84	8593755.28	530	0.28	0.31	0.01
273241.98	8593755.19	533	0.28	0.31	0.01
273231.11	8593755.11	449	0.26	0.26	0.01
273222.06	8593755.03	522	0.25	0.31	0.01
273207.58	8593754.92	600	0.25	0.35	0.01
273193.09	8593754.80	667	0.30	0.39	0.01
273184.04	8593754.73	652	0.30	0.38	0.01
273173.16	8593756.48	701	0.35	0.41	0.01
273164.12	8593754.57	741	0.32	0.44	0.01
273156.88	8593754.51	785	0.38	0.47	0.01
273142.40	8593754.39	803	0.39	0.48	0.01
273133.33	8593756.17	748	0.38	0.44	0.01
273120.66	8593756.06	769	0.36	0.46	0.01
273106.17	8593755.95	730	0.32	0.43	0.01
273100.76	8593754.06	750	0.41	0.44	0.01
273091.70	8593753.99	765	0.40	0.45	0.01
273079.00	8593757.57	686	0.33	0.41	0.01
273071.79	8593753.83	653	0.30	0.39	0.01
273057.30	8593753.71	765	0.33	0.45	0.01
273046.43	8593755.47	681	0.30	0.40	0.01
273030.13	8593755.34	574	0.25	0.34	0.01
273017.47	8593753.39	548	0.28	0.32	0.01
273004.77	8593756.98	474	0.25	0.28	0.01
272988.49	8593755.00	398	0.22	0.23	0.01
272977.64	8593753.07	405	0.16	0.23	0.01
272967.03	8593721.63	351	0.16	0.20	0.01
272979.69	8593723.58	387	0.19	0.22	0.01
272988.76	8593721.81	407	0.21	0.24	0.01
272999.62	8593721.89	380	0.19	0.22	0.01
273015.91	8593722.02	402	0.20	0.23	0.01
273023.16	8593722.08	383	0.19	0.22	0.01
273037.64	8593722.20	451	0.25	0.26	0.01
273046.69	8593722.27	509	0.28	0.30	0.01
273055.74	8593722.34	491	0.25	0.29	0.01
273066.61	8593722.43	520	0.26	0.30	0.01
273073.85	8593722.49	556	0.32	0.33	0.01
273082.90	8593722.56	496	0.31	0.29	0.01

UTM Eastings	UTM Northings	counts/ 100s	uGy/hr meas	uGy/hr calc	+-
273099.20	8593722.69	636	0.32	0.38	0.01
273111.88	8593720.95	608	0.33	0.36	0.01
273122.75	8593721.04	618	0.35	0.36	0.01
273129.98	8593722.94	646	0.31	0.38	0.01
273139.03	8593723.01	674	0.29	0.40	0.01
273166.20	8593721.39	661	0.37	0.39	0.01
273166.20	8593721.39	683	0.37	0.40	0.01
273177.06	8593721.47	655	0.31	0.39	0.01
273184.29	8593723.38	633	0.31	0.37	0.01
273196.98	8593721.63	635	0.28	0.37	0.01
273213.27	8593721.77	560	0.31	0.33	0.01
273220.52	8593721.82	532	0.25	0.31	0.01
273238.62	8593721.97	469	0.21	0.27	0.01
273247.67	8593722.04	408	0.19	0.24	0.01
273263.97	8593722.17	401	0.22	0.23	0.01
273052.53	8593897.53	373	0.2	0.21	0.01
273068.82	8593897.66	412	0.2	0.24	0.01
273079.68	8593897.75	522	0.3	0.31	0.01
273088.74	8593897.82	554	0.3	0.32	0.01
273101.41	8593897.92	599	0.35	0.35	0.01
273106.84	8593897.96	672	0.35	0.40	0.01
273119.52	8593898.07	653	0.35	0.38	0.01
273130.38	8593898.15	692	0.4	0.41	0.02
273139.43	8593898.23	690	0.4	0.41	0.02
273150.29	8593898.31	753	0.4	0.45	0.01
273162.97	8593898.41	807	0.5	0.48	0.02
273172.02	8593898.49	852	0.5	0.51	0.02
273190.13	8593898.63	854	0.5	0.51	0.02
273201	8593896.87	875	0.5	0.52	0.02
273208.25	8593896.93	796	0.45	0.47	0.02
273222.73	8593897.05	819	0.45	0.49	0.02
273233.59	8593897.14	703	0.35	0.42	0.01
273249.87	8593899.11	769	0.4	0.46	0.01
273258.94	8593897.34	677	0.4	0.40	0.02
273267.99	8593897.41	754	0.4	0.45	0.01
273255.57	8593865.96	843	0.5	0.50	0.02
273246.52	8593865.89	905	0.45	0.54	0.01
273235.66	8593865.8	966	0.5	0.58	0.02
273224.79	8593865.71	839	0.45	0.50	0.02
273217.55	8593865.65	884	0.45	0.53	0.02
273206.69	8593865.57	902	0.5	0.54	0.02
273197.63	8593865.49	898	0.5	0.53	0.02
273183.15	8593865.38	1208	0.6	0.72	0.02
273174.1	8593865.31	1006	0.55	0.60	0.02
273159.61	8593865.19	1255	0.8	0.75	0.02
273145.13	8593865.07	952	0.5	0.57	0.02
273128.84	8593864.94	892	0.5	0.53	0.02
273112.54	8593864.81	719	0.4	0.43	0.01
273099.87	8593864.71	577	0.35	0.34	0.01
273087.19	8593864.61	645	0.4	0.38	0.02
273074.5	8593866.35	537	0.3	0.31	0.01
273065.47	8593864.43	478	0.25	0.28	0.01

UTM Eastings	UTM Northing	counts/ 100s	uGy/hr meas	uGy/hr calc	+-
273050.98	8593864.32	410	0.2	0.24	0.01
273040.11	8593866.07	355	0.2	0.20	0.01
273054.87	8593831.15	1324	0.6	0.79	0.02
273063.92	8593831.22	1148	0.6	0.69	0.02
273071.17	8593831.28	1232	0.6	0.74	0.02
273092.89	8593831.46	1114	0.6	0.67	0.02
273100.13	8593831.51	1202	0.6	0.72	0.02
273109.19	8593831.59	1057	0.55	0.63	0.02
273116.43	8593831.65	1096	0.6	0.65	0.02
273125.48	8593831.72	1149	0.6	0.69	0.02
273134.53	8593831.79	1260	0.6	0.75	0.02
273147.21	8593831.89	1123	0.7	0.67	0.02
273163.5	8593832.02	779	0.4	0.46	0.01
273170.74	8593832.08	695	0.4	0.41	0.02
273188.85	8593832.23	519	0.25	0.30	0.01
273196.09	8593832.29	452	0.25	0.26	0.01
273210.57	8593832.4	831	0.4	0.49	0.01
273225.06	8593832.52	745	0.4	0.44	0.01
273237.73	8593832.62	654	0.35	0.39	0.01
273252.22	8593832.74	612	0.35	0.36	0.01
273266.7	8593832.85	627	0.35	0.37	0.01
273257.93	8593797.74	451	0.3	0.26	0.01
273241.62	8593799.45	492	0.3	0.29	0.01
273230.76	8593799.37	492	0.25	0.29	0.01
273219.89	8593799.28	597	0.3	0.35	0.01
273209.03	8593799.19	558	0.35	0.33	0.01
273196.36	8593799.09	604	0.35	0.36	0.01
273183.68	8593798.99	528	0.3	0.31	0.01
273174.63	8593798.92	495	0.25	0.29	0.01
273165.58	8593798.84	531	0.3	0.31	0.01
273158.34	8593798.78	611	0.25	0.36	0.01
273147.47	8593798.7	625	0.35	0.37	0.01
273136.61	8593798.61	854	0.5	0.51	0.02
273118.51	8593798.47	1040	0.5	0.62	0.02
273111.26	8593798.41	1140	0.6	0.68	0.02
273104.02	8593798.35	1940	1	1.17	0.02
273084.09	8593800.03	1215	0.7	0.73	0.02
273066	8593798.04	935	0.5	0.56	0.02
273053.31	8593799.79	832	0.45	0.49	0.02
273042.46	8593797.85	803	0.4	0.48	0.01
273027.96	8593799.58	907	0.5	0.54	0.02
273053.58	8593766.59	660	0.4	0.39	0.02
273060.82	8593766.65	712	0.4	0.42	0.01
273071.68	8593766.74	869	0.5	0.52	0.02
273078.93	8593766.79	1156	0.6	0.69	0.02
273087.98	8593766.87	972	0.55	0.58	0.02
273097.03	8593766.94	923	0.5	0.55	0.02
273109.7	8593767.04	849	0.5	0.50	0.02
273126	8593767.17	868	0.5	0.52	0.02
273135.05	8593767.24	995	0.6	0.59	0.02
273147.74	8593765.5	827	0.45	0.49	0.02
273154.97	8593767.4	577	0.35	0.34	0.01

UTM Eastings	UTM Northing	counts/ 100s	uGy/hr meas	uGy/hr calc	+-
273171.28	8593765.69	660	0.4	0.39	0.02
273176.71	8593765.73	678	0.4	0.40	0.02
273183.95	8593765.79	604	0.3	0.36	0.01
273193	8593765.87	526	0.3	0.31	0.01
273203.87	8593765.95	539	0.3	0.32	0.01
273218.35	8593766.07	562	0.3	0.33	0.01
273231.02	8593766.17	539	0.3	0.32	0.01
273243.7	8593766.27	531	0.3	0.31	0.01
273258.18	8593766.39	464	0.25	0.27	0.01
273258.45	8593733.19	390	0.25	0.22	0.01
273247.58	8593733.11	423	0.25	0.24	0.01
273236.72	8593733.02	436	0.25	0.25	0.01
273222.24	8593732.9	527	0.3	0.31	0.01
273213.18	8593732.83	557	0.3	0.33	0.01
273198.7	8593732.71	656	0.35	0.39	0.01
273191.46	8593732.66	681	0.35	0.40	0.01
273182.41	8593732.58	724	0.4	0.43	0.01
273169.73	8593732.48	660	0.35	0.39	0.01
273157.06	8593732.38	691	0.4	0.41	0.02
273142.57	8593732.26	719	0.4	0.43	0.01
273133.52	8593732.19	683	0.35	0.40	0.01
273117.23	8593732.06	625	0.35	0.37	0.01
273100.92	8593733.77	659	0.35	0.39	0.01
273090.06	8593733.69	625	0.35	0.37	0.01
273077.38	8593733.58	647	0.35	0.38	0.01
273066.52	8593733.5	503	0.3	0.29	0.01
273055.66	8593733.41	542	0.3	0.32	0.01
273044.79	8593733.32	540	0.3	0.32	0.01
273028.5	8593733.19	502	0.25	0.29	0.01
273017.63	8593733.1	399	0.2	0.23	0.01
273001.33	8593734.82	373	0.2	0.21	0.01
272983.22	8593734.67	350	0.16	0.20	0.01
272974.18	8593732.76	334	0.175	0.19	0.01
272963.32	8593732.67	358	0.2	0.21	0.01
272963.59	8593699.47	296	0.15	0.17	0.01
272976.26	8593699.57	323	0.2	0.18	0.01
272985.31	8593699.65	347	0.2	0.20	0.01
272997.99	8593699.75	325	0.2	0.18	0.01
273007.04	8593699.82	353	0.2	0.20	0.01
273016.09	8593699.89	345	0.2	0.20	0.01
273028.76	8593700	387	0.2	0.22	0.01
273045.06	8593700.13	425	0.25	0.25	0.01
273059.54	8593700.24	493	0.25	0.29	0.01
273072.22	8593700.35	494	0.25	0.29	0.01
273084.89	8593700.45	490	0.25	0.29	0.01
273097.56	8593700.55	463	0.25	0.27	0.01
273106.62	8593700.62	523	0.3	0.31	0.01
273113.86	8593700.68	499	0.25	0.29	0.01
273128.36	8593698.95	519	0.3	0.30	0.01
273139.21	8593700.88	596	0.35	0.35	0.01
273151.88	8593700.99	589	0.3	0.35	0.01
273166.38	8593699.26	563	0.35	0.33	0.01

UTM Eastings	UTM Northing	counts/ 100s	uGy/hr meas	uGy/hr calc	+-
273180.86	8593699.37	566	0.3	0.33	0.01
273195.35	8593699.49	474	0.25	0.28	0.01
273209.83	8593699.61	480	0.25	0.28	0.01
273224.31	8593699.72	451	0.25	0.26	0.01
273238.8	8593699.84	435	0.25	0.25	0.01
273249.66	8593699.93	308	0.15	0.17	0.01
273262.33	8593700.03	296	0.15	0.17	0.01
273271.39	8593700.1	241	0.15	0.13	0.01
273047.63	8593831.09	1289	0.7	0.77	0.02
273031.32	8593832.81	967	0.5	0.58	0.02
273018.65	8593832.7	1011	0.5	0.60	0.02
273009.61	8593830.79	525	0.3	0.31	0.01
272996.92	8593832.53	369	0.2	0.21	0.01
272982.44	8593832.41	338	0.175	0.19	0.01
272985.79	8593865.64	239	0.15	0.13	0.01
272996.65	8593865.73	264	0.15	0.15	0.01
273009.34	8593863.98	279	0.15	0.16	0.01
273022.01	8593864.08	336	0.175	0.19	0.01
273040.11	8593866.07	374	0.2	0.21	0.01
273041.66	8593897.44	387	0.2	0.22	0.01
273028.98	8593899.18	347	0.175	0.20	0.01
273019.92	8593899.11	308	0.15	0.17	0.01
273019.76	8593919.4	284	0.15	0.16	0.01
273030.62	8593919.48	340	0.175	0.19	0.01
273041.49	8593919.57	373	0.2	0.21	0.01

Appendix A4 γ dose rate results from survey between Anomalies 2A and 2B, and on top of Anomaly 2C (southwest of Anomaly 2A), conducted 8–10 October 2008.

UTM Easting	UTM Northing	counts/ 100s	uGy/hr meas	uGy/hr calc	+-
272574.28	8593701.88	267	0.13	0.14	0.01
272596.02	8593700.21	286	0.16	0.15	0.01
272626.82	8593698.61	295	0.15	0.16	0.01
272643.1	8593700.58	298	0.18	0.16	0.01
272666.63	8593700.77	263	0.15	0.14	0.01
272688.36	8593700.95	302	0.16	0.16	0.01
272706.46	8593701.09	282	0.14	0.15	0.01
272728.21	8593699.43	272	0.14	0.15	0.01
272746.31	8593699.57	291	0.16	0.16	0.01
272764.4	8593701.56	303	0.17	0.16	0.01
272787.95	8593699.91	277	0.15	0.15	0.01
272809.68	8593700.08	279	0.14	0.15	0.01
272835.01	8593702.13	295	0.18	0.16	0.01
272853.13	8593700.43	319	0.18	0.17	0.01
272871.24	8593700.58	315	0.19	0.17	0.01
272887.55	8593698.86	354	0.20	0.19	0.01
272912.88	8593700.91	303	0.19	0.16	0.01
272938.22	8593701.11	316	0.17	0.17	0.01
272963.59	8593699.47	315	0.16	0.17	0.01
272985.31	8593699.65	304	0.17	0.16	0.01
273016.09	8593699.89	320	0.18	0.17	0.01
273041.42	8593701.94	366	0.20	0.20	0.01
273064.97	8593700.29	461	0.23	0.25	0.01
273084.91	8593698.6	490	0.22	0.27	0.01
273115.67	8593700.69	521	0.29	0.29	0.01
273137.39	8593700.87	544	0.27	0.30	0.01
273151.89	8593699.14	602	0.32	0.34	0.01
273175.43	8593699.33	536	0.28	0.30	0.01
273224.28	8593703.41	467	0.26	0.26	0.01
273246.04	8593699.9	346	0.20	0.19	0.01
273274.99	8593701.97	283	0.15	0.15	0.01
273289.49	8593700.25	258	0.16	0.14	0.01
273268.25	8593639.21	449	0.24	0.25	0.01
273251.96	8593639.08	359	0.20	0.20	0.01
273222.98	8593640.69	274	0.20	0.15	0.01
273192.2	8593640.45	281	0.15	0.15	0.01
273170.47	8593640.27	333	0.18	0.18	0.01
273155.99	8593640.16	295	0.18	0.16	0.01
273123.38	8593641.74	344	0.20	0.19	0.01
273105.29	8593639.75	312	0.16	0.17	0.01
273087.17	8593641.45	331	0.20	0.18	0.01
273072.71	8593639.49	344	0.21	0.19	0.01
273052.79	8593639.33	348	0.20	0.19	0.01
273023.81	8593640.94	354	0.18	0.19	0.01
272994.84	8593640.71	359	0.18	0.20	0.01
272978.54	8593640.58	366	0.21	0.20	0.01
272940.54	8593638.43	448	0.22	0.25	0.01
272924.23	8593640.14	384	0.25	0.21	0.01
272897.07	8593639.92	378	0.19	0.21	0.01
272871.72	8593639.72	336	0.22	0.18	0.01

UTM Easting	UTM Northing	counts/ 100s	uGy/hr meas	uGy/hr calc	+-
272844.57	8593639.5	322	0.18	0.17	0.01
272815.6	8593639.27	350	0.20	0.19	0.01
272784.82	8593639.02	311	0.16	0.17	0.01
272768.51	8593640.73	363	0.16	0.20	0.01
272746.79	8593640.56	327	0.16	0.18	0.01
272732.3	8593640.44	334	0.17	0.18	0.01
272701.52	8593640.19	263	0.14	0.14	0.01
272683.42	8593640.05	300	0.16	0.16	0.01
272654.45	8593639.81	276	0.13	0.15	0.01
272630.91	8593639.62	279	0.14	0.15	0.01
272607.38	8593639.44	295	0.15	0.16	0.01
272582.03	8593639.23	316	0.17	0.17	0.01
272558.48	8593640.89	338	0.17	0.18	0.01
272573.45	8593580.14	262	0.15	0.14	0.01
272593.35	8593582.15	285	0.16	0.15	0.01
272627.77	8593580.58	250	0.14	0.13	0.01
272653.13	8593578.94	281	0.16	0.15	0.01
272682.08	8593581.02	278	0.15	0.15	0.01
272707.43	8593581.22	350	0.16	0.19	0.01
272732.78	8593581.43	323	0.17	0.17	0.01
272758.14	8593579.79	352	0.22	0.19	0.01
272779.86	8593579.96	423	0.19	0.23	0.01
272797.97	8593580.11	407	0.22	0.22	0.01
272816.07	8593580.25	447	0.24	0.25	0.01
272832.37	8593580.38	439	0.23	0.24	0.01
272850.47	8593580.53	504	0.23	0.28	0.01
272868.59	8593578.83	472	0.24	0.26	0.01
272886.68	8593580.82	311	0.21	0.17	0.01
272901.17	8593580.94	867	0.49	0.49	0.02
272933.77	8593579.35	369	0.22	0.20	0.01
272962.74	8593579.59	363	0.19	0.20	0.01
272984.46	8593579.76	431	0.22	0.24	0.01
273009.81	8593579.96	430	0.26	0.24	0.01
273027.92	8593580.11	459	0.26	0.25	0.01
273053.26	8593580.31	405	0.21	0.22	0.01
273074.99	8593580.49	357	0.19	0.19	0.01
273094.92	8593578.8	392	0.22	0.21	0.01
273120.25	8593580.85	335	0.19	0.18	0.01
273143.79	8593581.04	320	0.15	0.17	0.01
273167.33	8593581.23	298	0.18	0.16	0.01
273187.24	8593581.39	354	0.19	0.19	0.01
273212.59	8593581.59	371	0.22	0.20	0.01
273252.43	8593580.07	196	0.13	0.10	0.01
273281.4	8593580.3	180	0.07	0.09	0.01
272570.16	8593539.54	245	0.14	0.13	0.01
272590.07	8593539.7	248	0.14	0.13	0.01
272606.35	8593541.68	246	0.14	0.13	0.01
272631.73	8593538.19	285	0.14	0.15	0.01
272642.59	8593538.28	264	0.15	0.14	0.01
272630.07	8593519.74	323	0.16	0.17	0.01
272599.3	8593517.65	273	0.14	0.15	0.01
272577.55	8593521.16	232	0.15	0.12	0.01

UTM Eastings	UTM Northing	counts/ 100s	uGy/hr meas	uGy/hr calc	+-
272557.63	8593521	248	0.15	0.13	0.01
272574.09	8593500.84	276	0.14	0.15	0.01
272599.44	8593501.05	273	0.14	0.15	0.01
272621.16	8593501.22	301	0.16	0.16	0.01
272635.65	8593501.34	304	0.21	0.16	0.01
272628.66	8593469.93	887	0.58	0.50	0.02
272614.17	8593469.81	760	0.42	0.43	0.02
272599.69	8593469.7	440	0.30	0.24	0.01
272577.96	8593469.52	367	0.19	0.20	0.01
272559.86	8593469.38	310	0.18	0.17	0.01
272572.71	8593447.35	439	0.23	0.24	0.01
272594.41	8593451.21	504	0.22	0.28	0.01
272616.15	8593449.54	752	0.45	0.42	0.02
272636.06	8593449.7	1066	0.62	0.61	0.02
272630.79	8593429.37	592	0.22	0.33	0.01
272610.86	8593431.06	572	0.31	0.32	0.01
272587.34	8593429.02	569	0.30	0.32	0.01
272563.79	8593430.68	537	0.30	0.30	0.01
272573.01	8593410.47	698	0.46	0.39	0.01
272591.11	8593410.61	821	0.43	0.46	0.02
272611.03	8593410.77	713	0.45	0.40	0.02
272629.34	8593385.1	689	0.35	0.39	0.01
272603.99	8593384.89	572	0.38	0.32	0.01
272585.89	8593384.75	498	0.30	0.28	0.01
272562.34	8593386.4	527	0.31	0.29	0.01
272575.23	8593358.84	488	0.25	0.27	0.01
272595.13	8593360.85	360	0.28	0.20	0.01
272615.06	8593359.16	472	0.24	0.26	0.01
272636.79	8593359.34	484	0.31	0.27	0.01
272638.76	8593339.07	395	0.22	0.21	0.01
272620.64	8593340.77	411	0.20	0.22	0.01
272602.54	8593340.62	416	0.20	0.22	0.01
272586.24	8593340.49	454	0.22	0.24	0.01
272559.09	8593340.27	359	0.19	0.19	0.01
272539.17	8593340.11	396	0.20	0.21	0.01
272512.01	8593339.89	407	0.23	0.22	0.01
272499.36	8593337.94	367	0.20	0.19	0.01
272481.24	8593339.64	359	0.20	0.19	0.01
272448.65	8593339.38	397	0.20	0.21	0.01
272428.72	8593341.06	392	0.20	0.21	0.01
272432.78	8593285.77	342	0.19	0.18	0.01
272452.71	8593284.08	432	0.22	0.23	0.01
272474.42	8593286.1	437	0.24	0.23	0.01
272501.6	8593284.48	411	0.23	0.22	0.01
272528.75	8593284.7	583	0.25	0.31	0.01
272552.29	8593284.89	631	0.25	0.34	0.01
272575.81	8593286.92	627	0.40	0.34	0.01
272602.98	8593285.29	443	0.23	0.24	0.01
272621.09	8593285.44	369	0.24	0.19	0.01
272642.81	8593285.61	360	0.18	0.19	0.01
272621.7	8593209.83	338	0.20	0.18	0.01
272668.77	8593210.21	426	0.22	0.23	0.01

UTM Easting	UTM Northing	counts/ 100s	uGy/hr meas	uGy/hr calc	+-
272650.67	8593210.06	402	0.22	0.21	0.01
272637.98	8593211.8	375	0.20	0.20	0.01
272605.4	8593209.7	352	0.20	0.19	0.01
272585.49	8593209.54	362	0.18	0.19	0.01
272563.75	8593211.21	334	0.19	0.18	0.01
272536.6	8593209.14	385	0.20	0.20	0.01
272516.67	8593210.83	391	0.20	0.21	0.01
272498.57	8593210.68	334	0.20	0.18	0.01
272478	8593209	315	0.18	0.16	0.01
272458.75	8593208.52	267	0.15	0.14	0.01
272437	8593212.03	312	0.17	0.16	0.01
272422.56	8593206.38	315	0.20	0.16	0.01
272550.97	8593449.02	380	0.20	0.20	0.01
272529.23	8593450.69	289	0.20	0.15	0.01
272556.71	8593410.33	545	0.25	0.29	0.01
272531.37	8593410.13	383	0.20	0.20	0.01
272509.64	8593409.96	351	0.21	0.18	0.01
272543.86	8593432.36	443	0.23	0.24	0.01
272522.16	8593428.5	453	0.22	0.24	0.01
272500.42	8593430.17	333	0.18	0.17	0.01
272533.38	8593384.33	352	0.13	0.19	0.01
272513.45	8593386.01	334	0.20	0.18	0.01
272493.55	8593384.01	325	0.16	0.17	0.01
272473.64	8593383.84	315	0.20	0.16	0.01
272466.17	8593411.45	351	0.20	0.18	0.01
272471.44	8593431.78	309	0.18	0.16	0.01
272478.52	8593452.12	247	0.12	0.13	0.01
272442.32	8593449.99	353	0.15	0.19	0.01
272440.68	8593429.69	260	0.15	0.13	0.01
272440.84	8593409.4	360	0.20	0.19	0.01
272411.87	8593409.17	279	0.15	0.14	0.01
272433.81	8593383.52	359	0.20	0.19	0.01
272406.65	8593383.31	327	0.18	0.17	0.01
272384.91	8593384.97	313	0.18	0.16	0.01
272390.55	8593359.2	290	0.15	0.15	0.01
272417.71	8593359.42	348	0.18	0.18	0.01
272448.48	8593359.67	317	0.18	0.17	0.01
272479.26	8593359.91	336	0.19	0.18	0.01
272513.66	8593360.19	466	0.26	0.25	0.01
272551.68	8593360.5	463	0.25	0.25	0.01
272675.17	8593090.38	260	0.15	0.13	0.01
272662.49	8593090.28	292	0.15	0.15	0.01
272642.58	8593090.12	999	0.60	0.55	0.02
272626.28	8593089.99	366	0.26	0.19	0.01
272586.47	8593087.82	397	0.20	0.21	0.01
272597.32	8593089.75	395	0.25	0.21	0.01
272561.11	8593089.46	898	0.50	0.49	0.02
272541.18	8593091.14	673	0.42	0.36	0.01
272517.64	8593090.95	693	0.40	0.38	0.01
272495.91	8593090.78	921	0.50	0.50	0.02
272479.64	8593088.8	635	0.45	0.34	0.01
272461.52	8593090.5	652	0.35	0.35	0.01

UTM Eastings	UTM Northing	counts/ 100s	uGy/hr meas	uGy/hr calc	+-
272430.72	8593092.1	320	0.20	0.17	0.01
272414.43	8593091.97	272	0.16	0.14	0.01
272390.91	8593089.93	192	0.13	0.10	0.01
272378.25	8593087.99	188	0.12	0.09	0.01
272405.88	8593029.19	195	0.13	0.10	0.01
272440.27	8593031.31	190	0.10	0.09	0.01
272456.57	8593029.6	192	0.10	0.10	0.01
272476.5	8593027.92	183	0.11	0.09	0.01
272505.46	8593029.99	231	0.14	0.12	0.01
272525.39	8593028.31	229	0.10	0.12	0.01
272557.98	8593028.57	251	0.13	0.13	0.01
272588.75	8593028.82	201	0.10	0.10	0.01
272612.27	8593030.85	194	0.10	0.10	0.01
272630.39	8593029.16	201	0.10	0.10	0.01
272648.5	8593029.3	180	0.10	0.09	0.01
272661.17	8593029.4	192	0.11	0.10	0.01
272572.64	8593681.57	288	0.20	0.15	0.01
272592.63	8593672.51	306	0.20	0.16	0.01
272625	8593680	326	0.20	0.17	0.01
272661	8593680	247	0.15	0.13	0.01
272684.9	8593680.63	318	0.20	0.16	0.01
272701.21	8593678.92	301	0.20	0.16	0.01
272731.96	8593682.86	316	0.20	0.16	0.01
272759.15	8593679.39	281	0.20	0.14	0.01
272775.44	8593679.52	312	0.20	0.16	0.01
272808.03	8593679.78	314	0.15	0.16	0.01
272844.23	8593681.92	298	0.20	0.15	0.01
272871.4	8593680.29	309	0.20	0.16	0.01
272909.42	8593680.59	332	0.20	0.17	0.01
272936.59	8593678.97	369	0.20	0.19	0.01
272967.36	8593681.06	352	0.20	0.18	0.01
273005.39	8593679.52	353	0.20	0.18	0.01
273037.97	8593681.63	376	0.20	0.20	0.01
273066.95	8593680.02	373	0.20	0.20	0.01
273092.3	8593680.22	419	0.25	0.22	0.01
273123.06	8593682.31	437	0.25	0.23	0.01
273150.23	8593680.68	505	0.25	0.27	0.01
273186.44	8593680.98	378	0.20	0.20	0.01
273204.55	8593681.12	431	0.20	0.23	0.01
273226.27	8593681.3	308	0.20	0.16	0.01
273246.2	8593679.61	339	0.20	0.18	0.01
273262.5	8593679.74	322	0.15	0.17	0.01
273287.84	8593679.94	325	0.15	0.17	0.01
273266.61	8593618.91	472	0.30	0.25	0.01
273232.19	8593620.48	368	0.20	0.19	0.01
273194.17	8593620.18	324	0.20	0.17	0.01
273159.77	8593619.9	342	0.20	0.18	0.01
273128.99	8593619.65	391	0.20	0.21	0.01
273105.44	8593621.31	368	0.20	0.19	0.01
273071.06	8593619.19	377	0.20	0.20	0.01
273052.94	8593620.89	363	0.20	0.19	0.01
273033.04	8593618.88	381	0.20	0.20	0.01

UTM Easting	UTM Northing	counts/ 100s	uGy/hr meas	uGy/hr calc	+-
273016.73	8593620.6	436	0.22	0.23	0.01
273004.07	8593618.65	410	0.20	0.22	0.01
272989.57	8593620.38	421	0.23	0.22	0.01
272960.6	8593620.14	415	0.22	0.22	0.01
272926.2	8593619.87	389	0.22	0.20	0.01
272893.61	8593619.61	423	0.20	0.22	0.01
272864.65	8593619.37	371	0.15	0.19	0.01
272833.87	8593619.13	389	0.20	0.20	0.01
272803.07	8593620.72	351	0.20	0.18	0.01
272770.5	8593618.62	358	0.20	0.19	0.01
272746.95	8593620.27	366	0.20	0.19	0.01
272730.65	8593620.14	310	0.20	0.16	0.01
272703.5	8593619.92	314	0.20	0.16	0.01
272687.2	8593619.79	287	0.20	0.15	0.01
272665.48	8593619.62	329	0.20	0.17	0.01
272641.94	8593619.43	278	0.20	0.14	0.01
272611.16	8593619.18	320	0.20	0.17	0.01
272576.76	8593618.9	318	0.20	0.16	0.01
272558.64	8593620.6	325	0.20	0.17	0.01
272431.11	8593269.16	413	0.22	0.22	0.01
272452.83	8593269.33	498	0.27	0.27	0.01
272476.37	8593269.52	568	0.32	0.31	0.01
272501.72	8593269.72	590	0.32	0.32	0.01
272523.44	8593269.9	494	0.30	0.26	0.01
272548.79	8593270.1	578	0.38	0.31	0.01
272572.32	8593270.29	499	0.30	0.27	0.01
272595.88	8593268.64	406	0.24	0.22	0.01
272615.78	8593270.64	378	0.22	0.20	0.01
272642.95	8593269.02	418	0.22	0.22	0.01
272628.78	8593230.17	364	0.20	0.19	0.01
272668.61	8593230.49	393	0.24	0.21	0.01
272648.69	8593230.33	410	0.22	0.22	0.01
272637.83	8593230.25	381	0.20	0.20	0.01
272605.24	8593229.98	357	0.22	0.19	0.01
272583.51	8593229.81	377	0.22	0.20	0.01
272565.39	8593231.51	293	0.18	0.15	0.01
272545.49	8593229.5	408	0.22	0.22	0.01
272520.15	8593229.3	424	0.28	0.23	0.01
272498.41	8593230.97	455	0.26	0.24	0.01
272478.49	8593230.81	518	0.30	0.28	0.01
272456.78	8593228.79	420	0.25	0.22	0.01
272435.04	8593230.46	368	0.23	0.19	0.01
272418.75	8593230.33	386	0.22	0.20	0.01
272524.42	8593148.18	1224	0.80	0.67	0.02
272509.94	8593148.07	1065	0.60	0.58	0.02
272486.39	8593149.72	785	0.48	0.43	0.02
272461.03	8593151.36	728	0.40	0.40	0.01
272439.31	8593149.34	602	0.32	0.33	0.01
272415.78	8593149.15	594	0.35	0.32	0.01
272538.89	8593150.14	1060	0.60	0.58	0.02
272560.62	8593150.32	1037	0.59	0.57	0.02
272580.53	8593150.48	1254	0.68	0.69	0.02

UTM Easting	UTM Northing	counts/ 100s	uGy/hr meas	uGy/hr calc	+-
272600.45	8593150.64	1996	1.20	1.11	0.02
272620.38	8593148.96	2454	1.40	1.36	0.03
272642.1	8593149.13	3748	2.50	2.09	0.03
272660.19	8593151.12	3445	2.00	1.92	0.03
272683.73	8593151.31	807	0.45	0.44	0.02
272700.04	8593149.6	574	0.28	0.31	0.01
272721.76	8593149.77	373	0.18	0.20	0.01
272741.68	8593149.93	298	0.18	0.15	0.01
272763.4	8593150.11	308	0.16	0.16	0.01
272761.74	8593131.65	221	0.10	0.12	0.01
272741.84	8593129.65	241	0.12	0.13	0.01
272721.93	8593129.49	237	0.12	0.12	0.01
272698.38	8593131.14	348	0.17	0.19	0.01
272678.48	8593129.14	678	0.35	0.38	0.01
272658.55	8593130.82	1450	0.80	0.83	0.02
272645.89	8593128.87	3640	2.60	2.10	0.03
272631.39	8593130.6	2534	1.40	1.46	0.03
272611.49	8593128.6	2130	1.20	1.22	0.03
272591.56	8593130.28	1456	0.80	0.83	0.02
272569.83	8593130.11	1177	0.70	0.67	0.02
272549.92	8593129.95	1157	0.65	0.66	0.02
272530	8593129.78	999	0.56	0.57	0.02
272504.65	8593129.58	882	0.45	0.50	0.02
272484.74	8593129.42	737	0.45	0.41	0.02
272464.82	8593129.26	923	0.50	0.52	0.02
272446.72	8593129.11	761	0.45	0.43	0.02
272423.17	8593130.77	633	0.38	0.35	0.01
272403.25	8593130.61	472	0.26	0.26	0.01
272383.34	8593130.45	226	0.14	0.12	0.01
272361.61	8593130.27	198	0.10	0.10	0.01
272382.03	8593067.73	204	0.10	0.11	0.01
272401.92	8593071.58	209	0.10	0.11	0.01
272420.04	8593069.88	192	0.12	0.10	0.01
272443.57	8593070.07	254	0.13	0.13	0.01
272468.92	8593070.28	278	0.15	0.15	0.01
272487.03	8593070.42	413	0.20	0.23	0.01
272512.37	8593070.63	624	0.35	0.35	0.01
272534.1	8593070.8	758	0.45	0.43	0.02
272552.2	8593070.95	813	0.50	0.46	0.02
272573.94	8593069.28	376	0.18	0.21	0.01
272595.65	8593071.3	336	0.18	0.18	0.01
272617.39	8593069.63	351	0.17	0.19	0.01
272639.11	8593071.65	3008	1.80	1.73	0.03
272659.04	8593069.96	232	0.12	0.12	0.01
272680.76	8593070.14	167	0.11	0.08	0.01
272567.38	8593659.4	328	0.10	0.17	0.01
272587.28	8593661.41	287	0.08	0.15	0.01
272614.45	8593659.78	308	0.11	0.16	0.01
272632.56	8593659.93	276	0.11	0.14	0.01
272657.92	8593658.29	280	0.11	0.14	0.01
272683.25	8593660.33	263	0.07	0.13	0.01
272710.41	8593660.55	284	0.10	0.15	0.01

UTM Easting	UTM Northing	counts/ 100s	uGy/hr meas	uGy/hr calc	+-
272735.76	8593660.76	282	0.11	0.14	0.01
272766.54	8593661	285	0.11	0.15	0.01
272791.9	8593659.36	297	0.13	0.15	0.01
272824.49	8593659.62	324	0.12	0.17	0.01
272853.46	8593659.86	296	0.11	0.15	0.01
272886.05	8593660.12	308	0.13	0.16	0.01
272907.77	8593660.29	361	0.15	0.19	0.01
272936.74	8593660.53	390	0.15	0.21	0.01
272953.05	8593658.81	390	0.16	0.21	0.01
272978.38	8593660.86	400	0.16	0.21	0.01
273005.55	8593659.24	400	0.19	0.21	0.01
273029.09	8593659.42	373	0.17	0.20	0.01
273047.2	8593659.57	316	0.12	0.16	0.01
273070.73	8593659.76	381	0.14	0.20	0.01
273096.09	8593658.12	329	0.13	0.17	0.01
273128.67	8593660.22	353	0.03	0.18	0.01
273152.2	8593660.41	313	0.10	0.16	0.01
273175.74	8593660.6	264	0.10	0.13	0.01
273199.28	8593660.79	307	0.11	0.16	0.01
273222.83	8593659.14	299	0.11	0.15	0.01
273246.37	8593659.32	283	0.13	0.15	0.01
273269.9	8593659.51	304	0.15	0.16	0.01
273275.81	8593600.54	223	0.11	0.11	0.01
273246.84	8593600.31	450	0.17	0.24	0.01
273230.54	8593600.18	438	0.15	0.23	0.01
273208.82	8593600.01	349	0.14	0.18	0.01
273183.47	8593599.8	323	0.14	0.17	0.01
273147.25	8593601.36	390	0.14	0.21	0.01
273118.29	8593599.28	342	0.15	0.18	0.01
273098.38	8593599.12	436	0.15	0.23	0.01
273073.02	8593600.76	398	0.14	0.21	0.01
273049.48	8593600.57	374	0.13	0.20	0.01
273020.51	8593600.34	345	0.13	0.18	0.01
272993.35	8593600.12	401	0.14	0.21	0.01
272969.82	8593599.93	384	0.16	0.20	0.01
272948.09	8593599.76	347	0.12	0.18	0.01
272929.99	8593599.61	369	0.16	0.19	0.01
272904.64	8593599.41	453	0.15	0.24	0.01
272879.29	8593599.2	438	0.16	0.23	0.01
272857.57	8593599.03	437	0.14	0.23	0.01
272826.77	8593600.63	372	0.15	0.20	0.01
272801.43	8593600.42	342	0.14	0.18	0.01
272783.32	8593600.28	340	0.15	0.18	0.01
272759.78	8593600.09	334	0.10	0.17	0.01
272732.63	8593599.87	315	0.12	0.16	0.01
272714.51	8593601.57	294	0.10	0.15	0.01
272685.55	8593599.49	280	0.08	0.14	0.01
272658.4	8593599.27	260	0.10	0.13	0.01
272629.43	8593599.04	255	0.09	0.13	0.01
272611.31	8593600.74	274	0.09	0.14	0.01
272598.64	8593600.63	265	0.08	0.14	0.01
272578.73	8593598.63	276	0.09	0.14	0.01

UTM Easting	UTM Northing	counts/ 100s	uGy/hr meas	uGy/hr calc	+-
272564.25	8593598.51	306	0.08	0.16	0.01
272577.24	8593559.89	270	0.10	0.14	0.01
272595.34	8593560.03	259	0.12	0.13	0.01
272617.07	8593560.21	274	0.14	0.14	0.01
272640.6	8593560.4	287	0.13	0.15	0.01
272667.76	8593560.62	298	0.15	0.15	0.01
272698.54	8593560.86	387	0.17	0.20	0.01
272731.13	8593561.13	365	0.16	0.19	0.01
272752.87	8593559.46	413	0.20	0.22	0.01
272776.39	8593561.49	354	0.18	0.19	0.01
272801.75	8593559.85	405	0.21	0.21	0.01
272823.48	8593560.02	399	0.20	0.21	0.01
272854.26	8593560.27	413	0.17	0.22	0.01
272868.74	8593560.39	495	0.20	0.26	0.01
272895.91	8593558.76	568	0.23	0.30	0.01
272923.06	8593560.82	481	0.22	0.26	0.01
272946.59	8593561.01	433	0.20	0.23	0.01
272970.14	8593559.36	437	0.22	0.23	0.01
272995.49	8593559.56	593	0.28	0.32	0.01
273017.22	8593559.74	647	0.32	0.35	0.01
273033.51	8593559.87	645	0.32	0.35	0.01
273057.05	8593560.06	471	0.21	0.25	0.01
273086.02	8593560.29	442	0.22	0.23	0.01
273104.14	8593558.59	449	0.28	0.24	0.01
273129.47	8593560.64	342	0.19	0.18	0.01
273149.38	8593560.8	350	0.16	0.18	0.01
273171.12	8593559.13	305	0.16	0.16	0.01
273198.27	8593561.19	258	0.08	0.13	0.01
273225.42	8593561.41	196	0.09	0.10	0.01
273238.11	8593559.67	180	0.06	0.09	0.01
273258.03	8593559.83	198	0.06	0.10	0.01
273279.74	8593561.84	184	0.07	0.09	0.01
272640.81	8593309.57	404	0.20	0.21	0.01
272619	8593311	389	0.20	0.20	0.01
272601	8593310	479	0.23	0.25	0.01
272579.25	8593309.08	502	0.20	0.27	0.01
272557.53	8593308.9	508	0.30	0.27	0.01
272535.8	8593308.73	517	0.28	0.28	0.01
272518	8593312	526	0.30	0.28	0.01
272499.61	8593306.59	438	0.25	0.23	0.01
272474.22	8593311.92	394	0.18	0.21	0.01
272454.3	8593311.76	411	0.17	0.22	0.01
272427.13	8593313.39	441	0.20	0.23	0.01
272427.62	8593252.53	423	0.18	0.22	0.01
272449.36	8593250.86	457	0.25	0.24	0.01
272472.91	8593249.2	504	0.25	0.27	0.01
272500.05	8593251.27	574	0.30	0.31	0.01
272521.78	8593251.44	754	0.45	0.41	0.01
272545.3	8593253.48	547	0.30	0.29	0.01
272568.85	8593251.82	504	0.28	0.27	0.01
272592.37	8593253.86	432	0.21	0.23	0.01
272612.32	8593250.33	356	0.15	0.19	0.01

UTM Easting	UTM Northing	counts/ 100s	uGy/hr meas	uGy/hr calc	+-
272635.84	8593252.36	354	0.15	0.19	0.01
272614.63	8593187.64	511	0.30	0.27	0.01
272668.93	8593189.92	557	0.35	0.30	0.01
272645.41	8593187.89	736	0.50	0.40	0.01
272625.47	8593191.42	584	0.25	0.31	0.01
272598.32	8593189.35	416	0.20	0.22	0.01
272580.22	8593189.21	418	0.18	0.22	0.01
272560.3	8593189.05	351	0.15	0.18	0.01
272540.37	8593190.73	416	0.15	0.22	0.01
272515.04	8593188.68	471	0.20	0.25	0.01
272496.91	8593192.22	368	0.15	0.19	0.01
272480.66	8593186.56	345	0.15	0.18	0.01
272458.9	8593190.07	262	0.15	0.13	0.01
272433.56	8593189.87	346	0.15	0.18	0.01
272533.31	8593168.54	617	0.40	0.33	0.01
272511.6	8593166.52	706	0.40	0.38	0.01
272488.06	8593166.33	584	0.30	0.31	0.01
272473.56	8593168.06	631	0.30	0.34	0.01
272450.01	8593169.72	533	0.25	0.28	0.01
272421.05	8593169.48	499	0.20	0.27	0.01
272392.14	8593161.87	524	0.20	0.28	0.01
272551.45	8593165	617	0.30	0.33	0.01
272569.49	8593172.52	545	0.22	0.29	0.01
272591.25	8593169.01	596	0.22	0.32	0.01
272609.34	8593171	714	0.35	0.39	0.01
272632.89	8593169.34	926	0.50	0.50	0.02
272647.44	8593160.24	3365	2.00	1.86	0.03
272672.7	8593171.51	964	0.40	0.52	0.02
272692.63	8593169.82	893	0.40	0.48	0.02
272710.74	8593169.97	505	0.20	0.27	0.01
272730.65	8593170.13	409	0.15	0.22	0.01
272746.95	8593170.26	400	0.18	0.21	0.01
272768.67	8593170.44	311	0.15	0.16	0.01
272760.12	8593107.66	211	0.10	0.11	0.01
272740.19	8593109.35	218	0.10	0.11	0.01
272720.28	8593109.18	218	0.10	0.11	0.01
272700.36	8593109.02	231	0.10	0.12	0.01
272680.45	8593108.86	307	0.15	0.16	0.01
272660.52	8593110.55	611	0.20	0.33	0.01
272643	8593107	807	0.60	0.44	0.02
272622.48	8593112.09	903	0.35	0.49	0.02
272600.77	8593110.07	1276	0.70	0.70	0.02
272579.05	8593109.89	1006	0.50	0.55	0.02
272559.12	8593111.58	980	0.50	0.53	0.02
272539.22	8593109.57	902	0.40	0.49	0.02
272519.27	8593113.1	900	0.45	0.49	0.02
272503.02	8593107.44	648	0.35	0.35	0.01
272479.46	8593110.93	659	0.23	0.35	0.01
272455.95	8593107.06	646	0.20	0.35	0.01
272430.59	8593108.7	684	0.25	0.37	0.01
272407.05	8593108.51	293	0.13	0.15	0.01
272381.72	8593106.46	213	0.10	0.11	0.01

UTM Easting	UTM Northing	counts/ 100s	uGy/hr meas	uGy/hr calc	+-
272385.85	8593043.79	192	0.10	0.09	0.01
272402.07	8593053.14	207	0.10	0.10	0.01
272420.19	8593051.44	215	0.10	0.11	0.01
272441.93	8593049.77	193	0.10	0.10	0.01
272461.86	8593048.09	215	0.10	0.11	0.01
272485.35	8593053.81	201	0.10	0.10	0.01
272508.88	8593054	255	0.10	0.13	0.01
272530.63	8593052.33	386	0.15	0.20	0.01
272550.53	8593054.33	451	0.18	0.24	0.01
272577.73	8593049.02	283	0.10	0.15	0.01
272601.22	8593054.74	233	0.15	0.12	0.01
272621.18	8593049.37	198	0.10	0.10	0.01
272641.09	8593049.53	206	0.10	0.10	0.01
272660.95	8593057.07	194	0.10	0.10	0.01
272682.75	8593048.02	176	0.10	0.09	0.01

Appendix B Radon flux density

Appendix B Radon flux density results for individual charcoal canisters deployed during Anomaly 2 survey conducted 14–17 July 2009.

Can #	site	Easting	Northing	Deployed Date/time	Retrieved Date/time	Rn [mBq.m ⁻² .s ⁻¹]	ave±stdev	Soil type
							geomean	
100	1A	272968	8593810	14/07/2009 10:45	17/07/2009 10:37	252 ± 4	249±6	sandy
70	1A	272968	8593810	14/07/2009 10:45	17/07/2009 10:37	253 ± 4	249	loam
97	1A	272968	8593810	14/07/2009 10:45	17/07/2009 10:37	241 ± 4		
87	2A	273084	8593837	14/07/2009 11:07	17/07/2009 10:41	818 ± 7	694±411	fine
78	2A	273084	8593837	14/07/2009 11:07	17/07/2009 10:41	235 ± 4	583	gravel
92	2A	273084	8593837	14/07/2009 11:07	17/07/2009 10:41	1029 ± 7		
88	3A	273106	8593792	14/07/2009 11:25	17/07/2009 10:45	926 ± 7	1046±153	fine
68	3A	273106	8593792	14/07/2009 11:25	17/07/2009 10:45	1219 ± 8	1039	gravel
98	3A	273106	8593792	14/07/2009 11:25	17/07/2009 10:45	992 ± 7		
2E	4A	273141	8593890	14/07/2009 11:37	17/07/2009 10:48	771 ± 7	760±10	fine
10E	4A	273141	8593890	14/07/2009 11:37	17/07/2009 10:48	759 ± 7	760	gravel
80	4A	273141	8593890	14/07/2009 11:37	17/07/2009 10:48	750 ± 6		
19E	5A	273273	8593846	14/07/2009 11:45	17/07/2009 10:50	751 ± 7		
22E	5A	273273	8593846	14/07/2009 11:45	17/07/2009 10:50	894 ± 7	866±104	sandy
37E	5A	273273	8593846	14/07/2009 11:45	17/07/2009 10:50	952 ± 7	861	loam
38E	6A	273263	8593696	14/07/2009 11:54	17/07/2009 10:54	271 ± 4	290±48	sandy
83	6A	273263	8593696	14/07/2009 11:54	17/07/2009 10:54	254 ± 4	288	loam
24E	6A	273263	8593696	14/07/2009 11:54	17/07/2009 10:54	345 ± 5		
6E	7A	273200	8593597	14/07/2009 12:00	17/07/2009 10:55	864 ± 7	918±49	sandy
69	7A	273200	8593597	14/07/2009 12:00	17/07/2009 10:55	959 ± 7	917	loam
73	7A	273200	8593597	14/07/2009 12:00	17/07/2009 10:55	932 ± 7		
7E	8A	272988	8593601	14/07/2009 12:07	17/07/2009 10:58	209 ± 4	222±13	fine
61	8A	272988	8593601	14/07/2009 12:07	17/07/2009 10:58	235 ± 4	222	gravel
O	8A	272988	8593601	14/07/2009 12:07	17/07/2009 10:58	222 ± 4		
39E	9A	272793	8593599	14/07/2009 12:15	17/07/2009 11:01	286 ± 5	305±27	fine
12E	9A	272793	8593599	14/07/2009 12:15	17/07/2009 11:01	324 ± 5	305	gravel
15	9A	272793	8593599	14/07/2009 12:15	17/07/2009 11:01	N/A		
35E	10A	272606	8593588	14/07/2009 12:20	17/07/2009 11:04	155 ± 3	140±14	sandy
9E	10A	272606	8593588	14/07/2009 12:20	17/07/2009 11:04	129 ± 3	139	loam
74	10A	272606	8593588	14/07/2009 12:20	17/07/2009 11:04	136 ± 4		
4E	11A	272511	8593428	14/07/2009 12:28	17/07/2009 11:15	631 ± 6	612±27	sandy
29E	11A	272511	8593428	14/07/2009 12:28	17/07/2009 11:15	593 ± 6	612	loam
65	11A	272511	8593428	14/07/2009 12:28	17/07/2009 11:15	N/A		
63	12A	272712	8593449	14/07/2009 12:44	17/07/2009 11:18	6108 ± 17	6631±456	fine
8E	12A	272712	8593449	14/07/2009 12:44	17/07/2009 11:18	6946 ± 18	6621	gravel
31	12A	272712	8593449	14/07/2009 12:44	17/07/2009 11:18	6840 ± 18		
84	13A	272894	8593454	14/07/2009 12:55	17/07/2009 11:22	7541 ± 19	9983±3892	coarse
1E	13A	272894	8593454	14/07/2009 12:55	17/07/2009 11:22	7937 ± 19	9532	gravel
23E	13A	272894	8593454	14/07/2009 12:55	17/07/2009 11:22	14472 ± 27		
62	14A	272894	8593453	14/07/2009 13:05	17/07/2009 11:33	1022 ± 7	5216±5420	coarse
76	14A	272894	8593453	14/07/2009 13:05	17/07/2009 11:33	11336 ± 23	3366	gravel
16E	14A	272894	8593453	14/07/2009 13:05	17/07/2009 11:33	3289 ± 13		
86	15A	272856	8593432	14/07/2009 13:12	17/07/2009 11:30	2586 ± 11	4982±2238	gravel/
77	15A	272856	8593432	14/07/2009 13:12	17/07/2009 11:30	7019 ± 19	4594	sand on
95	15A	272856	8593432	14/07/2009 13:12	17/07/2009 11:30	5341 ± 16		rock
93	16A	272867	8593385	14/07/2009 13:20	17/07/2009 11:26	4840 ± 15	5726±815	sandy
67	16A	272867	8593385	14/07/2009 13:20	17/07/2009 11:26	6443 ± 18	5686	

79 Can #	16A site	272867 Easting	8593385 Northing	14/07/2009 13:20 Deployed Date/time	17/07/2009 11:26 Retrieved Date/time	5894 ± 17 Rn [mBq.m⁻².s⁻¹]	ave±stdev geomean	Soil type
94	17A	273092	8593445	14/07/2009 13:31	17/07/2009 11:42	93 ± 3	104±15	sandy
96	17A	273092	8593445	14/07/2009 13:31	17/07/2009 11:42	98 ± 3	103	loam
66	17A	273092	8593445	14/07/2009 13:31	17/07/2009 11:42	121 ± 4		
17E	18A	272798	8593299	14/07/2009 14:09	17/07/2009 11:49	143 ± 4	122±29	fine
27E	18A	272798	8593299	14/07/2009 14:09	17/07/2009 11:49	102 ± 3	121	gravel
28E	19A	272993	8593295	14/07/2009 13:56	17/07/2009 11:46	217 ± 3	229±24	sandy
26E	19A	272993	8593295	14/07/2009 13:56	17/07/2009 11:46	213 ± 3	228	loam
25E	19A	272993	8593295	14/07/2009 13:56	17/07/2009 11:46	256 ± 4		
81E	20A	272495	8593306	14/07/2009 14:22	17/07/2009 11:53	822 ± 7	926±147	sandy
62E	20A	272495	8593306	14/07/2009 14:22	17/07/2009 11:53	1030 ± 8	921	loam
40	21A	272416	8593047	14/07/2009 14:30	17/07/2009 12:00	8 ± 3	6±2	sandy
64	21A	272416.6	8593047	14/07/2009 14:30	17/07/2009 12:00	6 ± 3	6	loam
30E	21A	272416.6	8593047	14/07/2009 14:30	17/07/2009 12:00	4 ± 3		
20E	22A	272524.23	8593172.21	14/07/2009 14:38	17/07/2009 12:05	583 ± 6	556±26	sandy
3E	22A	272524.23	8593172.21	14/07/2009 14:38	17/07/2009 12:05	552 ± 6	555	loam
72	22A	272524.23	8593172.21	14/07/2009 14:38	17/07/2009 12:05	532 ± 6		
21E	23A	272598.93	8593113.71	14/07/2009 14:46	17/07/2009 12:08	2496 ± 11	3513±1331	sandy
85	23A	272598.93	8593113.71	14/07/2009 14:46	17/07/2009 12:08	5020 ± 16	3359	loam
34E	23A	272598.93	8593113.71	14/07/2009 14:46	17/07/2009 12:08	3024 ± 13		
75	24A	272643.81	8593165	14/07/2009 14:58	17/07/2009 12:14	15684 ± 27	8710±6718	Rocky
91	24A	272643.81	8593165	14/07/2009 14:58	17/07/2009 12:14	2280 ± 11	6634	heap
18E	24A	272643.81	8593165	14/07/2009 14:58	17/07/2009 12:14	8166 ± 20		
90	25A	272731.02	8593124	14/07/2009 15:05	17/07/2009 12:21	278 ± 5	231±66	sandy
11E	25A	272731.02	8593124	14/07/2009 15:05	17/07/2009 12:21	185 ± 4	227	loam

Appendix C Airborne radon activity concentrations

Appendix C Results of airborne radon activity concentrations [Bq·m⁻³] for sites 1A-25A.

Site	Rn [Bq.m ⁻³]	Rn average [Bq.m ⁻³]	Site	Rn [Bq.m ⁻³]	Rn average [Bq.m ⁻³]
4A	298±119	218±114	17A	72±29 255±10 2	164±129
	137±55				
8A	131±52	119±17	17A (30cm)	236±94 51±20	144±131
	107±43				
9A	39±16	45±8	17A (50cm)	82±33 57±23	70±18
	51±20				
2A	92±37	96±6	20A	131±52 198±79	165±47
	100±40				
3A	181±72	122±83	22A	244±98 168±67	206±54
	63±25				
3A (30cm)	175±70	206±43	23A	88±35 151±60	120±45
	236±94				
3A (50cm)	125±50	107±26	19A	131±52 119±48	125±8
	88±35				
12A	244±98	176±97	24A	221±88 236±94 252±10	229±11
	107±43				
18A	76±30	95±26	13A	1 193±77 3464±1	223±42
	113±45				
16A	463±185	331±187	13A (30cm)	386 525±21 0 545±21	1995±2078
	198±79				
21A	63±25	68±6	13A (50cm)	8 1173±4 69 422±16	859±444
	72±29				
21A (30cm)	n.r.	100±40	14A	9 432±17 3 1657±6	427±7
	100±40				
21A (50cm)	n.r.	20±8	14A (30cm)	63 1935±7 74 1225±4	1796±197
	20±8				
1A	82±33	113±44	14A (50cm)	90 1873±7 49 259±10	1549±458
	144±58				
25A	46±18	46±18	15A	4 306±12 2 267±10	283±33
	n.r.				
5A	224±90	159±92	15A (30cm)	7 535±21 4 607±24	401±190
	94±38				
6A	298±119	237±87	15A (50cm)	3	1233±885

Site	Rn [Bq.m³]	Rn average [Bq.m³]	Site	Rn [Bq.m³]	Rn average [Bq.m³]
7A	252±101 411±164	332±112	unexposed	15±6	15±6
10A	57±23 162±65	110±74			
11A	181±72 150±60	166±22			

n.r.: not reliable

Appendix D Soil activity concentrations

Appendix D Results of soil activity concentrations [$\text{Bq}\cdot\text{kg}^{-1}$] and gamma dose rate measurements [$\mu\text{Gy}\cdot\text{hr}^{-1}$] for sites 1A-25A at Anomaly 2. Soil activity concentrations were measured with the *eriss* HPGe gamma detectors. Eastings and Northings are given in Appendix B.

Site	U-238	Ra-226	Pb-210	Ra-228	Th-228	K-40	Dose rate
Site 1a	131±4	224±2	193±5	27±1	34±1	36±3	0.21 ± 0.01
Site 2a	656±9	1330±10	803±14	24±1	24±1	10±4	0.47 ± 0.02
Site 3a	970±10	1230±10	930±20	52±2	58±1	0±5	0.72 ± 0.02
Site 4a	533±8	766±6	560±10	28±1	33±1	38±5	0.47 ± 0.02
Site 5a	241±6	429±3	414±8	24±1	28±1	26±4	0.30 ± 0.01
Site 6a	93±3	91±1	141±4	24±1	25±1	15±2	0.14 ± 0.01
Site 7a	124±3	130±1	197±4	21±1	25±1	16±2	0.16 ± 0.01
Site 8a	162±4	212±2	168±5	51±1	56±1	17±2	0.22 ± 0.02
Site 9a	103±3	168±1	159±5	32±1	36±1	35±3	0.16 ± 0.01
Site 10a	133±4	171±2	227±6	56±1	62±2	69±4	0.14 ± 0.01
Site 11a	226±5	291±2	379±7	25±1	26±1	35±3	0.21 ± 0.01
Site 12a	987±11	1330±10	1300±20	29±2	31±1	75±6	0.8 ± 0.01
Site 13a	7775±31	10580±70	6510±90	38±4	45±2	182±16	5.25 ± 0.06
Site 14a	78073±107	110700±800	64800±830	N/A	N/A	N/A	21.0 ± 0.7
Site 15a	32219±61	41080±290	29010±370	78±7	113±5	290±25	11.4 ± 0.22
Site 16a	8692±29	7800±60	6910±90	42±3	43±2	80±11	2.07 ± 0.03
Site 17a	30±2	38±1	77±3	18±1	20±1	21±2	0.11 ± 0.01
Site 18a	75±3	79±1	107±4	26±1	30±1	37±3	0.14 ± 0.01
Site 19a	46±2	39±1	109±3	18±1	20±1	27±2	0.13 ± 0.01
Site 20a	264±5	213±2	267±6	21±1	25±1	24±3	0.23 ± 0.01
Site 21a	16±1	14±1	45±3	15±1	16±1	44±3	0.10± 0.04
Site 22a	275±6	502±4	420±8	20±1	23±1	22±4	0.38 ± 0.02
Site 23a	373±7	654±5	729±12	16±1	16±1	20±4	0.70 ± 0.01
Site 24a	6289±29	9950±70	7660±100	77±4	98±3	616±22	2.00 ± 0.02
Site 25a	29±1	30±1	80±3	15±1	16±1	45±3	0.12 ± 0.01